

2011

IMPROVING JET ATTRITION IN FLUIDIZED BEDS

Qi Zhang

Follow this and additional works at: <https://ir.lib.uwo.ca/digitizedtheses>

Recommended Citation

Zhang, Qi, "IMPROVING JET ATTRITION IN FLUIDIZED BEDS" (2011). *Digitized Theses*. 3399.
<https://ir.lib.uwo.ca/digitizedtheses/3399>

This Thesis is brought to you for free and open access by the Digitized Special Collections at Scholarship@Western. It has been accepted for inclusion in Digitized Theses by an authorized administrator of Scholarship@Western. For more information, please contact wlsadmin@uwo.ca.

THE UNIVERSITY OF WESTERN ONTARIO
School of Graduate and Postdoctoral Studies
IMPROVING JET ATTRITION IN FLUIDIZED BEDS

(Spine Title: Improving Jet Attrition in Fluidized Beds)

(Thesis Format: Integrated Article)

by

Qi Zhang

Graduate Program
In
Engineering Science
Department of Mechanical and Materials Engineering

A thesis submitted in partial fulfillment of the requirements for the degree of
Master of Engineering Science

The School of Graduate and Postdoctoral Studies
The University of Western Ontario

London, Ontario Canada

© Qi Zhang 2011

THE UNIVERSITY OF WESTERN ONTARIO

School of Graduate and Postdoctoral Studies

Certificate of Examination

Joint-Supervisor

Dr. Cedric Briens

Joint-Supervisor

Dr. Franco Berruti

Examiners

Dr. Anand Prakash

Dr. Chao Zhang

Dr. Ralph Buchal

The thesis by

Qi Zhang

entitled:

Improving Jet Attrition in Fluidized Beds

is accepted in partial fulfillment of the
requirements for the degree of
Master of Engineering Science

Date _____

Chair of the Thesis Examination Board

Abstract

Fluidized bed reactors are used extensively in many industrial applications due to attractive features such as good solids and gases mixing, and rapid heat and mass transfer. Fluid Coking is a process that utilizes these attractive properties. It is a non-catalytic thermal conversion process that is used to upgrade bitumen from oil sands in order to produce synthetic crude oil. Particle size control is crucial in Fluid Coking in order to maintain a well fluidized bed and a satisfactory production rate. Therefore, steam is injected through supersonic nozzles in the reactor section of the Fluid Coker, to attrit the coke particles and maintain the desired particle size distribution. Currently, a large quantity of steam is used by the Coker attrition nozzles. If the steam consumption of the attrition nozzles could be reduced, it would reduce the energy consumption and lead to a higher reactor throughput. This is the primary research objective for this thesis work.

The first portion of the research work was focused on the optimization of supersonic nozzle operating conditions, in terms of maximizing the grinding efficiency to minimize the flowrate of attrition gas. The attrition nozzle operating pressure, attrition time, and nozzle scale were tested to determine their effect on the grinding efficiency. Attrition gas consumptions were compared for the same new surface area created in order to find the optimal operating conditions, for which a minimum flowrate of attrition gas is used.

The effect of fluid bed hydrodynamics on jet attrition was investigated next. A specially designed fluidized bed was used to create two hydrodynamics zones, where the superficial gas velocity could be independently adjusted. Supersonic attrition jets were

tested under different hydrodynamic conditions, with different nozzle penetrations where the attrition jet could either straddle both hydrodynamic zones, or be completely enclosed within one hydrodynamic zone. Local bed pressure gradient was measured along the width of the bed to help explain the effect of bed hydrodynamics on jet attrition.

Authors:

Qi Zhang, Tarek J. Jamaileddine, Cedric Briens, Franco Berruti, Jennifer McMillan

Article Status: Unpublished

Finally, the effect of the nozzle inclination angle on jet attrition was studied. A supersonic nozzle was used and able to adjust from 0° to 90°. The optimal nozzle inclination angle was found, which generated the largest new surface area. Particle size distribution analysis was carried out to determine the amount of coarse particles ground and fine particles generated for each nozzle angle.

Article Title:

Effect of fluidized bed hydrodynamics on jet attrition

Authors:

Qi Zhang, Tarek J. Jamaileddine, Cedric Briens, Franco Berruti, Jennifer McMillan

Article Status:

Unpublished

Contributions:

Qi Zhang conducted all experimental work, data analysis and writing. Tarek J. Jamaileddine assisted in some of the experimental work. Cedric Briens, Franco Berruti and Jennifer McMillan provided guidance, supervision and revised drafts of the work.

Chapter 4

Article Title:

Effect of nozzle inclination on jet attrition

Authors:

Qi Zhang, Tarek J. Jamaileddine, Cedric Briens, Franco Berruti, Jennifer McMillan, Majid Hamidi

Article Status:

Unpublished

Contributions:

Qi Zhang conducted all experimental work, data analysis and writing. Majid Hamidi assisted in some of the experimental work. Cedric Briens, Franco Berruti and Jennifer McMillan provided guidance, supervision and revised drafts of the work.

Keywords: Fluidized bed, fluid coking, supersonic nozzles, particle attrition, fluid bed hydrodynamics, nozzle inclination angle

Co-Authorship

Chapter 2

Article Title: Influence of operation conditions for supersonic attrition nozzles in jet attrition
Authors: Qi Zhang, Tarek J. Jamaledidine, Cedric Briens, Franco Berruti, Jennifer McMillan
Article Status: Unpublished
Contributions: Qi Zhang conducted all experimental work, data analysis and writing. Tarek J. Jamaledidine assisted with setting up the fluidized bed, also assisted in some of the experimental work. Cedric Briens, Franco Berruti and Jennifer McMillan provided guidance, supervision and revised drafts of the work.

Chapter 3

Article Title: Effect of fluidized bed hydrodynamics on jet attrition
Authors: Qi Zhang, Tarek J. Jamaledidine, Cedric Briens, Franco Berruti, Jennifer McMillan
Article Status: Unpublished
Contributions: Qi Zhang conducted all experimental work, data analysis and writing. Tarek J. Jamaledidine assisted in some of the experimental work. Cedric Briens, Franco Berruti and Jennifer McMillan provided guidance, supervision and revised drafts of the work.

Chapter 4

Article Title: Effect of nozzle inclination on jet attrition
Authors: Qi Zhang, Tarek J. Jamaledidine, Cedric Briens, Franco Berruti, Jennifer McMillan, Majid Hamidi
Article Status: Unpublished
Contributions: Qi Zhang conducted all experimental work, data analysis and writing. Majid Hamidi assisted in some of the experimental work. Cedric Briens, Franco Berruti and Jennifer McMillan provided guidance, supervision and revised drafts of the work.

Acknowledgements

First, I would like to express my gratitude to my supervisors Dr. Cedric Briens and Dr. Franco Berruti from the Institute of Chemicals and Fuels from Alternative Resources (ICFAR) at the University of Western Ontario, for their guidance and support throughout the completion of my thesis work. Dr. Briens and Dr. Berruti kindly shared their knowledge and expertise to help on my research work, I am truly thankful for all of that. I would especially like to thank Dr. Tarek J. Jamaledine, a post-doctoral fellow of ICFAR for providing me valuable advices and assistance on all my experimental works. I would like to thank Dr. Jennifer McMillan, of Syncrude Canada, for providing valuable feedback and ensuring that my research was industrially relevant. Special thanks to Rob Taylor and Ganesh Raj for their help on my experimental equipments. I also wish to acknowledge all my colleagues from ICFAR. It was great to know you all and thank you for all your help in my research work.

At last, my deepest gratitude goes to my parents, Yongxi Zhang and Kun Jiang, for their unconditional support and love. I would not have been able to pursue my education in Canada and complete my Master degree if you had not always believed in me. I would like to dedicate this thesis to my beloved parents.

Table of Contents

Certificate of Examination.....	ii
Abstract.....	iii
Co-Authorship	v
Acknowledgements.....	vi
List of Figures.....	ix
List of Tables	xi
Chapter 1: Introduction.....	1
1.1 Present Thesis Work	1
1.2 Fluid Coking Process	1
1.3 Review of Particle Attrition Studies in Fluidized Bed.....	4
1.3.1 Particle attrition in fluidized bed	4
1.3.2 Modes of particle breakage.....	5
1.3.3 Subsonic jet-induced attrition in fluidized beds	5
1.3.4 Supersonic jet-induced attrition in fluidized beds	6
1.3.5 Effect of fluidized bed hydrodynamics on jet attrition.....	7
1.3.6 Methods of improving jet attrition.....	8
1.4 Research Objectives	10
1.5 Nomenclature	11
1.6 References	11
Chapter 2: Effect of Nozzle Operating Conditions on Jet Attrition	15
2.1 Introduction.....	15
2.2 Experimental Setup	18
2.3 Results and Discussion.....	22
2.3.1 Effect of attrition pressure on the attrition gas consumption.....	22
2.3.2 Effect of nozzle scale on the attrition gas consumption	26
2.4 Analysis of Particle Size Distribution.....	32
2.4.1 Effect of attrition pressure on particle size distribution.....	33
2.4.2 Effect of nozzle scale on particle size distribution	36
2.5 Conclusion	38
2.6 Nomenclature	39
2.7 References	39
Chapter 3: Effect of Fluidized Bed Hydrodynamics on Jet Attrition	42
3.1 Introduction.....	42

3.2	Experimental Setup.....	45
3.3	Results and Discussion.....	49
3.3.1	Effect of uneven fluidization gas distribution and nozzle insertion depth	49
3.3.2	Effect of nozzle scale with uneven gas distribution	60
3.3.3	Effect of inserted baffle underneath the attrition jet.....	62
3.4	Conclusion	64
3.5	Nomenclature	64
3.6	References	65
Chapter 4:	Effect of Nozzle Inclination on Jet Attrition.....	68
4.1	Introduction.....	68
4.2	Experimental Setup.....	71
4.3	Results and Discussion.....	74
4.3.1	Effect of nozzle inclination on jet attrition.....	74
4.3.2	Effect of baffle on jet attrition	82
4.4	Conclusion	84
4.5	References.....	85
Chapter 5:	Conclusions and Recommendations	87
5.1	Conclusions.....	87
5.2	Recommendations.....	88
Curriculum Vitae	89
Figure 2.17:	Effect of nozzle scale on the grinding of coarse particles	37
Figure 2.18:	Relationship between the generation of fines smaller than 30 µm and the grinding of particles larger than 10 µm	37
Figure 3.1:	Experimental Set-up	46
Figure 3.2:	Attrition nozzle positions	47
Figure 3.3:	Annal type nozzle, $D_g = 2.4$ mm	48
Figure 3.4:	Laval type nozzle, $D_g = 2.8$ mm	49
Figure 3.5:	New surface area created versus uneven fluidization velocities – Nozzle penetration at 25% bed width (the first velocity is the fluidization velocity in the bed half nearer the nozzle port)	50
Figure 3.6:	New surface area created versus uneven fluidization velocities – Nozzle penetration at 75% bed width (the first velocity is the fluidization velocity in the bed half nearer the nozzle port)	50
Figure 3.7:	New surface area created versus uneven fluidization velocities – Nozzle penetration at 50% bed width (the first velocity is the fluidization velocity in the bed half nearer the nozzle port)	51
Figure 3.8:	Effect of uneven gas distribution and nozzle penetration on new surface area created	52
Figure 3.9a:	Estimated jet tip location for nozzle penetration at 24.4 cm	53

List of Figures

Figure 1.1: Schematic diagram of the fluid coking process (adapted from House, 2007).....	2
Figure 2.1a: Experimental Set-up.....	19
Figure 2.1b: Photographic view of the experimental set-up.....	20
Figure 2.2: Laval type nozzle, $D_{th} = 2.4$ mm.....	21
Figure 2.3: Laval type nozzle, $D_{th} = 2.8$ mm.....	21
Figure 2.4: Effect of attrition pressure on new surface area created with 2.4 mm Laval-type nozzle (Dash lines show 95% confidence interval).....	23
Figure 2.5 Mass of attrition gas versus new surface area created for 2.4 mm nozzle.....	24
Figure 2.6: Effect of attrition pressure on new surface area created with 2.8 mm Laval-type nozzle (Dash lines show 95% confidence interval).....	25
Figure 2.7: Mass of attrition gas versus new surface area created for 2.8 mm nozzle.....	26
Figure 2.8: Effect of nozzle scale on new surface area created at an attrition pressure of 1.5 MPa (Dash lines show 95% confidence interval).....	27
Figure 2.9: New surface area created versus mass of attrition gas at 1.5 MPa.....	28
Figure 2.10: Effect of nozzle scale on new surface area created at an attrition pressure of 2.2 MPa (Dash lines show 95% confidence interval).....	29
Figure 2.11: New surface area created versus mass of attrition gas at 2.2 MPa.....	30
Figure 2.12: New surface area created versus mass of attrition gas.....	31
Figure 2.13: Effect of attrition pressure on the generation of fine particles – 2.4 mm Laval-type nozzle.....	33
Figure 2.14: Effect of attrition pressure on the grinding of coarse particles – 2.4 mm Laval-type nozzle.....	34
Figure 2.15: Relationship between the generation of fines smaller than 30 μm and the grinding of particles larger than 105 μm	35
Figure 2.16: Effect of nozzle scale on the generation of fine particles.....	36
Figure 2.17: Effect of nozzle scale on the grinding of coarse particles.....	37
Figure 2.18: Relationship between the generation of fines smaller than 30 μm and the grinding of particles larger than 105 μm	37
Figure 3.1: Experimental Set-up.....	46
Figure 3.2: Attrition nozzle positions.....	47
Figure 3.3: Laval type nozzle, $D_{th} = 2.4$ mm.....	48
Figure 3.4: Laval type nozzle, $D_{th} = 2.8$ mm.....	49
Figure 3.5: New surface area created versus uneven fluidization velocities -- Nozzle penetration at 25% bed width (the first velocity is the fluidization velocity in the bed half nearer the nozzle port).....	50
Figure 3.6: New surface area created versus uneven fluidization velocities -- Nozzle penetration at 37.5% bed width (the first velocity is the fluidization velocity in the bed half nearer the nozzle port).....	50
Figure 3.7: New surface area created versus uneven fluidization velocities -- Nozzle penetration at 50% bed width (the first velocity is the fluidization velocity in the bed half nearer the nozzle port).....	51
Figure 3.8: Effect of uneven gas distribution and nozzle penetration on new surface area created.....	52
Figure 3.9a: Estimated jet tip location for nozzle penetration at 24.4 cm.....	53

Figure 3.9b: Estimated jet tip location for nozzle penetration at 36.7 cm.....	53
Figure 3.9c: Estimated jet tip location for nozzle penetration at 48.9 cm.....	53
Figure 3.10: Pressure taps used to determine bubble volume fraction.....	55
Figure 3.11: Bubble volume fraction profile along the width of bed at 0.1 m/s.....	57
Figure 3.12: Bubble volume fraction profile along the width of bed at 0.5 m/s.....	57
Figure 3.13: Average bubble volume fraction versus excess fluidization velocity.....	58
Figure 3.14: Bubble volume fraction profile along the width of bed at 0.5 m/s and 0.1m/s.....	59
Figure 3.15: Effect of nozzle scale with uneven gas distribution (the first velocity is the fluidization velocity in the bed half nearer the nozzle port).....	60
Figure 3.16: Effect of fluidization velocity on new surface area creation (the first velocity is the fluidization velocity in the bed half nearer the nozzle port).....	61
Figure 3.17: Inserted baffle under attrition nozzle.....	62
Figure 3.18: Effect of inserted baffle.....	63
Figure 4.1: Experimental Set-up.....	72
Figure 4.2: Laval type nozzle, $D_{th}=2.4$ mm.....	73
Figure 4.3: Nozzle layout.....	75
Figure 4.4: New surface area created vs. nozzle inclination angle.....	76
Figure 4.5: Electrodes on wooden window.....	77
Figure 4.6: Horizontal jet tip contour.....	78
Figure 4.7: Vertical jet tip contour.....	78
Figure 4.8: Coefficient of variation for horizontal jet.....	79
Figure 4.9: Coefficient of variation for vertical jet.....	80
Figure 4.10: Grinding of coarse particles versus the nozzle inclination angle.....	81
Figure 4.11: Generation of fine particles versus the nozzle inclination angle.....	81
Figure 4.12: Nozzle position relative to baffle.....	82
Figure 4.13: New surface area created vs. nozzle inclination angle (with baffle inserted for the 60° case).....	83
Figure 4.14: Grinding of coarse particles versus the nozzle inclination angle (with baffle inserted for the 60° case).....	84
Figure 4.15: Generation of fine particles versus the nozzle inclination angle (with baffle inserted for the 60° case).....	84

Chapter 1 List of Tables

Table 2.1: Generation of fines for a given new surface area created by the 2.4 mm nozzle.....	35
Table 2.2: Generation of fines for a given new surface area created by the two nozzles at 2.1 MPa.....	38

particle attrition with convergent-divergent nozzles in gas-solid fluidized beds. Fluidized beds have been used in numerous industrial applications due to attractive features such as good solids and gases mixing, and rapid heat and mass transfer. Fluid Coking is one application that utilizes these attractive properties, and it is used in heavy oil upgrading. The motivation and main objective of the thesis is to improve the efficiency of particle attrition in the Fluid Coking process, by reducing the consumption of attrition gas.

The following chapters focus on experimental studies of jet-induced particle attrition in fluidized beds. However, an overview of the Fluid Coking process will be presented first. Recent research on jet-induced particle attrition will be reviewed next. At last, research objectives for this thesis will be outlined to conclude this chapter.

1.2 Fluid Coking Process

Canada has approximately 170 billion barrels of oil reserves, ranking the third in the world behind Saudi Arabia and Venezuela (Government of Alberta-Oil sands industry, 2011). 170 billion barrels out of the total oil reserves are contained in the oil sands, which are located in Alberta and are currently recoverable. However, 115 billion barrels are ultimately recoverable once necessary technology is developed (Government of Alberta-Energy, 2009). Oil sands contain a mixture of water, mineral rich clay material and a form of heavy oil called bitumen. Bitumen is a black, asphalt-like oil in its raw

Chapter 1: Introduction

1.1 Present Thesis Work

The research work presented in this thesis deals with experimental studies on particle attrition with convergent-divergent nozzles in gas-solid fluidized beds. Fluidized beds have been used in numerous industrial applications due to attractive features such as flexibility and low greenhouse gas emissions. Syncrude Canada Ltd. is one of the largest manufacturers of crude oil from Canada's oil sands, with the three largest Fluid Cokers in application that utilizes these attractive properties, and it is used in heavy oil upgrading. The motivation and main objective of the thesis is to improve the efficiency of particle attrition in the Fluid Coking process, by reducing the consumption of attrition gas.

The following chapters focus on experimental studies of jet-induced particle attrition in fluidized beds. However, an overview of the Fluid Coking process will be presented first. Recent research on jet-induced particle attrition will be reviewed next. At last, research objectives for this thesis will be outlined to conclude this chapter.

1.2 Fluid Coking Process

Canada has approximately 179 billion barrels of oil reserves, ranking the third in the world behind Saudi Arabia and Venezuela (Government of Alberta-Oil sands industry, 2011). 170 billion barrels out of the total oil reserves are bitumen from the oil sands, which are located in Alberta and are currently recoverable. However, 315 billion barrels are ultimately recoverable once necessary technology is developed (Government of Alberta-Energy, 2009). Oil sands contain a mixture of water, mineral rich clay material and a form of heavy oil called bitumen. Bitumen is a black, asphalt-like oil in its raw

Figure 1.1: Schematic diagram of the fluid coking process (adapted from House, 2007)

state, and cannot be processed in oil refineries. It requires upgrading before it can be transported by pipeline and used by conventional refineries.

Fluid Coking is a non-catalytic thermal conversion process that is used to upgrade heavy oil such as bitumen into synthetic crude oil. Fluid Coking has become a popular choice for upgrading oil sands bitumen due to its continuous operation, high reliability, flexibility and low greenhouse gas emissions. Syncrude Canada Ltd. is one of the largest manufacturers of crude oil from Canada's oil sands, with the three largest Fluid Cokers in the world. Syncrude Canada Ltd. produced 107 million barrels crude oil from oil sands bitumen in 2010 and is capable to supply 15% of Canada's petroleum requirements (Syncrude Canada Ltd., 2011).

The Fluid Cokers used by Syncrude Canada utilize a two vessels system, which includes a fluid bed reactor and a fluid bed burner, as shown in Figure 1.1 (House, 2007).

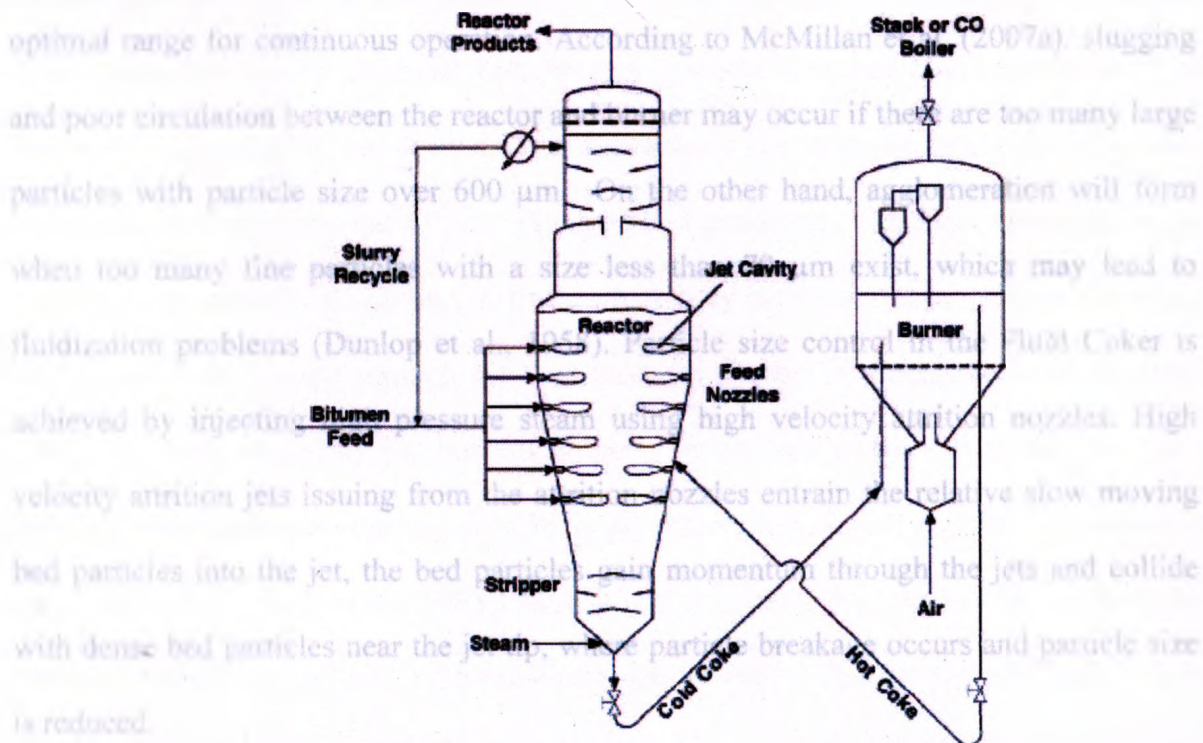


Figure 1.1: Schematic diagram of the fluid coking process (adapted from House, 2007)

Coke particles are heated to temperatures ranging from 600-680 °C by the fluidized bed burner and transported to the top of reactor section to contact with bitumen feed, which is at a temperature ranging from 300-400°C. Hot coke particles provide the heat needed for bitumen to thermally crack on its surface at temperatures ranging from 510 to 550 °C. The thermally cracked vapours flow through the cyclones at the top of the reactor before going through the condenser further downstream, which helps to transport the entrained coke particles back to the reactor. The coke particles lose some heat after the thermal cracking process and fall through the reactor, and are then transported back to the burner for reheating.

1.3.1 Particle attrition in fluidized bed

During the Fluid Coking process, coke is formed and deposited on the surface of coke particles as a reaction by-product. This causes a gradual increase in the particle size of coke. The Fluid Coking process requires that the coke particles size remains within an optimal range for continuous operation. According to McMillan et al. (2007a), slugging and poor circulation between the reactor and burner may occur if there are too many large particles with particle size over 600 µm. On the other hand, agglomeration will form when too many fine particles with a size less than 70 µm exist, which may lead to fluidization problems (Dunlop et al., 1958). Particle size control in the Fluid Coker is achieved by injecting high pressure steam using high velocity attrition nozzles. High velocity attrition jets issuing from the attrition nozzles entrain the relative slow moving bed particles into the jet, the bed particles gain momentum through the jets and collide with dense bed particles near the jet tip, where particle breakage occurs and particle size is reduced.

In the Fluid Coking process, the jet attrition process accounts for about 40% of the total steam consumption (Li, 2011). If the steam consumed by the attrition nozzles could be reduced, the same superficial gas velocity in the freeboard would be obtained with a higher injection rate of feedstock, which would lead to higher production of synthetic crude oil. This is also the motivation for the research work performed in this thesis, whose goal is to reduce steam consumption in the Fluid Coking process through improvements in the jet attrition process.

1.3 Review of Particle Attrition Studies in Fluidized Bed

1.3.1 Particle attrition in fluidized bed

Particle attrition in fluidized beds has been studied extensively. Particle attrition may be caused by many factors such as particle to particle and particle to bed wall interactions, due to the vigorous motion of the fluidized particles. The attrition rate needs to be monitored in the fluidized bed, because particle breakage could be desirable or unwanted depending on the fluidized bed application. For example, catalyst attrition is a concern in the development of new fluidized bed processes. The main consequence of catalyst attrition is the generation of fines, which may result in loss of valuable materials as the fines may escape through the dust recovery system (Reppenhagen and Werther, 1999). Attrition caused by gas bubbles, impacts in cyclones or gas jets issuing from the gas distributor have also been studied by many researchers (Lin et al, 1980; Arastoopour and Chen, 1983; Stein et al., 1998). Models for predicting the attrition rate induced by subsonic distributor gas jets, with maximum gas velocities that are typically well below 50 m/s, were also proposed by these researchers. Vaux and Keairns (1980) also proposed that particle attrition may be affected by the mechanical stress applied to the particles by

different regions of the fluidized bed. Patel et al. (1986) classified the numerous variables that affect attrition into two categories: particle properties and fluidized bed environment properties. Particle properties include size, shape, surface roughness and strength. Fluidized bed environment properties include excess fluidization velocity ($U-U_{mf}$), bed height, temperature and attrition pressure.

1.3.2 Modes of particle breakage

There are two main modes of particle breakage, which are abrasion and fragmentation (Pell, 1990; Xiao et al., 2011). During abrasion, a thin layer is removed from the particulate material due to shear and frictional forces inside the bed. This mode of particle attrition is associated with the production of fine particles and is characterized by marginal changes to the initial size distribution of the original particles. On the contrary, during fragmentation, particles break into similar sizes and substantial changes to the initial size of the original particles occur. Ray and Jiang (1987) also argued that the particle strength and breaking force supplied in a fluidized bed may determine the particle breakage modes. If the breaking force supplied increases, the breakage mechanism can change from abrasion to fragmentation. Fragmentation is a more desirable attrition mode in the Fluid Coking process, because too many fine particles will reduce fluidization quality and increase dust emissions (Dunlop et al., 1958).

1.3.3 Subsonic jet-induced attrition in fluidized beds

A number of studies on particle attrition with subsonic jets in fluidized beds have been performed (Pacek and Nienow, 1991; Ghadiri et al., 1994; Wu et al., 1999; Werther and Xi, 1993; Benthams et al., 2004; Boerefijn et al., 2000). Pacek and Nienow (1991) found that the efficiency of jet grinding depends on jet velocity and particle strength

primarily. Ghadiri et al. (1994) indicated that the attrition rate is proportional to the orifice velocity raised to a power 3. Werther and Xi (1993) proposed a model to consider the efficiency of the attrition process, by relating the surface energy created by the process to the kinetic energy spent on producing the surface area. The attrition rate was found to be proportional to the jet gas density, the orifice diameter and the jet exit velocity. It is presented in the following equation:

$$R_a = \rho_o d_o^2 u_o^3 \quad (1.1)$$

1.3.4 Supersonic jet-induced attrition in fluidized beds

Studies on jet induced particle attrition with high velocity gas jets in fluidized beds are limited. Tasirin and Geldart (1999) used straight tube nozzles at high velocity and found that the mean particle size decreased as the jet velocity increased. Moreover, they claimed that the grinding rate was a power law function of the free jet velocity.

In Fluid Coking, high velocity convergent-divergent Laval-type nozzles are used for particle attrition. The Laval-type nozzle is able to provide a supersonic velocity jet as the gas expands in the divergent section. When the high velocity jet is injected in the fluidized bed, fluidized particles near the nozzle are rapidly drawn into the path of the jet cavity and are accelerated to a high velocity. Then, they collide with each other and relatively slow moving dense phase bed particles near the jet tip and cause particle breakage (McMillan et al., 2007a).

Segraves (1958) first proposed a supersonic Laval-type nozzle used in combination with a draft tube for jet attrition in a Fluid Coker. Segraves (1958) claimed that this combination could improve attrition as the draft tube could enhance particle collisions with other particles and the draft tube wall. However, draft tube erosion is an

issue in this application. The high velocity nozzles were also found in studies of jet mill grinding (Mebtoul et al., 1996; Benz et al., 1996). In recent years, McMillan et al. (2007a), Cruz et al. (2010) and Li (2011) used Laval-type nozzles to study jet attrition in fluidized beds. McMillan et al. (2007a) studied the effect of operating conditions on jet attrition in a fluidized bed, such as attrition pressure, fluidization velocities, attrition gas properties and nozzle scale. They concluded that larger diameter nozzles operating at high flowrates, and using low density gases gave the highest grinding efficiencies. Cruz et al. (2010) studied the supersonic nozzle by relating thrust and equivalent velocity with grinding efficiency. They defined thrust as the reaction force created by the ejection of high velocity attrition gas from the supersonic nozzle. In order to maximize the thrust, Cruz et al. (2010) also studied the design of the supersonic nozzle and claimed that the divergent angle of the Laval-type nozzle needs to be optimized. That is because if the divergent angle is too large, shocks will develop and energy will be dissipated, while if it is too small, excessive friction will occur. They found that the optimum half angle of the divergent section should be between 3° and 8° . Li et al. (2011) studied particle attrition with a Laval-type nozzle in a fluidized bed at high temperature. They concluded that the grinding efficiency is positively affected by operation temperature, and also found that larger scale Laval-type nozzles with a high gas flowrate, operating at high attrition gas temperature with a low molar mass gas would produce the highest grinding efficiency.

1.3.5 Effect of fluidized bed hydrodynamics on jet attrition

Studies on the effect of fluidized bed hydrodynamics on jet attrition have not been found. Researchers have mainly studied the hydrodynamics of fluidized beds without attrition jets involved. For example, Olowson and Almstedt (1990) and Wiman and

Almstedt (1998) investigated the effect of excess gas velocities on the hydrodynamics of a fluidized bed, with silica sand particles with mean particle diameters of 0.45 mm and 0.7 mm respectively. The two studies showed similar hydrodynamics results in terms of mean bubble rise velocity, the mean bubble volume fraction and visible bubble flowrate. All of them were increased with excess gas velocity. Song et al. (2004) studied the hydrodynamics of Fluid Cokers in a pressurized, fully cylindrical cold model with similar reactor section geometrically and dynamically, by matching key dimensionless groups. They found that a denser annular region exists surrounding a more dilute core region. Song et al. (2006) further studied the hydrodynamics in the Fluid Coker using two kinds of solids (Fluidized cracking catalyst and fluid coke). Similar hydrodynamic behaviours were found, such as voidage distributions, differential pressure fluctuations and solids momentum flux distribution for both solids in their study. However, the effect of fluidized bed hydrodynamics on jet attrition has not been studied. This will be investigated in Chapter 3 of this work.

1.3.6 Methods of improving jet attrition

Numerous studies have been done on how to improve jet attrition in fluidized beds. Possible methods include placing a target plate downstream of the nozzle, installing a shroud near the nozzle tip, using two opposing jets instead of one jet and changing nozzle orientations. Dunlop et al. (1958) placed a target plate downstream of the attrition jet, which enhanced grinding by promoting particles and target collisions. Tasirin et al. (1999) studied the effect of separation distance between nozzle and target plate. They found that the grinding rate increased as the separation distance decreased. McMillan et al. (2007) also studied the separation distances of a nozzle and target plate. They found

that the grinding efficiency increased as the target moved away from the nozzle while remaining within reach of the jet, as the volume of particles entrained into the jet increased so that more particles were able to slam on the target. However, these researchers found that target plate erosion and unwanted fine particles generation were usually the drawbacks for this method.

Yates et al. (1991) studied particle attrition of opposing vertical jets in their overlap region and found that the discharge location of gases affect the attrition rate. When the gases from opposing jets were discharged close to the wall, they found it had a significant influence on attrition. Tasirin et al. (1999) compared the grinding rate of both horizontal and vertical opposing jets with that of a single jet. They found that two opposing horizontal nozzles gave only a slight increase in grinding when compared to a single horizontal jet. Tasirin et al. (1999) concluded that it is not advantageous to use two interacting opposing jets, as the region between them has a lower particle concentration, which lead to fewer particle-particle collisions.

Hulet et al. (2007) studied the effect of a shroud on solid entrainment into a gas jet. They found that the shroud helped the jet entrain more particles and less gas, as the attrition pressure, nozzle scale and attrition time were tested. More specifically, the bubbles approaching the nozzle tip were diverted by the shroud, thereby minimizing the attrition gas consumption for a given new surface area creation was compared. In order to effect of cross flow on the jet momentum. McMillan et al. (2007) further studied the effect of a shroud on jet attrition in a fluidized bed. They found that the attrition rate was improved as more particles were entrained into the jet, due to the increase in particle collisions near the tip of the jet.

The effect of nozzle angle on particle attrition was only studied by a few researchers. Werther and Xi (1993) studied the effect of gas jet orientation and found that

horizontal and upward jets achieved similar attrition rates. However, the attrition rate for a downward jet was significantly higher. Tuunila and Nystrom (1998) studied the effect of nozzle angle on particle attrition. They varied the angle of the nozzle in three levels, which were 23°, 33° and 43° and found the largest angle (43°) gave the highest grinding rate. Midoux et al. (1999) used three different jet mills with two nozzle angles (63° and 67°) and found that the nozzle angle affected the grinding ratio of the product. Moreover, most of the jet attrition studies were done with a straight tube nozzle. Therefore, the effect of nozzle angle on particle attrition with supersonic jet needs to be systematically studied, with a wide range of nozzle angles. This study will be revealed in Chapter 4.

1.4 Research Objectives

This work aims to improve jet attrition with supersonic attrition nozzles in gas-solid fluidized beds, and ultimately reduce steam consumption and increase overall reactor throughput in the Fluid Coking process.

The objective of the first study is to determine the best operating conditions of a supersonic Laval-type nozzle for attrition in a fluidized bed. Operating conditions such as attrition pressure, nozzle scale and attrition time were tested. More specifically, the attrition gas consumption for a given new surface area creation was compared, in order to determine which operating condition is most advisable. In order to maintain good fluidization in a Fluid Coker, the size distribution of the particles need to be within the desired range. Particle size distribution analysis was introduced to help determine the grinding of coarse particles, and monitor the generation of fine particles at different operating conditions.

1.6 References
 Arastoopour, H.; Chen, C. Attrition of char agglomerates. *Powder Technol* 1983, 16, 99.
 Ibrahim, A.; Swan, C.; Boerefijn, R.; Ghadiri, M.; Huchach-bai Jet milling of pharmaceutical powders. *Powder Technol* 2004, 141, 233-238.

The objective of the second study is to study the effect of fluidized bed operating parameters. *Int. J. Miner. Process.* 1996, 44-45, 507-519.

Boerefijn, R.; Gude, N. J.; Ghadiri, M. Review of attrition of fluid cracking catalyst a hydrodynamic condition that can help improve particle attrition. Two hydrodynamic zones were created by a specially designed fluidized bed. Experiments were conducted with a supersonic attrition jet either straddling both hydrodynamic zones, or completely enclosed within one hydrodynamic zone. *Chemical Engineering and Processing: Process Intensification* 2010, 49, 225-234.

Dunlop D., Griffin, L., Moser, J., Particle size control in fluid coking. 1958, 34, 39-41.

The objective of the third study is to investigate the effect of nozzle inclination for a supersonic nozzle in the attrition process. The aim is to determine the optimal nozzle inclination angle to give the highest grinding efficiency. A high velocity Laval-type nozzle was used and the nozzle was adjusted from 0° to 90°. Particle size analysis was also conducted to monitor the generation of fine particles, and the grinding of coarse particles. http://www.energy.alberta.ca/Org/pdf/Alberta_Energy_Overview.pdf, 2009, Government of Alberta. *Alberta Oil Sands Industry – Quarterly Update, summer 2011*, 2011.

Lin, L.; Sears, J. T.; Wen, C. Y. Elutriation and attrition of char from a large fluidized bed. *Particle attrition with supersonic nozzles in a high temperature fluidized bed*. Ph.D. dissertation. The University of Western Ontario, London, Canada, 2011.

1.5 Nomenclature

- d_o Orifice diameter (m) *Particle attrition with supersonic nozzles in a high temperature fluidized bed*. Ph.D. dissertation. The University of Western Ontario, London, Canada, 2011.
- R_a Jet attrition rate (kg/s) *Particle attrition with supersonic nozzles in a high temperature fluidized bed*. Ph.D. dissertation. The University of Western Ontario, London, Canada, 2011.
- u_o Jet velocity (m/s) *Particle attrition with supersonic nozzles in a high temperature fluidized bed*. Ph.D. dissertation. The University of Western Ontario, London, Canada, 2011.
- Greek letters**
- ρ_o Jet gas density (kg/m³) *Particle attrition with supersonic nozzles in a high temperature fluidized bed*. Ph.D. dissertation. The University of Western Ontario, London, Canada, 2011.

1.6 References

- Arastoopour, H.; Chen, C. Attrition of char agglomerates. *Powder Technol* 1983, 36, 99-106.
- Bentham, A., Kwan, C., Boerefijn, R., Ghadiri, M., Fluidised-bed jet milling of pharmaceutical powders. *Powder Technol* 2004, 141, 233-238.

- Benz, M.; Herold, H.; Ulfik, B. Performance of a fluidized bed jet mill as a function of operating parameters. *Int. J. Miner. Process.* **1996**, 44-45, 507-519.
- Boerefijn, R.; Gudde, N. J.; Ghadiri, M. Review of attrition of fluid cracking catalyst particles. *Advanced Powder Technology* **2000**, 11, 145-174.
- Cruz, N.; Briens, C.; Berruti, F. Supersonic attrition nozzles in gas-solid fluidized beds. *Chemical Engineering and Processing: Process Intensification* **2010**, 49, 225-234.
- Dunlop D., Griffin, L., Moser, J., Particle size control in fluid coking. **1958**, 54, 39-43.
- Ghadiri, M.; Cleaver, J. A. S.; Tuponogov, V. G.; Werther, J. Attrition of FCC powder in the jetting region of a fluidized bed. *Powder Technol* **1994**, 80, 175-178.
- Government of Alberta, *Alberta's Energy Industry (An Overview 2009)*; <<http://www.energy.alberta.ca/Org/pdfs/Alberta_Energy_Overview.pdf>>, **2009**.
- Government of Alberta, *Alberta Oil Sands Industry – Quarterly Update, summer 2011*; <<http://albertacanada.com/documents/AOSID_QuarterlyUpdate_Summer2011.pdf>>, **2011**.
- Li, F., Particle attrition with supersonic nozzles in a high temperature fluidized bed. Ph.D. dissertation. The University of Western Ontario, London, Canada. **2011**.
- Lin, L.; Sears, J. T.; Wen, C. Y. Elutriation and attrition of char from a large fluidized bed. *Powder Technol.* **1980**, 27.
- House, P. Interaction of gas-liquid jets with gas-solid fluidized beds: Effect on liquid-solid contact and impact on fluid coker operation. Ph.D. dissertation. The University of Western Ontario, London, Canada, **2007**.
- Hulet, C.; McMillan, J.; Briens, C.; Berruti, F.; Chan, E. W. Visualization of the effect of a shroud on entrainment of fluidized solids into a gas jet. *International Journal of Chemical Reactor Engineering* **2007**, 5.
- McMillan, J.; Briens, C.; Berruti, F.; Chan, E. High velocity attrition nozzles in fluidized beds. *Powder Technol* **2007a**, 175, 133-141.
- McMillan, J.; Briens, C.; Berruti, F.; Chan, E. Particle attrition mechanism with a sonic gas jet injected into a fluidized bed. *Chemical Engineering Science* **2007b**, 62, 3809-3820.
- McMillan, J.. Characterization of the interactions between high velocity jets and fluidized particles. Ph.D. dissertation, The University of Western Ontario, London, Canada. **2007**.

- Mebtoul, M.; Large, J. F.; Guigon, P. High velocity impact of particles on a target - An experimental study. *Int. J. Miner. Process.* **1996**, 44-45, 77-91.
- Midoux, N.; Hošek, P.; Pailleres, L.; Authelin, J. R. Micronization of pharmaceutical substances in a spiral jet mill. *Powder Technol* **1999**, 104, 113-120.
- Olowson, P. A.; Almstedt, A. E. Influence of pressure and fluidization velocity on the bubble behaviour and gas flow distribution in a fluidized bed. *Chemical Engineering Science* **1990**, 45, 1733-1741.
- Pacek, A. W.; Nienow, A. W. An application of jet grinding to fluidised bed granulation. *Powder Technol* **1991**, 65, 305-310.
- Patel, K.; Nienow, A. W.; Milne, I. P. Attrition of urea in a gas-fluidised bed. *Powder Technol* **1986**, 47, 257-261.
- Pell, M., In *Gas Fluidization; Handbook of Powder Technology*; Elsevier: Amsterdam, 1990; Vol. 8, pp 97.
- Ray, Y.; Jiang, T.; Wen, C. Y. PARTICLE ATTRITION PHENOMENA IN A FLUIDIZED BED. *Powder Technol* **1987**, 49, 193-206.
- Segraves, W., Supersonic jet grinding means and methods. *United States Patent*: 2 832 545, **1958**
- Stein, M.; Seville, J. P. K.; Parker, D. J. Attrition of porous glass particles in a fluidised bed. *Powder Technol.* **1998**, 100, 242-250.
- Song, X.; Bi, H.; Jim Lim, C.; Grace, J. R.; Chan, E.; Knapper, B.; McKnight, C. Hydrodynamics of the reactor section in fluid cokers. *Powder Technol* **2004**, 147, 126-136.
- Song, X.; Grace, J. R.; Bi, H.; Lim, C. J.; Chan, E.; Knapper, B.; McKnight, C. Experimental simulation of the reactor section of fluid cokers: Comparison of FCC and fluid coke particles. *Can. J. Chem. Eng.* **2006**, 84, 161-169.
- Syncrude Canada Ltd., <<<http://www.syncrude.ca/users/folder.asp>>>, **2011**
- Tasirin, S. M.; Geldart, D. Experimental investigation on fluidized bed jet grinding. *Powder Technol* **1999**, 105, 337-341.
- Tuunila, R.; Nyström, L. Technical note: Effects of grinding parameters on product fineness in jet mill grinding. *Minerals Eng* **1998**, 11, 1089-1094.
- Vaux, W. G.; Keairns, D. L. Particle Attrition in fluid-bed processes. *Journal of Technical Writing and Communication.* **1980**, 437-444.

Werther, J.; Xi, W. Jet attrition of catalyst particles in gas fluidized beds. *Powder Technol* **1993**, 76, 39-46.

Werther, J.; Reppenhagen, J. Catalyst attrition in fluidized-bed systems. *AIChE J.* **1999**, 45, 2001-2010.

Wiman, J.; Almstedt, A. E. Influence of pressure, fluidization velocity and particle size on the hydrodynamics of a freely bubbling fluidized bed. *Chemical Engineering Science* **1998**, 53, 2167-2176.

Wu, S.; Baeyens, J.; Chu, C. -. Effect of the grid-velocity on attrition in gas fluidized beds. *Can. J. Chem. Eng.* **1999**, 77, 738-744.

Xiao, G.; Grace, J. R.; Lim, C. J. Attrition characteristics and mechanisms for limestone particles in an air-jet apparatus. *Powder Technol* **2011**, 207, 183-191.

Yates, J. G.; Cobbinah, S. S.; Cheesman, D. J.; Jordan, S. P. In *In Particle attrition in fluidized beds containing opposing jets*; AIChE Symposium Series; 1991; Vol. 87, pp 13-19.

In Fluid Coking, solid coke that is produced as a reaction by-product deposits on the fluidized coke particles. This increases the particle size and, if unchecked, would lead to fluidization problems in the Fluid Coker. Therefore, steam is injected through high velocity attrition nozzles to attrit the coke particles and maintain their size within an optimum range, in order to maintain good fluidization in the Fluid Coker. Currently, a large quantity of steam is used by the Coker attrition nozzles. If the steam consumption of the attrition nozzles could be reduced, it would reduce sour water treatment and lead to a higher reactor throughput (Pougatch et al., 2010; McMillan et al., 2007a).

Particle attrition in fluidized beds had been studied extensively. The two main modes of particle attrition are abrasion and fragmentation (Pell, 1990; Xiao et al., 2011). During abrasion, a thin layer is removed from the particulate material due to shear and frictional forces inside the bed. This mode of particle attrition is associated with the production of fine particles and is characterized by marginal changes to the initial size distribution of the original particles. On the contrary, during fragmentation, particles

Chapter 2: Effect of Nozzle Operating Conditions on Jet Attrition

2.1 Introduction

Fluidized bed reactors are used extensively in many industrial applications due to attractive features such as good solids and gases mixing, and rapid heat and mass transfer. Fluid Coking is a process that utilizes these attractive properties. Fluid Coking is one application that is used for upgrading heavy oils, such as bitumen extracted from oil sands, with non-catalytic thermal cracking to produce lighter, synthetic crude oil. During this process, injected bitumen contacts with hot, fluidized coke particles that provide the heat required to start the coking reaction.

In Fluid Coking, solid coke that is produced as a reaction by-product deposits on the fluidized coke particles. This increases the particle size and, if unchecked, would lead to fluidization problems in the Fluid Coker. Therefore, steam is injected through high velocity attrition nozzles to attrit the coke particles and maintain their size within an optimum range, in order to maintain good fluidization in the Fluid Coker. Currently, a large quantity of steam is used by the Coker attrition nozzles. If the steam consumption of the attrition nozzles could be reduced, it would reduce sour water treatment and lead to a higher reactor throughout (Pougatch et al., 2010; McMillan et al., 2007a).

Particle attrition in fluidized beds had been studied extensively. The two main modes of particle attrition are abrasion and fragmentation (Pell, 1990; Xiao et al., 2011). During abrasion, a thin layer is removed from the particulate material due to shear and frictional forces inside the bed. This mode of particle attrition is associated with the production of fine particles and is characterized by marginal changes to the initial size distribution of the original particles. On the contrary, during fragmentation, particles

break into similar sizes and substantial changes to the initial size of the original particles occur. Fragmentation is a more desirable attrition mode in the Fluid Coking process, because too many fine particles will reduce fluidization quality and increase dust emissions (Dunlop et al., 1958). In addition, Forsythe and Hertwig (1949) discovered that fine particles may slow down particle breakage by providing an additional cushioning effect, requiring higher flowrates of attrition steam to maintain the optimum particle size in a Fluid Coker. Therefore, the generation of fine particles during the attrition process should be monitored and controlled during the Fluid Coking process.

Fluidized particles may undergo attrition when they interact with each other and the wall of the bed. Researchers have studied this type of attrition, which can be caused by gas bubbles, impacts in cyclones or gas jets issuing from the gas distributor convergent-divergent, Laval-type nozzle for the attrition process in a fluidized bed. They related grinding efficiency to thrust and equivalent velocity, and stated that there are certain design constraints for the nozzle, such as the divergence angle of the nozzle. This with maximum gas velocities that are typically well below 50 m/s, were also proposed by these researchers. Vaux and Keairns (1980) proposed that mechanical stress applied to the particles by different regions of the fluidized bed may also affect particle attrition. Patel et al. (1986) classified the numerous variables that affect attrition into two categories: particle properties and fluidized bed environment properties. Particle properties include size, shape, surface roughness and strength. Fluidized bed environment properties include excess fluidization velocity ($U-U_{mf}$), bed height, temperature and attrition pressure.

In the Fluid Coking process, sonic or supersonic velocity attrition nozzles are used to control the particle size distribution. Straight tube nozzles were used in most of the

previous particle attrition studies (McMillan et al., 2007a). Benz et al. (1996) used a nozzle with convergent-divergent geometry. This Laval type nozzle is able to provide supersonic velocities, and the grinding efficiency with this supersonic nozzle was studied by a group of researchers (McMillan et al., 2007a; Cruz et al., 2010; Li, 2011). McMillan et al. (2007a) defined a grinding efficiency to characterize the particle attrition, which was the amount of new surface area created per mass of attrition gas used:

$$\eta = \frac{\text{new particle surface created by attrition}}{\text{mass of required attrition gas}} = \frac{\text{m}^2/\text{s}}{\text{kg/s}} = \frac{\text{m}^2}{\text{kg}} \quad (2.1)$$

McMillan et al. (2007a) found that operating conditions such as nozzle geometry, nozzle scale, attrition pressure, fluidization velocities, particle properties and attrition gas properties may all affect the grinding efficiency. Cruz et al. (2010) further studied the convergent-divergent, Laval-type nozzle for the attrition process in a fluidized bed. They related grinding efficiency to thrust and equivalent velocity, and stated that there are certain design constraints for the nozzle, such as the divergence angle of the nozzle. This important design parameter needs to be optimized in order to produce the highest possible thrust that leads to higher nozzle exit and equivalent velocity. Cruz et al. (2010) had found that the optimum half angle for the divergent section of the nozzle should be maintained between 3° to 8°. Li et al. (2011) have also studied the effects of particle properties and fluidized bed operating conditions on particle attrition with supersonic nozzles. The effect of temperature on the grinding efficiency was also examined. The authors reported that a higher grinding efficiency can be obtained by increasing the fluidized bed temperature.

Mehtoul et al. (1996) stated that about only 2% of energy provided is used to create new surfaces in a jet grinding process. The jet attrition process in a Fluid Coker is

also energy consuming. If the energy consumed by the attrition nozzles is reduced in terms of steam usage, the same superficial gas velocity in the freeboard will be obtained with a higher injection rate of feedstock, leading to a higher production level for the Coker. Therefore, the objective of this study is to optimize the operating conditions of supersonic Laval type nozzles, in terms of maximizing the grinding efficiency to minimize the flowrate of attrition gas. In this paper, the attrition nozzle operating pressure, attrition time, and nozzle scale were tested in order to determine their effect on the grinding efficiency. Attrition gas consumptions were compared for same new surface area created. This will help in determining the optimal operating conditions in terms of attrition pressure, attrition time and nozzle size, so a minimum flowrate of attrition gas is used. Analysis of the particle size distribution was introduced in this study, to determine the mass of generated fines (with a diameter below 30 microns), as well as the mass of coarse particles (larger than 105 microns) that were ground.

2.2 Experimental Setup

Attrition experiments were conducted in a fluidized bed with a height of 3.2 m and a rectangular cross section of 1 m by 0.3 m as shown in Figure 2.1a and Figure 2.1b. The bed is equipped with two external cyclones in series, a primary cyclone that normally returns entrained material to the bed through a dipleg, and a secondary cyclone with a collection container. Compressed air is supplied to fluidize the unit and a set of sonic nozzles controls its flowrate with a pressure regulator. High pressure nitrogen gas is injected into the bed using high performance attrition nozzles to attrit the fluidized material.

The bed was initially filled with coke particles to a height of 0.75 m – 0.80 m to top the height of screw type sampling ports located at 0.12 and 0.56 m above the distributor plate, and was fluidized with air. Particles collected by the primary cyclone were fed back into the bed by a dipleg (0.54 m above the gas distributor) during the attrition process, but were diverted for collection during the elutriation process. Particles from the secondary cyclone were also collected at the end of each run to determine their mass and size distribution.

The attrition nozzle was arranged so that the attrition gas was injected horizontally into the bed. The nozzle was placed inside the bed at a height of 0.25 m above the gas distributor. The attrition gas was supplied from a high pressure nitrogen tank. The mass flow rates were determined from the pressure upstream of the nozzles, measured with a pressure transducer, using a prior calibration.

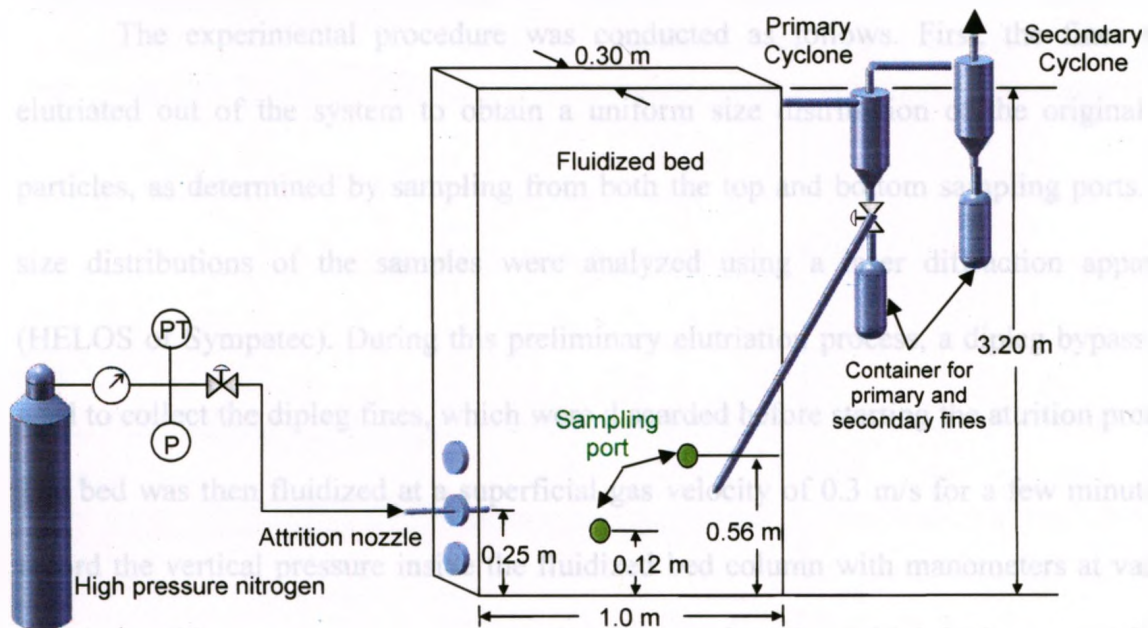


Figure 2.1a: Experimental Set-up



Figure 2.1b: Photographic view of the experimental set-up

The experimental procedure was conducted as follows. First, the fines were elutriated out of the system to obtain a uniform size distribution of the original bed particles, as determined by sampling from both the top and bottom sampling ports. The size distributions of the samples were analyzed using a laser diffraction apparatus (HELOS of Sympatec). During this preliminary elutriation process, a dipleg bypass was used to collect the dipleg fines, which were discarded before starting the attrition process. The bed was then fluidized at a superficial gas velocity of 0.3 m/s for a few minutes to record the vertical pressure inside the fluidized bed column with manometers at various locations; this measurement was used to determine the initial bed mass. All the experiments were conducted with this superficial gas velocity (0.3 m/s). The attrition process was then initiated using the attrition nozzle. During this process, the dipleg bypass was closed and particles collected by the primary cyclone were returned back to

the bed. At the end of the attrition process, the dipleg bypass was opened and the elutriation process was initiated. Bed samples were collected at the end of the elutriation process from both sampling ports. Samples collected from both cyclones and the sampling ports were then analysed for their particle size distribution. Although some

2.3 Results and Discussion

The objective was to achieve maximum grinding in terms of creating the largest new surface area while using a minimum amount of attrition gas for a predefined attrition time. The new surface area created was calculated from the difference between the sum of surface areas created from the final (after attrition) bed samples and the generated fines; and the surface area of the original bed sample. Surface areas created by attrition under different conditions are discussed in the following section.

In order to determine the effect of nozzle scale on the new surface area created, two attrition nozzles were tested. The nozzles used for the attrition experiments are convergent-divergent, Laval-type nozzles with 2.4 mm and 2.8 mm nozzle throat diameter as shown in Figures 2.2 and 2.3 respectively.

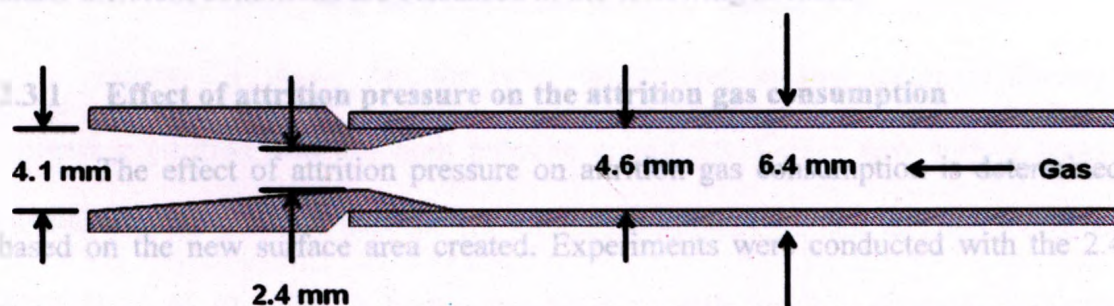


Figure 2.2: Laval type nozzle, $D_{th} = 2.4$ mm

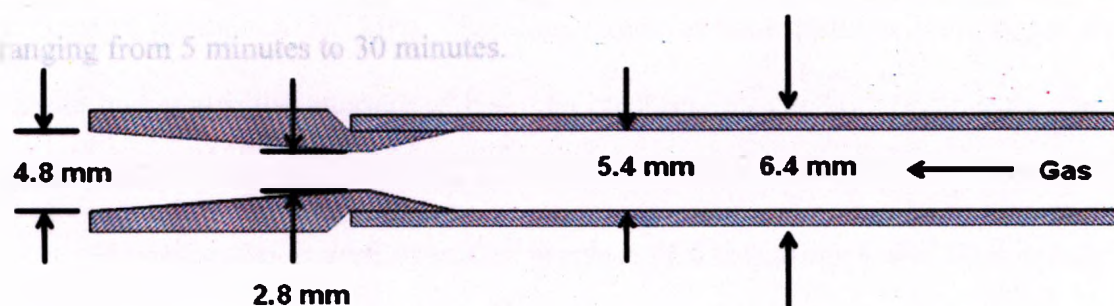


Figure 2.3: Laval type nozzle, $D_{th} = 2.8$ mm

Two attrition pressures (pressure upstream of the attrition nozzle), 1.5 MPa and 2.2 MPa were tested in order to determine the effect of attrition pressure on the new

surface area created. Attrition times ranging from 5 minutes to 30 minutes were adopted for the above studies. Results obtained were then compared to determine the optimal operating conditions for the traditional supersonic nozzles.

2.3 Results and Discussion

The objective was to achieve maximum grinding in terms of creating the largest new surface area while using a minimum amount of attrition gas for a predefined attrition time. The new surface area created was calculated from the difference between the sum of surface areas created from the final (after attrition) bed samples and the generated fines; and the surface area of the original bed sample. Surface areas created by attrition under different conditions are discussed in the following section.

2.3.1 Effect of attrition pressure on the attrition gas consumption

The effect of attrition pressure on attrition gas consumption is determined first based on the new surface area created. Experiments were conducted with the 2.4 mm Laval type nozzle. Two attrition pressures, 1.5 MPa and 2.2 MPa were tested in order to obtain results with different attrition gas flowrates. Several attrition times were tested ranging from 5 minutes to 30 minutes.

However, the desired operating pressure of this 2.4 mm Laval type nozzle is the pressure that uses minimum attrition gas. The attrition nozzles were all calibrated prior to an experiment at different attrition pressures, which gave the attrition mass flowrate at a specific attrition pressure. Figure 2.5 shows a plot of new surface area created versus mass of attrition gas. It shows that for 30 minutes of attrition at 1.5 MPa, the amount of

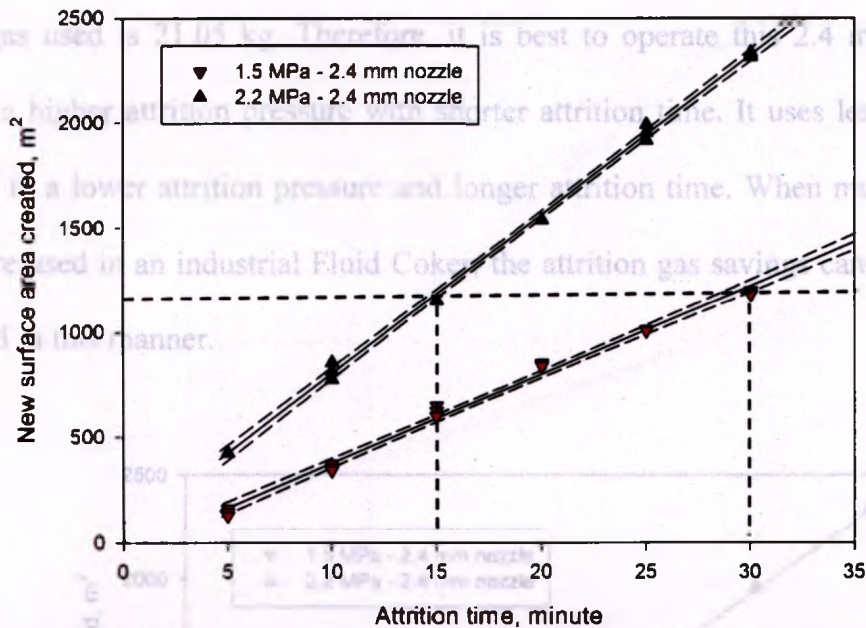


Figure 2.4: Effect of attrition pressure on new surface area created with 2.4 mm Laval-type nozzle (Dash lines show 95% confidence interval)

Figure 2.4 shows that the new surface area created increases linearly with increasing attrition time for both pressure conditions. Larger new surface areas were created with the 2.2 MPa than the 1.5 MPa attrition pressure. One can easily compare the times required to create a given new surface, with the two attrition pressures. For example, 30 minutes of attrition at 1.5 MPa can create the same new surface area as 15 minutes of attrition at 2.2 MPa. Therefore, lower attrition pressure with longer attrition time or higher attrition pressure with shorter attrition time can both produce the same new surface area.

However, the desired operating pressure of this 2.4 mm Laval type nozzle is the pressure that uses minimum attrition gas. The attrition nozzles were all calibrated prior to an experiment at different attrition pressures, which gave the attrition mass flowrate at a specific attrition pressure. Figure 2.5 shows a plot of new surface area created versus mass of attrition gas. It shows that for 30 minutes of attrition at 1.5 MPa, the amount of

attrition gas used is 30.02 kg. For 15 minutes of attrition at 2.2 MPa, the amount of attrition gas used is 21.05 kg. Therefore, it is best to operate this 2.4 mm Laval type nozzle at a higher attrition pressure with shorter attrition time. It uses less attrition gas compared to a lower attrition pressure and longer attrition time. When multiple attrition nozzles are used in an industrial Fluid Coker, the attrition gas savings can be substantial if operated in this manner.

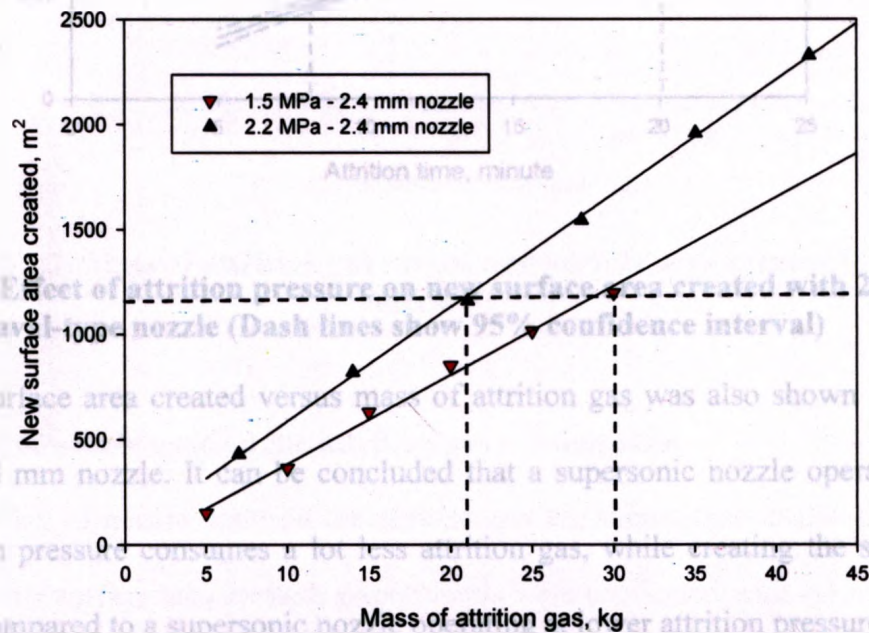


Figure 2.5 Mass of attrition gas versus new surface area created for 2.4 mm nozzle

Figure 2.6 shows a similar plot of the new surface area created versus the attrition time with a 2.8 mm Laval type nozzle at pressures of 1.5 MPa and 2.2 MPa. The same general trends can be observed as in Figure 2.4. The new surface area created increases as the attrition time progresses. Higher pressure gives a larger new surface area creation as well.

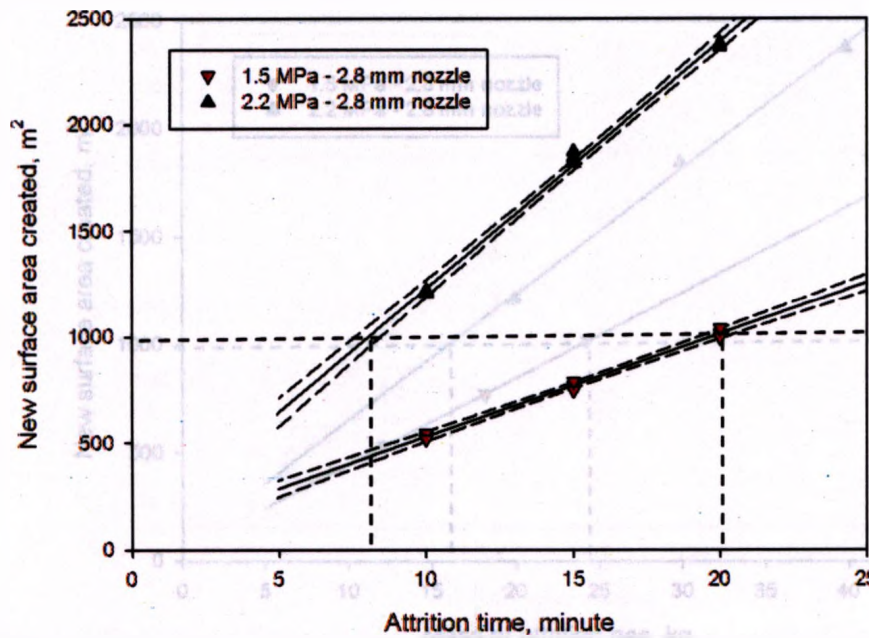


Figure 2.6: Effect of attrition pressure on new surface area created with 2.8 mm Laval-type nozzle (Dash lines show 95% confidence interval)

New surface area created versus mass of attrition gas was also shown in Figure 2.7 for the 2.8 mm nozzle. It can be concluded that a supersonic nozzle operating at a higher attrition pressure consumes a lot less attrition gas, while creating the same new surface area. The effect of nozzle scale on the attrition gas consumption was also determined based on the new surface area created. Experiments were conducted with 2.4 mm and 2.8 mm Laval type nozzles at attrition pressures of 1.5 MPa and 2.2 MPa. The attrition time ranged from 5 minutes to 30 minutes. Figure 2.8 shows a plot of attrition time versus the new surface area created for the 2.4 mm and 2.8 mm Laval type nozzles at 1.5 MPa.

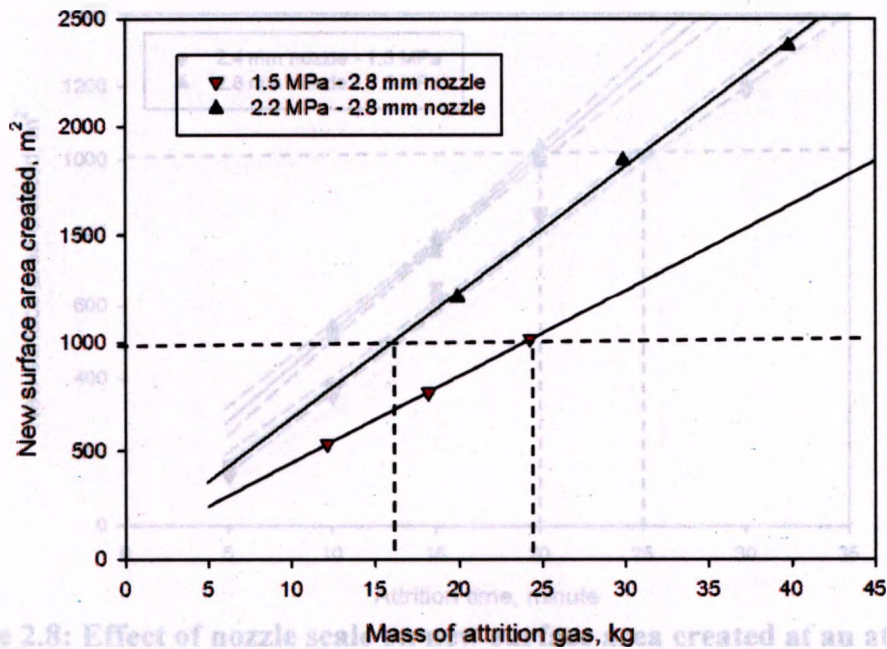


Figure 2.8: Effect of nozzle scale on the attrition gas consumption at an attrition pressure of 1.5 MPa (Dash lines show 95% confidence interval)

Figure 2.7: Mass of attrition gas versus new surface area created for 2.8 mm nozzle

2.3.2 Effect of nozzle scale on the attrition gas consumption

The effect of nozzle scale on the attrition gas consumption was also determined based on the new surface area created. Experiments were conducted with 2.4 mm and 2.8 mm Laval type nozzles at attrition pressures of 1.5 MPa and 2.2 MPa. The attrition time ranged from 5 minutes to 30 minutes. Figure 2.8 shows a plot of attrition time versus the new surface area created for the 2.4 mm and 2.8 mm Laval type nozzles at 1.5 MPa.

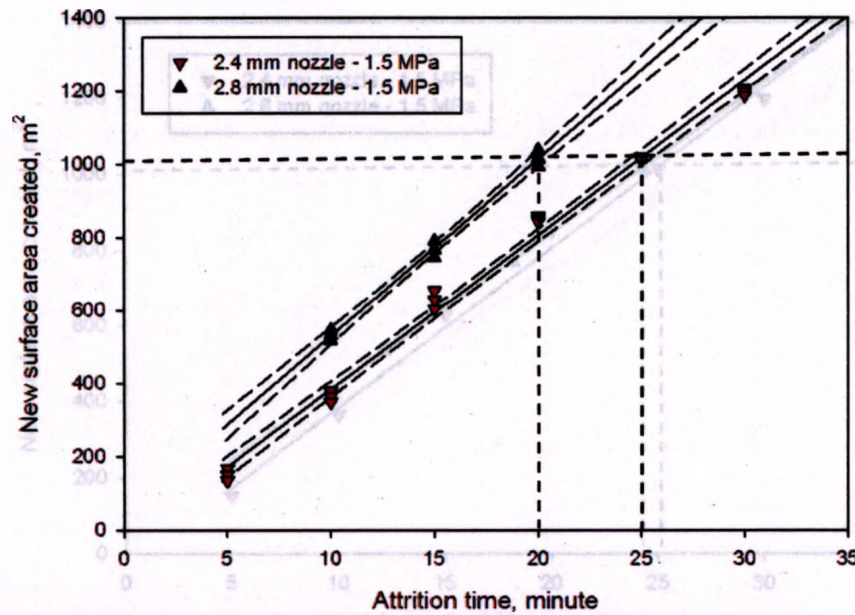


Figure 2.8: Effect of nozzle scale on new surface area created at an attrition pressure of 1.5 MPa (Dash lines show 95% confidence interval)

Figure 2.8 shows that the new surface area created increases linearly as the attrition time increases for both nozzle sizes. Larger surface areas were created with a larger nozzle than a smaller nozzle. However, the larger nozzle consumes more attrition gas. Therefore, it is only fair to judge which nozzle is better in term of attrition gas consumption when the same new surface area created is considered. Figure 2.9 shows the new surface area created versus the mass of attrition gas for the two nozzles at 1.5 MPa.

Figure 2.10 shows a plot of attrition time versus new surface area created for the 2.4 mm and 2.8 mm Laval type nozzle at 2.2 MPa.

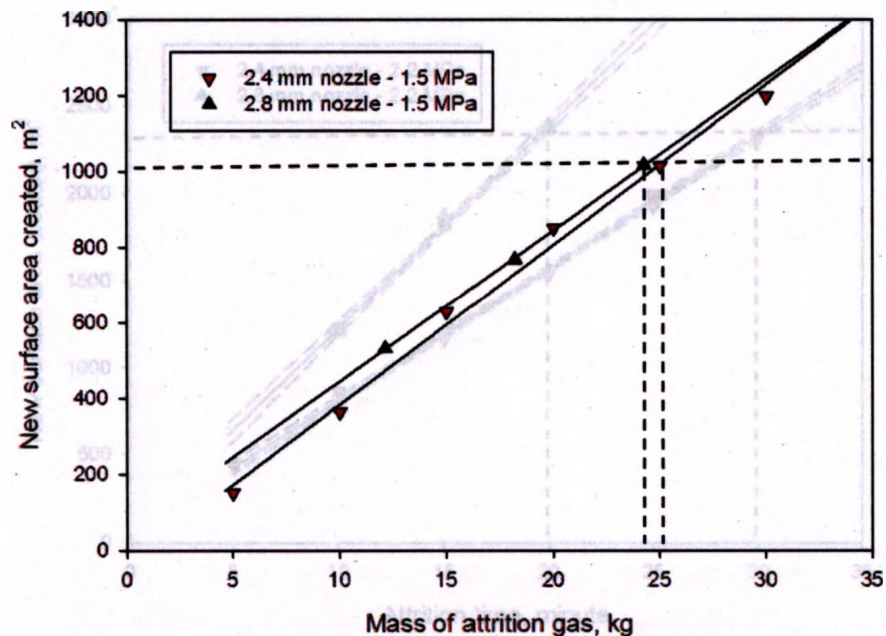


Figure 2.9: New surface area created versus mass of attrition gas at 1.5 MPa

It can be concluded that the larger nozzle uses slightly less attrition gas to generate the same new surface area compared to the smaller nozzle. Although the saving on attrition gas is not significant in this plot, it is mainly because of the low attrition pressure used in this case for the two nozzles. In the next section, same attrition nozzles were operated at a higher attrition pressure (2.2 MPa) for further investigation of the effect of the nozzle scale on attrition gas consumption.

Figure 2.10 shows a plot of attrition time versus new surface area created for the 2.4 mm and 2.8 mm Laval type nozzle at 2.2 MPa.

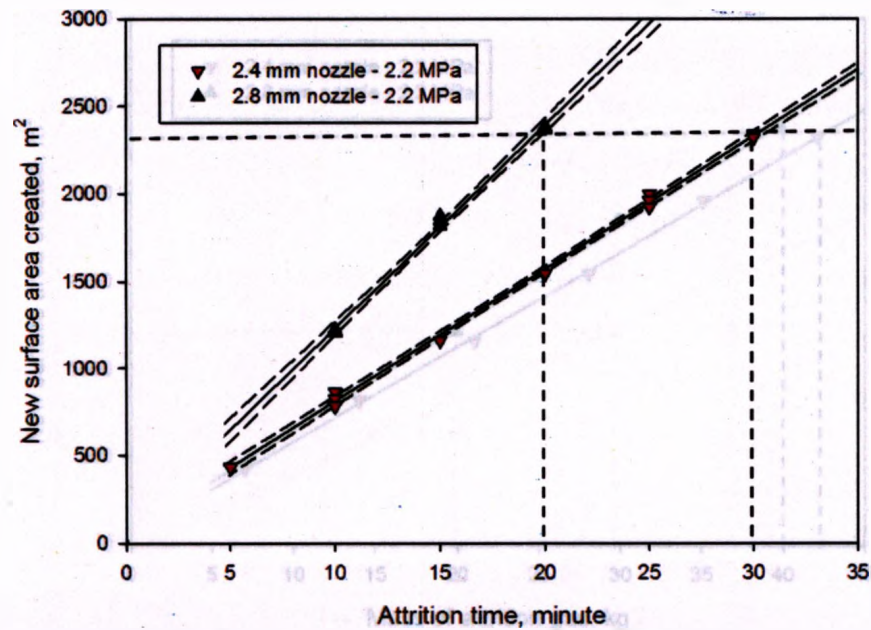


Figure 2.10: Effect of nozzle scale on new surface area created at an attrition pressure of 2.2 MPa (Dash lines show 95% confidence interval)

2.3.3 Effect of attrition pressure and nozzle scale combined on attrition gas consumption
The same conclusion can be drawn as before; new surface area created increases linearly with the attrition time for both nozzle sizes. Larger surface areas were also

created by the bigger nozzle than the smaller nozzle.

Figure 2.12 shows a plot of new surface area created versus attrition gas consumption for a 2.8 mm Laval nozzle operating at 2.2 MPa, compared to a 2.4 mm

The new surface area created versus the attrition gas consumption for the two Laval nozzle operating at 1.5 MPa. The attrition gas used for a given surface area with nozzles at 2.2 MPa is shown in Figure 2.11. It shows that the bigger nozzle consumes less attrition gas than the smaller nozzle for a given new surface area. It is important to emphasize that the saving on attrition gas will be more substantial when a larger number of attrition nozzles are used in an industrial Fluid Coker.

This combination will save the most attrition gas while creating the same new surface area compared to a small nozzle operating at low attrition pressure.

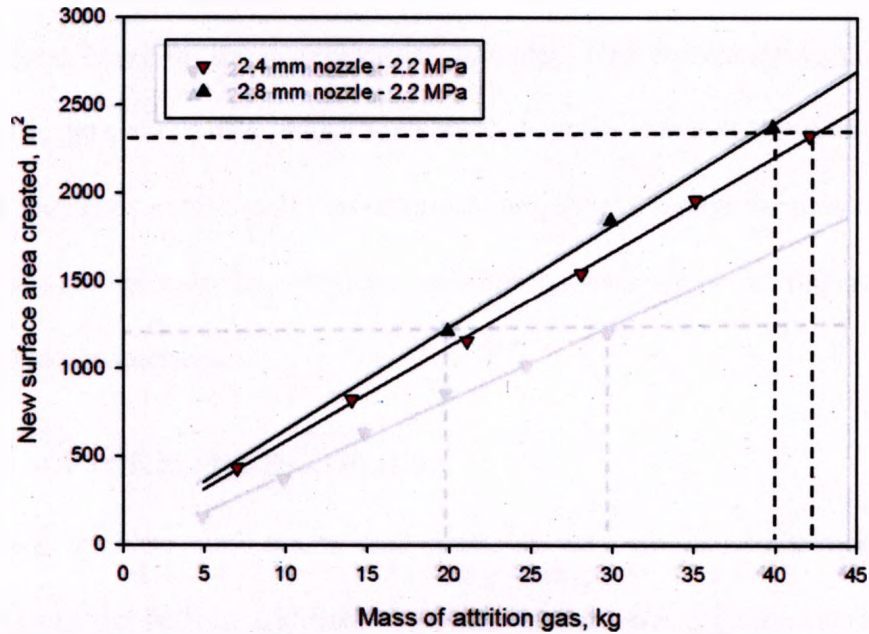


Figure 2.11: New surface area created versus mass of attrition gas at 2.2 MPa

2.3.3 Effect of attrition pressure and nozzle scale combined on attrition gas consumption

Figure 2.12 shows a plot of new surface area created versus attrition gas consumption for a 2.8 mm Laval nozzle operating at 2.2 MPa, compared to a 2.4 mm Laval nozzle operating at 1.5 MPa. The attrition gas used for a given surface area with the two nozzles at their respective pressures can be determined from this plot. From the analysis of the effect of attrition pressure and nozzle scale on attrition gas consumption, it can be concluded that it is best to operate a bigger supersonic Laval type nozzle at higher pressure. This combination will save the most attrition gas while creating the same new surface area compared to a small nozzle operating at low attrition pressure.

$$\frac{L_m}{D_e} = 5.52 \left[\frac{\rho_e U_e^2}{(\rho_p - \rho_e) g D_e} \right]^{0.37} \quad (2.2)$$

where ρ_e is the density at the nozzle exit and it can be found through the density at the

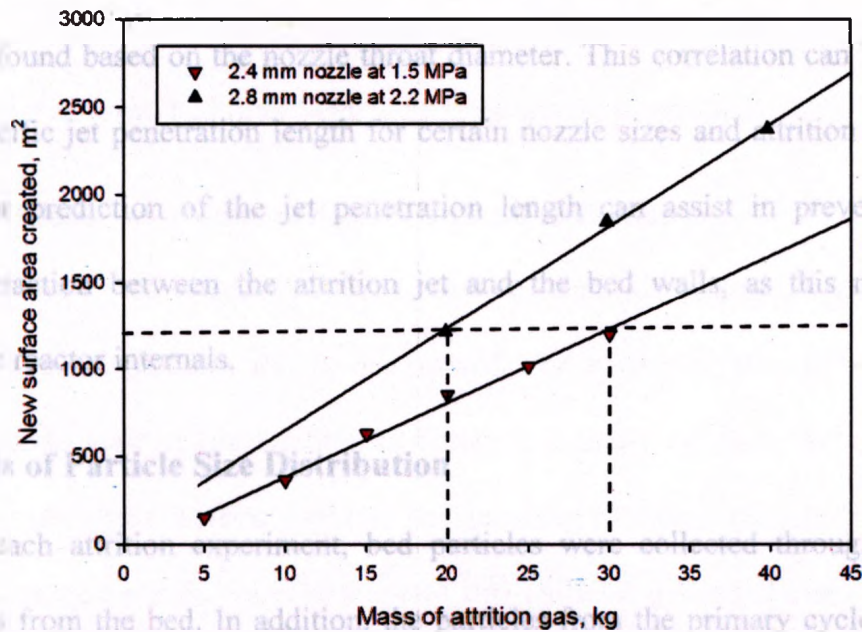


Figure 2.12: New surface area created versus mass of attrition gas

Although it might be more beneficial to operate large supersonic nozzles at higher attrition pressure, a limitation to how far this approach can be applied exists. Dawe et al. (2008) studied the jet penetration length of horizontal supersonic jets in a fluidized bed. They found that a bigger nozzle and higher pressure lead to higher gas density and higher gas mass flowrate of the jet. Both of these two factors increase the jet penetration length. Therefore, the width of the fluidized bed (or the diameter of the Fluid Coker) needs to be considered when selecting the nozzle size and operating pressure, in order to prevent the jet tip hitting the bed wall and causing erosion.

Benjelloun et al. (1995) developed an empirical correlation to predict the jet penetration length from a horizontal gas jet in a fluidized bed as shown in Equation 2.2:

$$\frac{L_{jet}}{D_e} = 5.52 \left[\frac{\rho_e U_e^2}{(\rho_p - \rho_e) g D_e} \right]^{0.27} \quad (2.2)$$

where ρ_e is the density at the nozzle exit and it can be found through the density at the

nozzle throat based on the attrition pressure used. D_e is the diameter at the nozzle exit, which can be found based on the nozzle throat diameter. This correlation can be used to obtain the specific jet penetration length for certain nozzle sizes and attrition pressures. Hence, a prior prediction of the jet penetration length can assist in preventing any undesired interaction between the attrition jet and the bed walls, as this may cause damages to the reactor internals.

2.4 Analysis of Particle Size Distribution

After each attrition experiment, bed particles were collected through the two sampling ports from the bed. In addition, the particles from the primary cyclone dipleg and the secondary cyclone dipleg were collected and weighed. Then, the particle size distributions were measured for the bed particles and cyclones catch by the laser diffraction sensor HELOS of Sympatec apparatus. The results were then combined to obtain the average size distribution of the particle mix after attrition, including all the ground particles and the particles that had not yet been ground. The results were reported with three size cuts: 0-30 μm (fines particles), 30-105 μm and particles greater than 105 μm (coarse particles). The 30 μm size cut was selected because there were no particles smaller than 30 μm in the bed before attrition and all particles smaller than 30 μm were, therefore, the result of attrition. Similarly, the 105 μm size cut was selected because there were no particles larger than 105 μm in the elutriated fines.

In the Fluid Coking process, supersonic attrition nozzles are used to control the size of coke particles, in order to maintain good fluidization of the coke particles. However, too many fine particles created by attrition would cause poor fluidization in the reactor as fine particles tend to agglomerate; it would also result in increased dust

emission from the burner. Therefore, the generation of fine particles should be monitored and kept as low as possible during the attrition process. From the particle size distribution analysis, the mass of unwanted fines being generated should be checked.

2.4.1 Effect of attrition pressure on particle size distribution

In this section, the effect of attrition pressure on the generation of fine particles and grinding of coarse particles will be determined. The same analysis will be done for the effect of nozzle scale in later section. In Figure 2.13 and 2.14, the effect of attrition pressure on the generation of fine particles and grinding of coarse particles for the 2.4 mm Laval type nozzle are shown. The mass of fine particles generated and grinding of coarse particles increases as the attrition time increases. Furthermore, higher attrition pressure created more fine particles and ground more coarse particles.

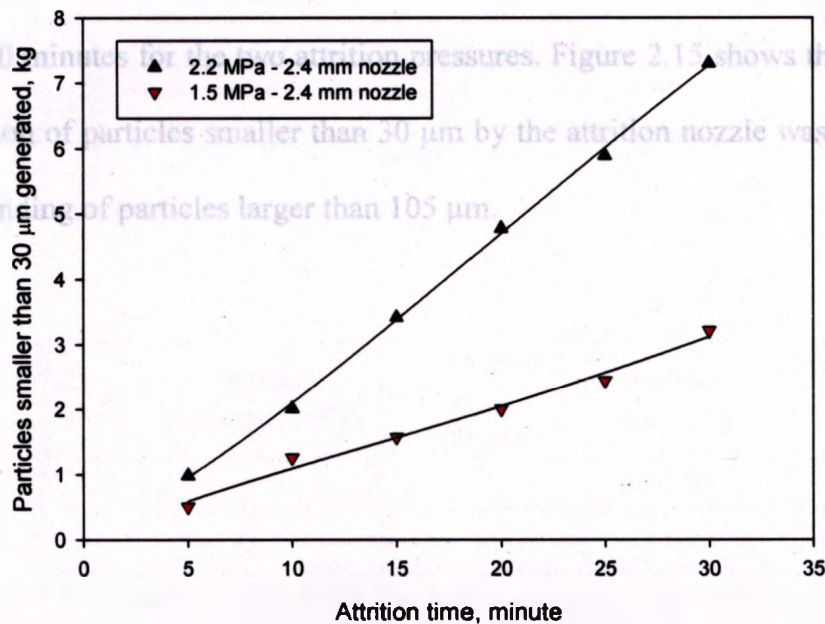


Figure 2.13: Effect of attrition pressure on the generation of fine particles – 2.4 mm Laval-type nozzle

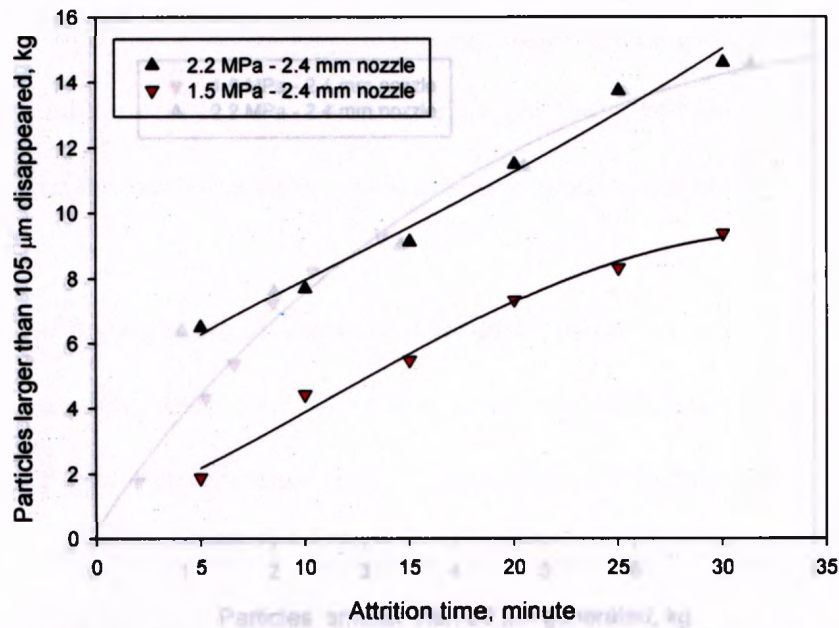


Figure 2.14: Effect of attrition pressure on the grinding of coarse particles – 2.4 mm Laval-type nozzle

However, the generation of fine particles for a given new surface area needs to be checked. Figure 2.15 shows a plot of the particles larger than 105 µm ground versus the particles smaller than 30 µm generated for the 2.4 mm nozzle. The attrition time ranged from 5 to 30 minutes for the two attrition pressures. Figure 2.15 shows that, as expected, the generation of particles smaller than 30 µm by the attrition nozzle was well correlated with the grinding of particles larger than 105 µm.

New surface area created (m ²)	Attrition pressure (MPa)	Attrition time (minute)	Attrition mass (kg)	Mass of fines generated (kg)
1170	1.5	30	30.02	3.21
	2.2	15	21.05	3.42

Table 2.1: Generation of fines for a given new surface area created by the 2.4 mm nozzle

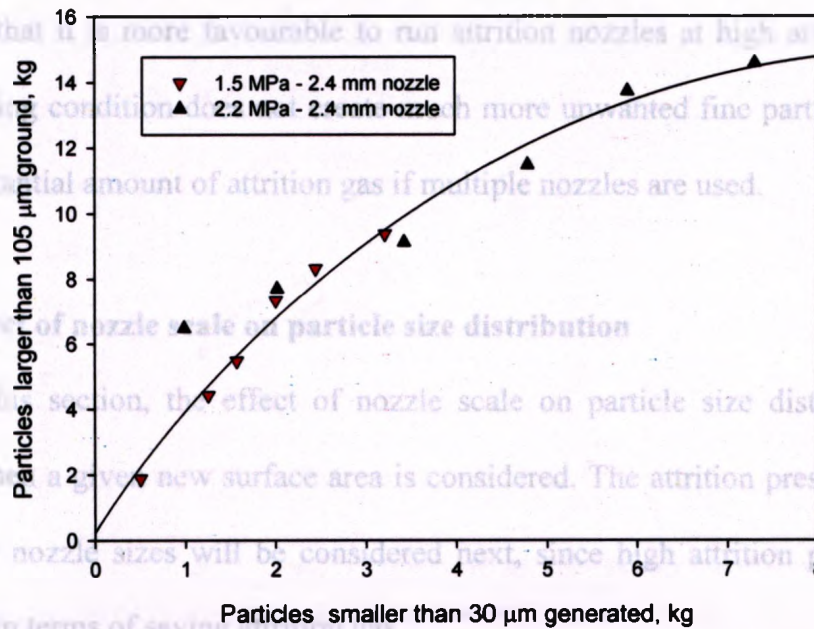


Figure 2.15: Relationship between the generation of fines smaller than 30 µm and the grinding of particles larger than 105 µm

However, the generation of fine particles for a given new surface area needs to be checked for the two attrition pressures. This will help to determine if running attrition nozzle at a high attrition pressure is truly beneficial. The same example used in section 2.3.1 with the mass of fine particles is summarized in Table 2.1. From the table, it shows that the two attrition pressures generate roughly the same amount of fine particles for a given new surface area.

New surface area created (m ²)	Attrition pressure (MPa)	Attrition time (minute)	Attrition mass (kg)	Mass of fines generated (kg)
1170	1.5	30	30.02	3.21
	2.2	15	21.05	3.42

Table 2.1: Generation of fines for a given new surface area created by the 2.4 mm nozzle

Therefore, it can be concluded from the particle size analysis and the above discussion that it is more favourable to run attrition nozzles at high attrition pressures. This operating condition does not create much more unwanted fine particles, but it does save a substantial amount of attrition gas if multiple nozzles are used.

2.4.2 Effect of nozzle scale on particle size distribution

In this section, the effect of nozzle scale on particle size distribution will be revealed when a given new surface area is considered. The attrition pressure at 2.2 MPa for the two nozzle sizes will be considered next, since high attrition pressure is more favourable in terms of saving attrition gas.

Figure 2.16 and 2.17 show that the generation of fine particles and coarse particles ground increases with the attrition time for both nozzles. The larger nozzle also created more fine particles and ground more coarse particles.

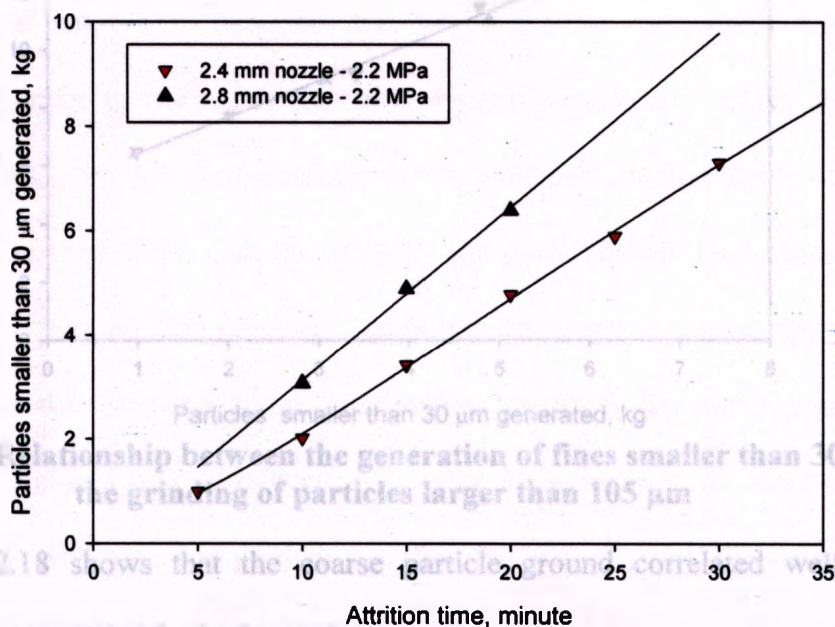


Figure 2.16: Effect of nozzle scale on the generation of fine particles

In section 2.3.2, the effect of nozzle scale on attrition gas consumption was thoroughly discussed. It was shown that the larger attrition nozzle uses less attrition gas for the same surface area created. However, it is also necessary to monitor the mass of fines generated to ensure stable reactor operation. Table 2.2 summarized the results obtained from before; it also shows the mass of fine particles generated for the two cases.

New surface area created (m ²)	Nozzle size (mm)	Attrition time (minute)	Attrition mass (kg)	Mass of fines generated (kg)
23.0	2.4	30	42.09	7.30
23.0	2.8	20	39.80	6.40

Table 2.2: Generation of fines for a given new surface area created by the two nozzles at 2.2 MPa

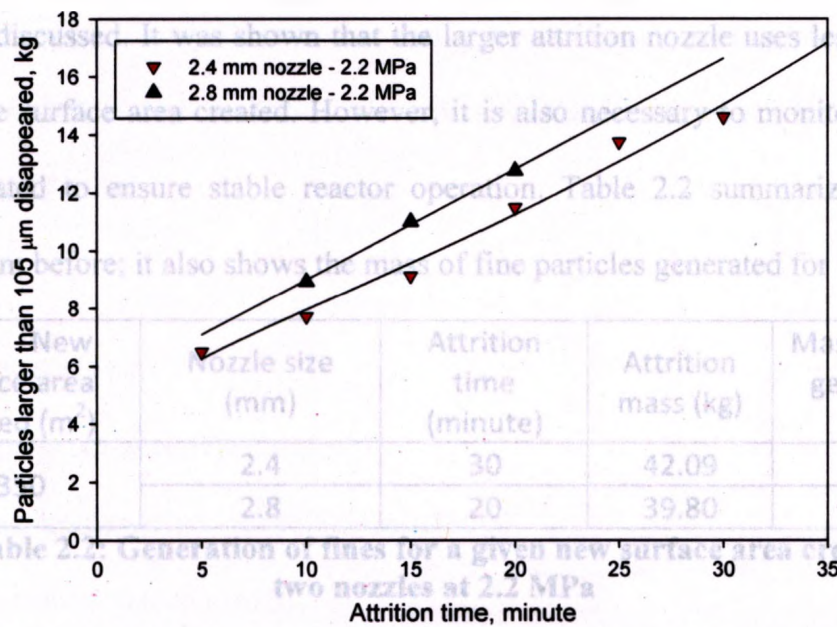


Figure 2.17: Effect of nozzle scale on the grinding of coarse particles

attrition gas for a given surface area creation compared to the smaller attrition nozzle, but, also generates less unwanted fine particles.

2.5 Conclusion

Supersonic convergent-divergent, Laval-type nozzles were used in a gas-solid fluidized bed in order to determine the best operating conditions during the attrition process in a Fluid Coker. Attrition pressure, nozzle scale and attrition time were tested in order to determine their effects on the attrition gas consumption. Experimental results have shown that higher attrition pressures and bigger attrition nozzles are more effective. They can generate the same new surface area while consuming less attrition gas. Particle size distribution analysis of the fines generated by the two nozzles showed that the 2.8 mm nozzle generated roughly the same amount of unwanted fine particles while consuming less attrition gas.

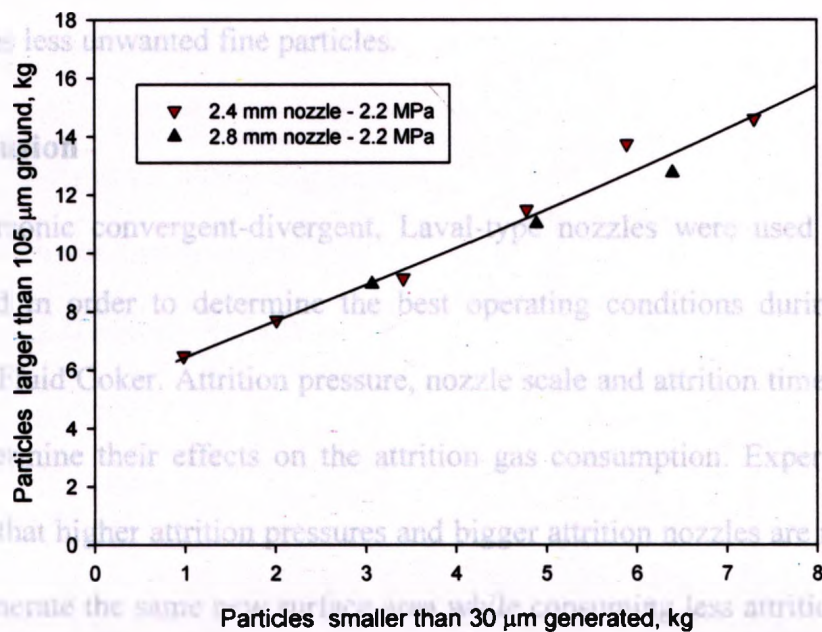


Figure 2.18: Relationship between the generation of fines smaller than 30 μm and the grinding of particles larger than 105 μm

Figure 2.18 shows that the coarse particle ground correlated well with the generation of fine particles for both nozzles.

generated roughly the same amount of unwanted fine particles while consuming less

In section 2.3.2, the effect of nozzle scale on attrition gas consumption was thoroughly discussed. It was shown that the larger attrition nozzle uses less attrition gas for the same surface area created. However, it is also necessary to monitor the mass of fines generated to ensure stable reactor operation. Table 2.2 summarized the results obtained from before; it also shows the mass of fine particles generated for the two cases.

New surface area created (m ²)	Nozzle size (mm)	Attrition time (minute)	Attrition mass (kg)	Mass of fines generated (kg)
2350	2.4	30	42.09	7.30
	2.8	20	39.80	6.40

Table 2.2: Generation of fines for a given new surface area created by the two nozzles at 2.2 MPa

Therefore, it can be concluded that larger attrition nozzle not only uses less attrition gas for a given surface area creation compared to the smaller attrition nozzle, but also generates less unwanted fine particles.

2.5 Conclusion

Supersonic convergent-divergent, Laval-type nozzles were used in a gas-solid fluidized bed in order to determine the best operating conditions during the attrition process in a Fluid Coker. Attrition pressure, nozzle scale and attrition time were tested in order to determine their effects on the attrition gas consumption. Experimental results have shown that higher attrition pressures and bigger attrition nozzles are more effective. They can generate the same new surface area while consuming less attrition gas. Particle size distribution analysis was introduced to monitor the generation of fine particles and grinding of coarse particles. The particle size distribution analysis further confirmed the benefit of using higher attrition pressures and bigger attrition nozzles. It showed that they generated roughly the same amount of unwanted fine particles while consuming less

attrition gas compared to the case where lower attrition pressures and smaller attrition jets into atmospheric fluidized bed. *Proc. Fluidization-VIII*, J-F. Large and C. nozzles are used. The only limitation is that potential erosion of fluidized bed internals should be avoided, as higher attrition pressures and larger attrition nozzles resulted in jets that penetrated further.

Dunlop D., Griffin, L., Moser, J., Particle size control in fluid coking. 1958, 34, 39-43.

Dawe, M.; Briens, C.; Berruti, F., Study of horizontal sonic gas jets in gas-solid fluidized beds. *Can. J. Chem. Eng.* 2008, 86, 506-513.

2.6 Nomenclature

Foraythe, W., Hertwig, W. Attrition characteristics of fluid cracking catalysts. *Ind. Eng. De* Diameter at the nozzle exit (m)

L_{jet} Jet penetration depth of attrition nozzle (m)
dissertation, The University of Western Ontario, London, Canada, 2011.

U Fluidization velocity (m/s)

Lin, L.; Sears, J. T.; Wen, C. Y. Elutriation and attrition of char from a large fluidized be Gas velocity at the nozzle exit (m/s)

U_{mf} Minimum fluidization velocity (m/s)
beds. *Powder Technol.* 2007a, 173, 133-141.

McMillan, J.; Briens, C.; Berruti, F.; Char, E. Particle attrition mechanism with a sonic Greek letters
injected into a fluidized bed. *Chemical Engineering Science*, 2007b, 62, 33-45.

ρ_e Gas density at the nozzle exit (kg/m^3)

ρ_p Bed particles density (kg/m^3)
High velocity impact of particles on a target - An experimental study. *Int. J. Miner. Process.* 1996, 44-45, 77-91.

η Grinding efficiency (m^2/kg)

Patel, K.; Nienow, A. W.; Milne, J. P. Attrition of urea in a gas-fluidised bed. *Powder Technol* 1986, 47, 237-251.

Bell, M., In *Gas Fluidization: Handbook of Powder Technology*; Elsevier: Amsterdam, 1997; pp 97.

2.7 References

Pouyatch, K.; Salcudean, M.; McMillan, J. Simulation of particle attrition by supersonic Arastoopour, H.; Chen, C. Attrition of char agglomerates. *Powder Technol* 1983, 36, 99-106.

Stein, M.; Seville, J. P. K.; Parker, D. J. Attrition of porous glass particles in a fluidised Benz, M.; Herold, H.; Ulfik, B. Performance of a fluidized bed jet mill as a function of operating parameters. *Int. J. Miner. Process.* 1996, 44-45, 507-519.

Vaux, W. G.; Kearns, D. L. Particle Attrition in fluid-bed processes. *Journal of Technical Writing and Communication*, 1980, 437-444.

- Benjelloun, F., Vanderschuren, J., and Liegeois, R., Penetration length of horizontal gas jets into atmospheric fluidized bed. *Proc. Fluidization-VIII*, J-F. Large and C. Laguerie Eds., Engineering Foundation, N.Y., **1995**, 239-246.
- Xiao, Q.; Grace, J. R.; Lim, C. J. Attrition characteristics and mechanisms for limestone. Cruz, N.; Briens, C.; Berruti, F. Supersonic attrition nozzles in gas-solid fluidized beds. *Chemical Engineering and Processing: Process Intensification* **2010**, 49, 225-234.
- Dunlop D., Griffin, L., Moser, J., Particle size control in fluid coking. **1958**, 54, 39-43.
- Dawe, M.; Briens, C.; Berruti, F. Study of horizontal sonic gas jets in gas-solid fluidized beds. *Can. J. Chem. Eng.* **2008**, 86, 506-513.
- Forsythe, W., Hertwig, W. Attrition characteristics of fluid cracking catalysts. *Ind. Eng. Chem* **1949**, 41, 1200-1206.
- Li, F., Particle attrition with supersonic nozzles in a high temperature fluidized bed. Ph.D. dissertation, The University of Western Ontario, London, Canada. **2011**.
- Lin, L.; Sears, J. T.; Wen, C. Y. Elutriation and attrition of char from a large fluidized bed. *Powder Technol.* **1980**, 27.
- McMillan, J.; Briens, C.; Berruti, F.; Chan, E. High velocity attrition nozzles in fluidized beds. *Powder Technol.* **2007a**, 175, 133-141.
- McMillan, J.; Briens, C.; Berruti, F.; Chan, E. Particle attrition mechanism with a sonic gas jet injected into a fluidized bed. *Chemical Engineering Science*, **2007b**, 62, 3809-3820.
- Mebtoul, M.; Large, J. F.; Guigon, P. High velocity impact of particles on a target - An experimental study. *Int. J. Miner. Process.* **1996**, 44-45, 77-91.
- Patel, K.; Nienow, A. W.; Milne, I. P. Attrition of urea in a gas-fluidised bed. *Powder Technol* **1986**, 47, 257-261.
- Pell, M., In *Gas Fluidization; Handbook of Powder Technology*; Elsevier: Amsterdam, 1990; Vol. 8, pp 97.
- Pougatch, K.; Salcudean, M.; McMillan, J. Simulation of particle attrition by supersonic gas jets in fluidized beds. *Chemical Engineering Science*. **2010**, 65, 4829-4843.
- Stein, M.; Seville, J. P. K.; Parker, D. J. Attrition of porous glass particles in a fluidised bed. *Powder Technol.* **1998**, 100, 242-250.
- Vaux, W. G.; Keairns, D. L. Particle Attrition in fluid-bed processes. *Journal of Technical Writing and Communication*. **1980**, 437-444.

Werther, J.; Reppenhagen, J. Catalyst attrition in fluidized-bed systems. *AIChE J.* **1999**, *45*, 2001-2010.

Xiao, G.; Grace, J. R.; Lim, C. J. Attrition characteristics and mechanisms for limestone particles in an air-jet apparatus. *Powder Technol* **2011**, *207*, 183-191.

Fluid Coking is a non-catalytic thermal conversion process that is used to upgrade bitumen extracted from oil sands in order to produce synthetic crude oil. The thermal cracking process is initiated in a fluidized bed where injected bitumen contacts hot coke particles. During this process, solid coke that is produced as reaction by-product deposits on the surface of fluidized coke particles, which become larger. Furthermore, coke particles stick together and form agglomerates due to poor feed distribution (McMillan et al., 2007a). If the bed particles become too large, slugging and poor circulation ensue. On the other hand, too many fine particles will reduce fluidization quality and increase dust emissions (Dunlop et al., 1958). Therefore, it is very important to keep the coke particle size within an optimum range (Li, 2011).

Steam is injected through supersonic attrition nozzles in the reactor section of the Fluid Coker, to attrit the coke particles and maintain the desired particle size distribution. Bed particles are entrained and accelerated by the high velocity gas jets; these particles collide with slow moving bed particles near the tip of the jet cavity, causing particle breakage (McMillan et al., 2007b). If the steam consumption of the attrition nozzles could be reduced, it would reduce the energy consumption and increase the reactor throughput.

Particle attrition with subsonic jets has been studied extensively in the past (Pacek and Nienow, 1991; Wu et al., 1999; Werther and Xu, 1993; Benthum et al., 2004; Boerefijn et al., 2000). Pacek and Nienow (1991) found that the efficiency of jet grinding depends primarily on the jet velocity and the particles strength. Fluidization velocity also

Chapter 3: Effect of Fluidized Bed Hydrodynamics on Jet Attrition

3.1 Introduction

Fluid Coking is a non-catalytic thermal conversion process that is used to upgrade bitumen extracted from oil sands in order to produce synthetic crude oil. The thermal cracking process is initiated in a fluidized bed, where injected bitumen contacts hot coke particles. During this process, solid coke that is produced as reaction by-product deposits on the surface of fluidized coke particles, which become larger. Furthermore, coke particles stick together and form agglomerates due to poor feed distribution (McMillan et al., 2007a). If the bed particles become too large, slugging and poor circulation ensue. On the other hand, too many fine particles will reduce fluidization quality and increase dust emissions (Dunlop et al., 1958). Therefore, it is very important to keep the coke particle size within an optimum range (Li, 2011).

Steam is injected through supersonic attrition nozzles in the reactor section of the Fluid Coker, to attrit the coke particles and maintain the desired particle size distribution. Bed particles are entrained and accelerated by the high velocity gas jets; these particles collide with slow moving bed particles near the tip of the jet cavity, causing particle breakage (McMillan et al., 2007a). If the steam consumption of the attrition nozzles could be reduced, it would reduce the energy consumption and increase the reactor throughput.

Particle attrition with subsonic jets has been studied extensively in the past (Pacek and Nienow, 1991; Wu et al., 1999; Werther and Xi, 1993; Bentham et al., 2004; Boerefijin et al., 2000). Pacek and Nienow (1991) found that the efficiency of jet grinding depends primarily on the jet velocity and the particles strength. Fluidization velocity also

had some effect on the efficiency of jet grinding, but to a lesser extent. Werther and Xi (1993) studied the grid jet attrition both theoretically and experimentally. They proposed a model which considered the efficiency of the attrition process by relating the surface energy created by the process to the kinetic energy which was spent to produce the surface area. The attrition rate was found to be proportional to the jet gas density, the orifice diameter and the jet exit velocity. It is presented in the following equation:

$$R_a = \rho_o d_o^2 u_o^3 \quad (3.1)$$

The effect of jet orientation was also studied by Werther and Xi (1993). They found that horizontal and upward jets achieve the same attrition rate, but the downward jet outperform the other two cases significantly. Bentham et al. (2004) mentioned that particle breakage is a result of particle-particle collisions in a more recent study. They found that the breakage mechanism involves the entrainment of particles into the subsonic jet cavity. Particles were entrained from the dense phase region and accelerated by the high velocity jets into the dilute jet cavity, where particles collide with each other and impact on the dense phase region above the jet.

McMillan et al. (2007a) mentioned that only a few researchers had studied high velocity attrition jets in fluidized beds (Dunlop et al., 1958; Forsythe and Hertwig, 1949; Tasirin and Geldart, 1999). All of their studies were conducted with straight tube nozzles. Tasirin and Geldart (1999) had found that the mean size of particles decreased as the jet velocity increased. Furthermore, they found that the rate of grinding was a power law function of the free jet velocity.

Mebtoul et al. (1996) and Benz et al. (1996) used convergent-divergent Laval-type nozzles in their studies on grinding in a jet mill. In a Laval-type nozzle, the fluid

reaches sonic velocity at the throat, and supersonic conditions are obtained as the gas jet expands fully in the divergent section of the nozzle (Smith, 1996). McMillan et al. (2007a) also used Laval-type nozzles to study the attrition process in fluidized beds. They examined the attrition process through the effect of different operating conditions and found that larger diameter nozzles operating at high flowrates, and using low density gases gave the highest grinding efficiencies. Cruz et al. (2010) further studied supersonic attrition nozzles in a fluidized bed by relating thrust and equivalent velocity with grinding efficiency. They defined thrust as the reaction force created by the ejection of high velocity attrition gas from the supersonic nozzle. Cruz et al. (2010) also claimed that the divergent angle of the nozzle needs to be optimized in order to achieve the highest thrust and grinding efficiency: if the divergent angle is too large, shocks will develop and energy will be dissipated, while if it is too small, excessive friction will occur. They found that the optimum half angle of the divergent section should be between 3° and 8° .

3.3 Experimental Setup

Li et al. (2011) studied particle attrition with a Laval-type nozzle in a fluidized bed at high temperature. They concluded that the grinding efficiency is positively affected by a rectangular cross section of 1 m by 0.3 m as shown in Figure 3.1. The wind-box operation temperature, and also found that larger scale Laval-type nozzles with a high gas flowrate, operating at high attrition gas temperature with a low molar mass gas would fluidized at different velocities (there was no physical separation within the bed). The produce the highest grinding efficiency.

Effect of fluidized bed hydrodynamics on the jet attrition process with supersonic nozzles. The bed was initially filled with coke particles to a height of 0.75 m – 0.80 m to top the height of the screw type sampling ports, and was fluidized with air. Screw and Wiman and Almstedt (1998) investigated the effect of excess gas velocities on the hydrodynamics of a fluidized bed with silica sand particles with mean particle diameters of 0.45 mm and 0.7 mm, respectively. They found similar hydrodynamic results for the particles were separated from the gas using two external cyclones in series. Most of the

two different particle sizes. For example, the mean bubble rise velocity, the mean bubble volume fraction and the visible bubble flow rate were found to increase with excess gas velocity. Song et al. (2004) studied the hydrodynamics of Fluid Cokers in a pressurized, fully cylindrical cold model with a similar reactor section geometrically and dynamically, by matching key dimensionless groups. They discovered a relatively dense annular region and a dilute core region through the investigation of voidage distributions and solids flow structure.

The objective of this study is to investigate the effect of fluid bed hydrodynamics on the jet attrition process. A specially designed fluidized bed was used to create two hydrodynamic zones, where the superficial gas velocity could be independently adjusted. Tests were conducted with a supersonic attrition jet either straddling both hydrodynamic zones, or completely enclosed within one hydrodynamic zone.

3.2 Experimental Setup

Attrition experiments were conducted in a fluidized bed with a height of 3.2 m and a rectangular cross section of 1 m by 0.3 m as shown in Figure 3.1. The wind-box was partitioned into two halves, so that the bed could be split into two zones that could be fluidized at different velocities (there was no physical separation within the bed). The fluidization velocity to each zone was controlled with a pressure regulator and a bank of sonic nozzles. The bed was initially filled with coke particles to a height of 0.75 m – 0.80 m to top the height of the screw type sampling ports, and was fluidized with air. Screw type sampling ports were located at two positions (shown in Figure 3.1) under the bed height, to take representative bed samples while the bed is fluidized. The entrained particles were separated from the gas using two external cyclones in series. Most of the

entrained particles were collected by the primary cyclone and normally returned to the bed through a dipleg during the attrition process, but were diverted for collection during the elutriation process. The secondary cyclone is equipped with a collection container; particles collected at the end of each run were weighed and analyzed. Although some small amount of the fines were lost in the exhaust air, their impact on the final results were negligible.

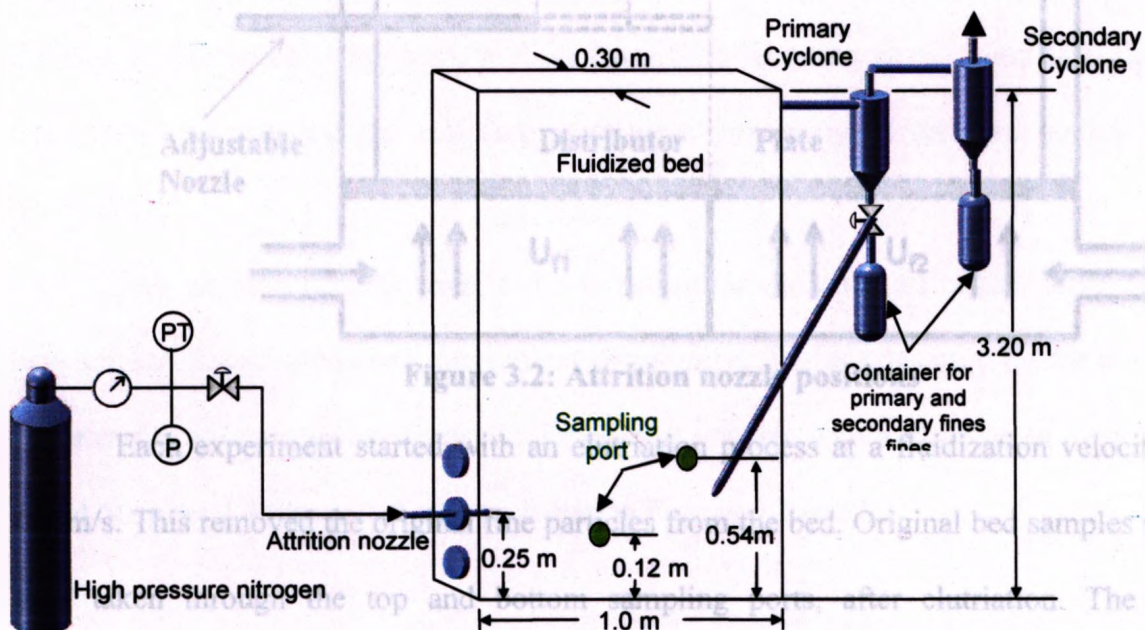


Figure 3.1: Experimental Set-up

The attrition nozzle was arranged for horizontal injection of the attrition gas into the bed. The nozzle was placed inside the bed at a height of 0.25 m above the gas distributor. The attrition gas was supplied from a high pressure nitrogen tank. The mass flow rates were determined from the pressure upstream of the nozzles, measured with a pressure transducer, using a prior calibration (because there was sonic flow through the nozzles, its gas flowrate was independent of downstream pressure). In order to check if

nozzle insertion depth may affect attrition, three nozzle penetrations were selected and shown in Figure 3.2.

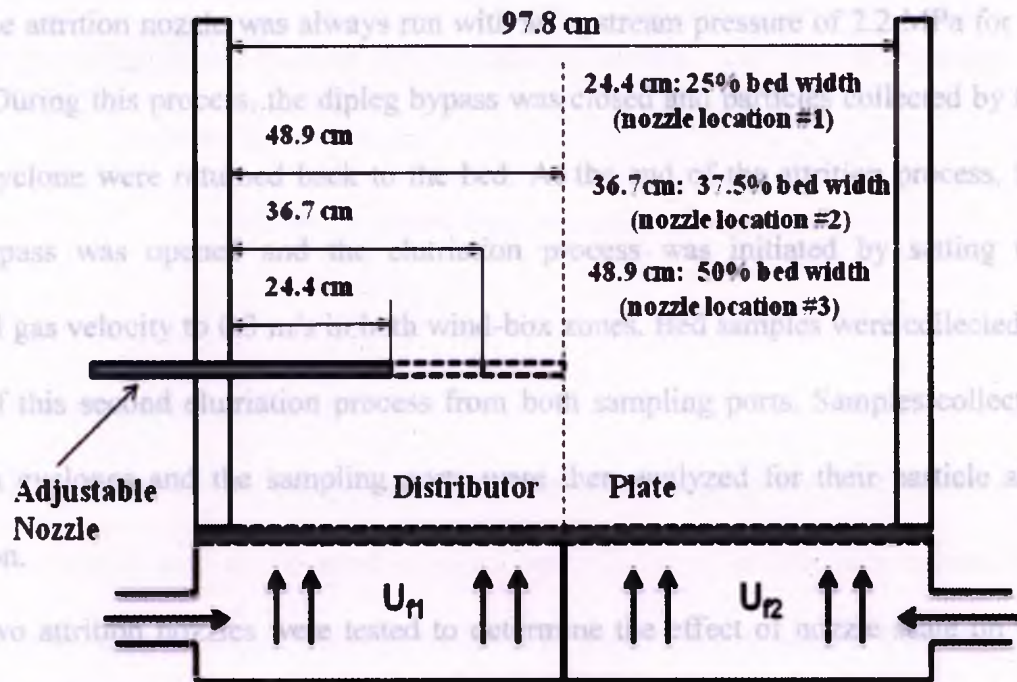


Figure 3.2: Attrition nozzle positions

Each experiment started with an elutriation process at a fluidization velocity of 0.3 m/s. This removed the original fine particles from the bed. Original bed samples were then taken through the top and bottom sampling ports, after elutriation. The size distributions of the samples were obtained with a laser diffraction apparatus (HELOS of Sympatec). During the preliminary elutriation, a dipleg bypass was used to collect the dipleg fines, which were discarded before starting the attrition process. In addition, the fluidized bed vertical pressure profile was recorded with manometers at various locations to determine the initial bed mass.

In order to study the effect of uneven gas distribution, specific superficial gas velocities were set in the two wind-box zones. The average fluidization velocity was

maintained at 0.3 m/s so that the total fluidization gas mass flowrate was kept constant for all the experiments.

The attrition nozzle was always run with an upstream pressure of 2.2 MPa for 20 minutes. During this process, the dipleg bypass was closed and particles collected by the primary cyclone were returned back to the bed. At the end of the attrition process, the dipleg bypass was opened and the elutriation process was initiated by setting the superficial gas velocity to 0.3 m/s in both wind-box zones. Bed samples were collected at the end of this second elutriation process from both sampling ports. Samples collected from both cyclones and the sampling ports were then analyzed for their particle size distribution.

Two attrition nozzles were tested to determine the effect of nozzle scale on the new surface area created under uneven gas distribution. The nozzles used for the attrition experiments are convergent-divergent, Laval-type nozzles with a diameter at the nozzle throat of either 2.4 mm or 2.8 mm, as shown in Figures 3.3 and 3.4.

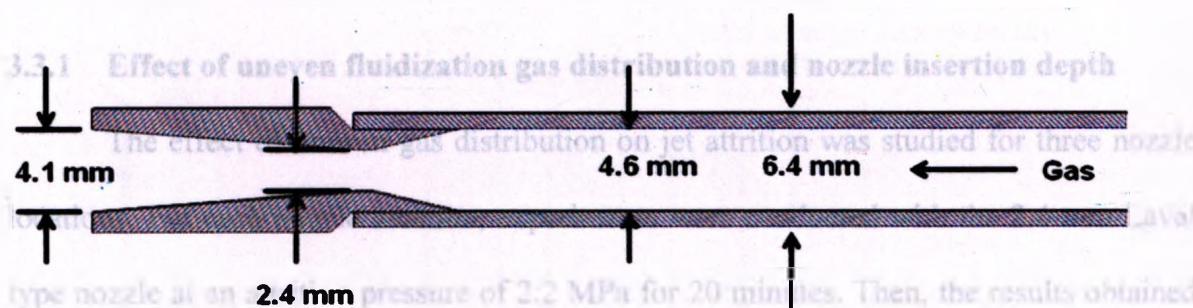


Figure 3.3: Laval type nozzle, $D_{th} = 2.4$ mm

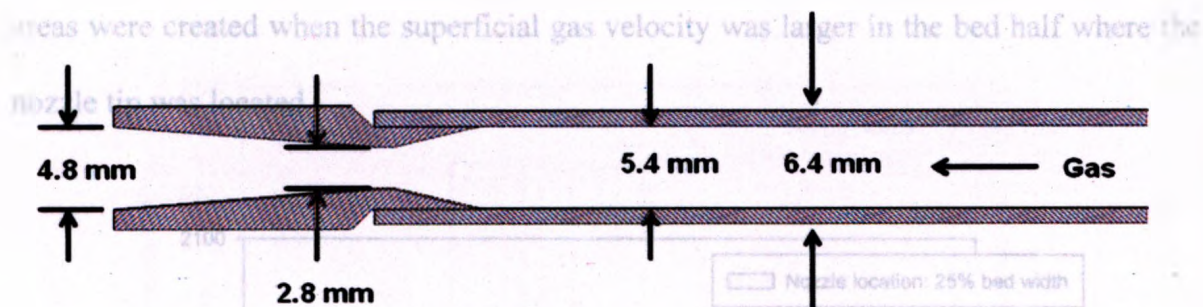


Figure 3.4: Laval type nozzle, $D_{th} = 2.8$ mm

3.3 Results and Discussion

The objective in this study was to maximize grinding in terms of creating the largest new surface area in the same attrition time. The new surface area created was calculated from the difference between the sum of surface areas created from the final (after attrition) bed samples and the generated fines; and the surface area of the original penetration at 25% bed width (the first velocity is the fluidization velocity in the bed). Surface areas created by attrition under different conditions are discussed in the following section.

3.3.1 Effect of uneven fluidization gas distribution and nozzle insertion depth

The effect of uneven gas distribution on jet attrition was studied for three nozzle locations. For each nozzle location, experiments were conducted with the 2.4 mm Laval type nozzle at an attrition pressure of 2.2 MPa for 20 minutes. Then, the results obtained for each nozzle location were compared with each other to determine the effect of nozzle insertion depth.

Figures 3.5 to 3.7 show the new surface area created versus the uneven fluidization velocities for three nozzle locations. The plots show that larger new surface area

Figure 3.6: New surface area created versus uneven fluidization velocities – Nozzle penetration at 37.5% bed width (the first velocity is the fluidization velocity in the bed half nearer the nozzle port).

areas were created when the superficial gas velocity was larger in the bed half where the nozzle tip was located.

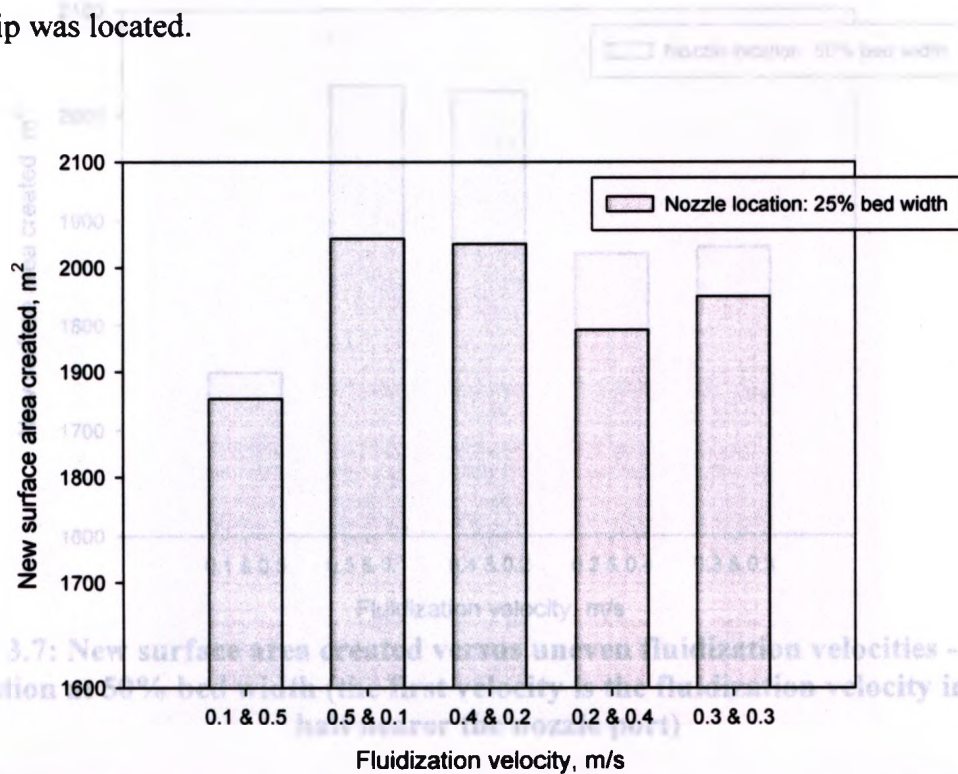


Figure 3.5: New surface area created versus uneven fluidization velocities -- Nozzle penetration at 25% bed width (the first velocity is the fluidization velocity in the bed half nearer the nozzle port)

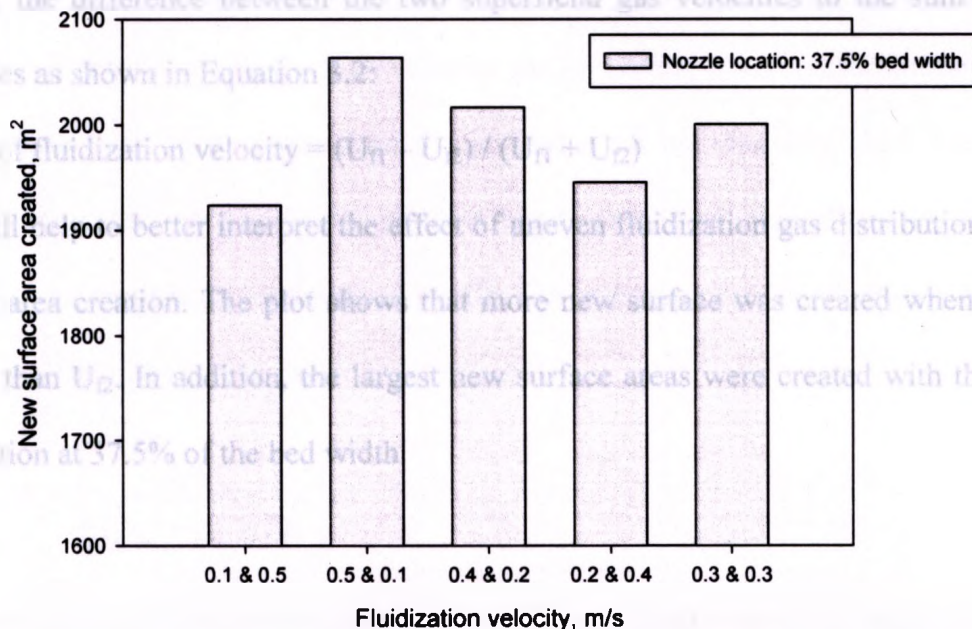


Figure 3.6: New surface area created versus uneven fluidization velocities -- Nozzle penetration at 37.5% bed width (the first velocity is the fluidization velocity in the bed half nearer the nozzle port)

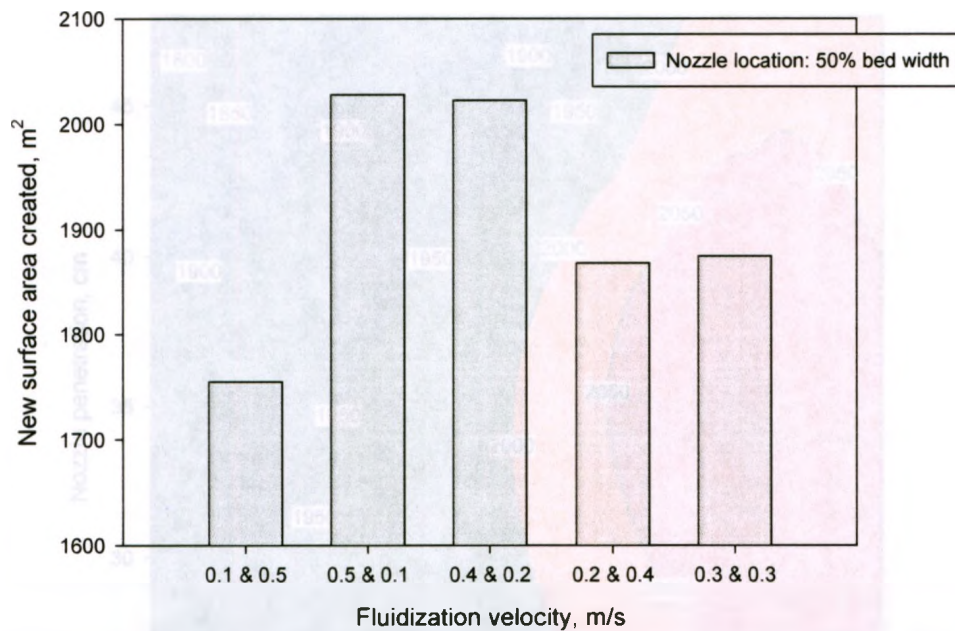


Figure 3.7: New surface area created versus uneven fluidization velocities -- Nozzle penetration at 50% bed width (the first velocity is the fluidization velocity in the bed half nearer the nozzle port)

Figure 3.8 summarizes the new surface area created versus uneven fluidization velocities for all three nozzle locations. The ratio of fluidization velocity is defined as the ratio of the difference between the two superficial gas velocities to the sum of these velocities as shown in Equation 3.2:

$$\text{Ratio of fluidization velocity} = (U_{f1} - U_{f2}) / (U_{f1} + U_{f2}) \quad (3.2)$$

This will help to better interpret the effect of uneven fluidization gas distribution on new surface area creation. The plot shows that more new surface was created when U_{f1} was greater than U_{f2} . In addition, the largest new surface areas were created with the nozzle penetration at 37.5% of the bed width.

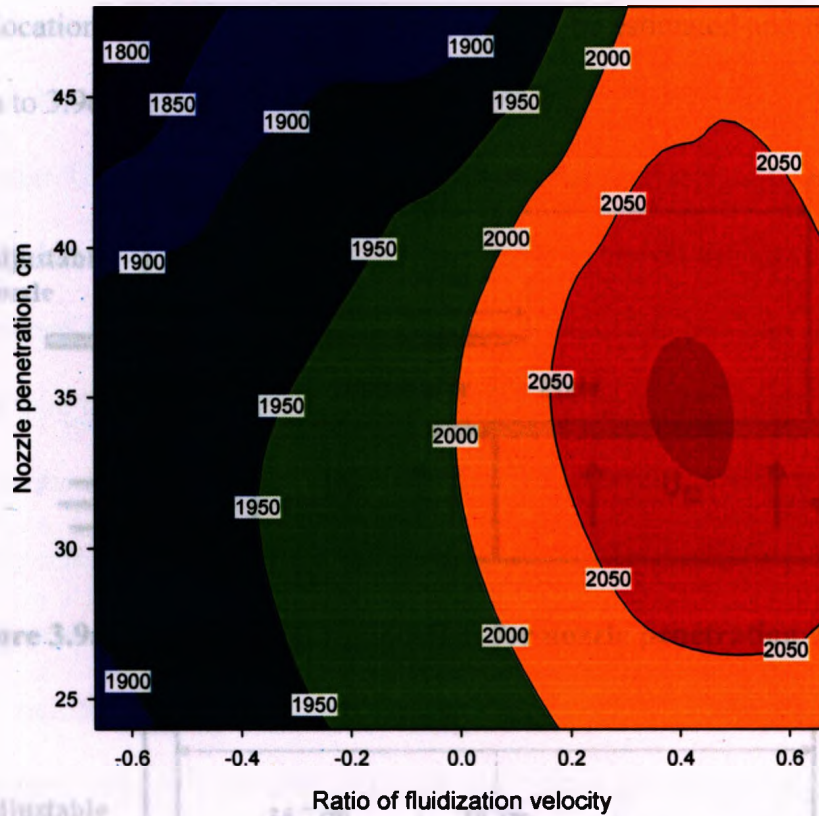


Figure 3.8: Effect of uneven gas distribution and nozzle penetration on new surface area created

According to a study done by McMillan et al. (2007b) on supersonic nozzles, bed particles are entrained into the high velocity gas jet issuing from an attrition nozzle. The bed particles gain momentum from the jet and slam on relatively slow moving bed particles near the jet tip, where particle breakage occurs. Benjelloun et al. (1995) developed an empirical correlation to predict the jet penetration length from a horizontal gas jet in a fluidized bed as shown in Equation 3.3:

$$\frac{L_{jet}}{D_e} = 5.52 \left[\frac{\rho_e U_e^2}{(\rho_p - \rho_e) g D_e} \right]^{0.27} \quad (3.3)$$

This correlation will help to determine the location of jet tip relative to the hydrodynamic zone. By applying the above correlation to the experimental conditions in this study, the

jet penetration depth for a 2.4 mm nozzle operating at 2.2 MPa is about 30 cm. Therefore, the jet tip location for each nozzle penetration could be estimated and they are shown in Figure 3.9a to 3.9c.

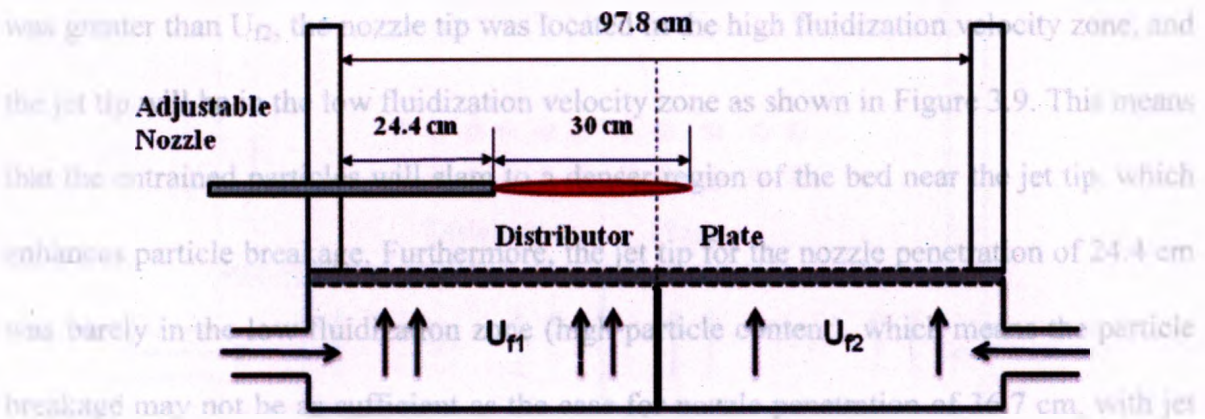


Figure 3.9a: Estimated jet tip location for nozzle penetration at 24.4 cm

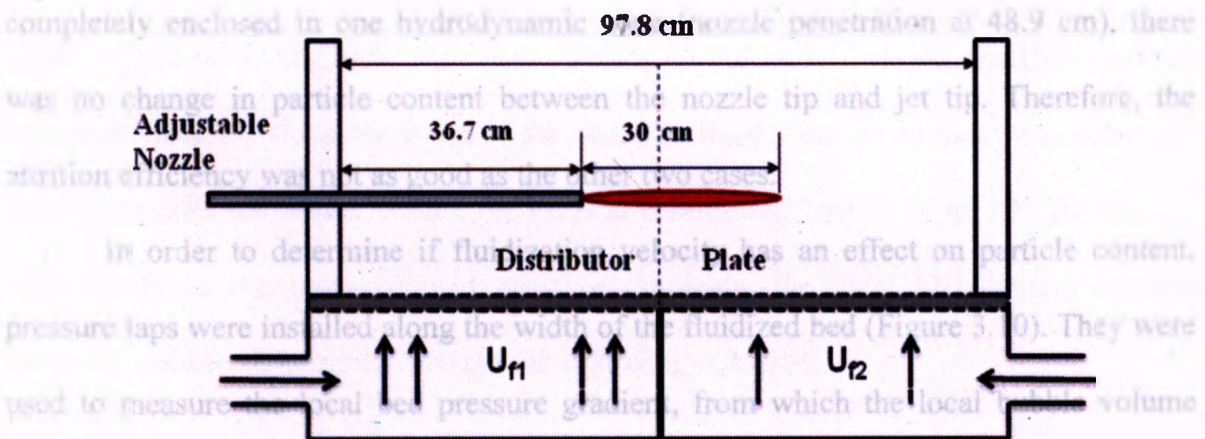


Figure 3.9b: Estimated jet tip location for nozzle penetration at 36.7 cm

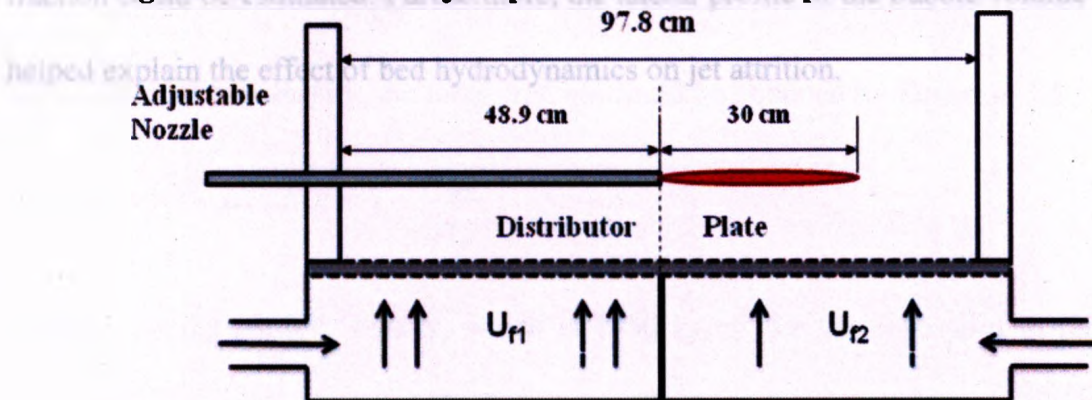


Figure 3.9c: Estimated jet tip location for nozzle penetration at 48.9 cm

Song et al. (2004) mentioned in their study that low fluidization velocity in fluidized bed reactor gave high particle content. In the two cases where the attrition jet straddles both hydrodynamic zones (nozzle penetration at 24.4 cm and 36.7 cm) and U_{f1} was greater than U_{f2} , the nozzle tip was located in the high fluidization velocity zone, and the jet tip will be in the low fluidization velocity zone as shown in Figure 3.9. This means that the entrained particles will slam to a denser region of the bed near the jet tip, which enhances particle breakage. Furthermore, the jet tip for the nozzle penetration of 24.4 cm was barely in the low fluidization zone (high particle content), which means the particle breakage may not be as sufficient as the case for nozzle penetration of 36.7 cm, with jet tip located completely in the low fluidization zone.

For the case where attrition jet was completely enclosed in one hydrodynamic zone (nozzle penetration at 48.9 cm), there was no change in particle content between the nozzle tip and jet tip. Therefore, the attrition efficiency was not as good as the other two cases.

In order to determine if fluidization velocity has an effect on particle content, pressure measurement is one of the easiest ways to study the hydrodynamics of fluidized bed (Bi et al., 2000; Ellis et al., 2002). As Figure 3.10 shows, multiple pressure taps were installed along the width of the bed. The local pressure gradient was measured with a pressure transducer, which recorded at a sampling frequency of 100 Hz for 120 seconds. From the time-averaged pressure gradients, the local bed density at each pressure taps were installed along the width of the fluidized bed (Figure 3.10). They were used to measure the local bed pressure gradient, from which the local bubble volume fraction could be estimated. Furthermore, the lateral profile of the bubble volume fraction helped explain the effect of bed hydrodynamics on jet attrition.

$$\rho_{bed} = \rho_p(1 - \epsilon) \Rightarrow \epsilon = 1 - \frac{\rho_{bed}}{\rho_p} \quad (3.3)$$

Where ρ_p is the particle density, which is 1450 kg/m³ for the coke used in this study.

From the voidage, the bubble volume fraction was determined through Equation 3.6:

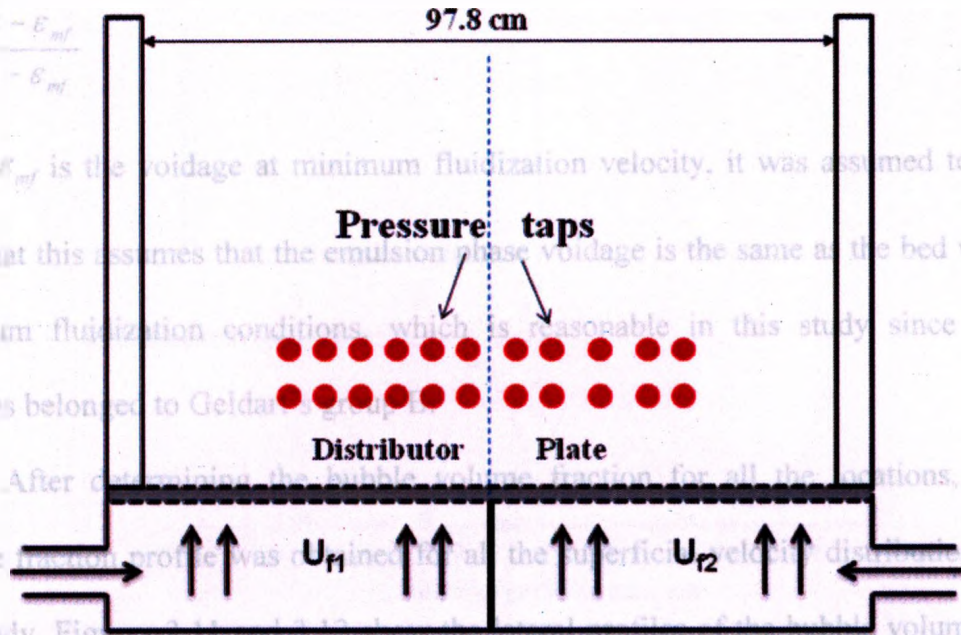


Figure 3.10: Pressure taps used to determine bubble volume fraction

Pressure measurement is one of the easiest ways to study the hydrodynamics of fluidized bed (Bi et al., 2000; Ellis et al., 2002). As Figure 3.10 shows, multiple pressure taps were installed along the width of the bed. The local pressure gradient was measured with a pressure transducer, which recorded at a sampling frequency of 100 Hz for 120 seconds. From the time-averaged pressure gradients, the local bed density at each location could be determined through the following equation:

$$\Delta P = \rho_{bed} gh \Rightarrow \rho_{bed} = \frac{\Delta p}{gh} \quad (3.4)$$

From the local bed density, the local voidage could be obtained by Equation 3.5:

$$\rho_{bed} = \rho_p (1 - \varepsilon) \Rightarrow \varepsilon = 1 - \frac{\rho_{bed}}{\rho_p} \quad (3.5)$$

Where ρ_p is the particle density, which is 1450 kg/m^3 for the coke used in this study.

From the voidage, the bubble volume fraction was determined through Equation 3.6:

$$X_b = \frac{\varepsilon - \varepsilon_{mf}}{1 - \varepsilon_{mf}} \quad (3.6)$$

where ε_{mf} is the voidage at minimum fluidization velocity, it was assumed to be 0.42. Note that this assumes that the emulsion phase voidage is the same as the bed voidage at minimum fluidization conditions, which is reasonable in this study since the coke particles belonged to Geldart's group B.

After determining the bubble volume fraction for all the locations, a bubble volume fraction profile was obtained for all the superficial velocity distributions used in this study. Figures 3.11 and 3.12 show the lateral profiles of the bubble volume fraction for the two extreme cases. 0.1 m/s was the lowest fluidization velocity, 0.5 m/s was the highest fluidization velocity in the experiments conducted for the study of uneven gas distribution. Figure 3.11 shows that the overall bubble volume fraction was very low and close to zero at some locations for a fluidization velocity of 0.1 m/s. However, the overall bubble volume fraction was a lot higher for the case of 0.5 m/s fluidization velocity, as Figure 3.12 shows.

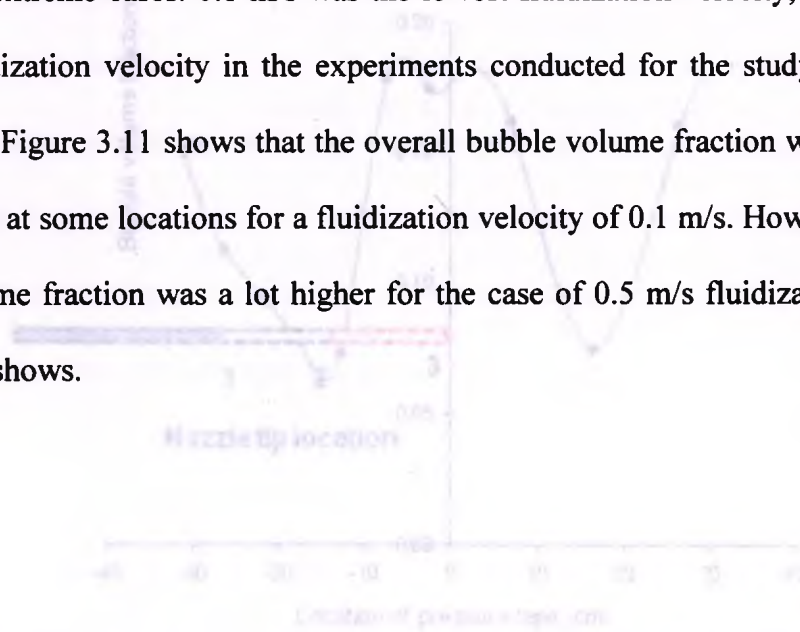


Figure 3.12: Bubble volume fraction profile along the width of bed at 0.5 m/s

The average bubble volume fraction at each fluidization velocity was also determined by taking the average of all the values obtained from each location. Figure 3.13 shows a plot of average bubble volume fraction versus the excess fluidization

velocity ($U=U_{mf}$). Figure 3.13 shows that the average bubble volume fraction increases linearly with the excess fluidization velocity, as expected.

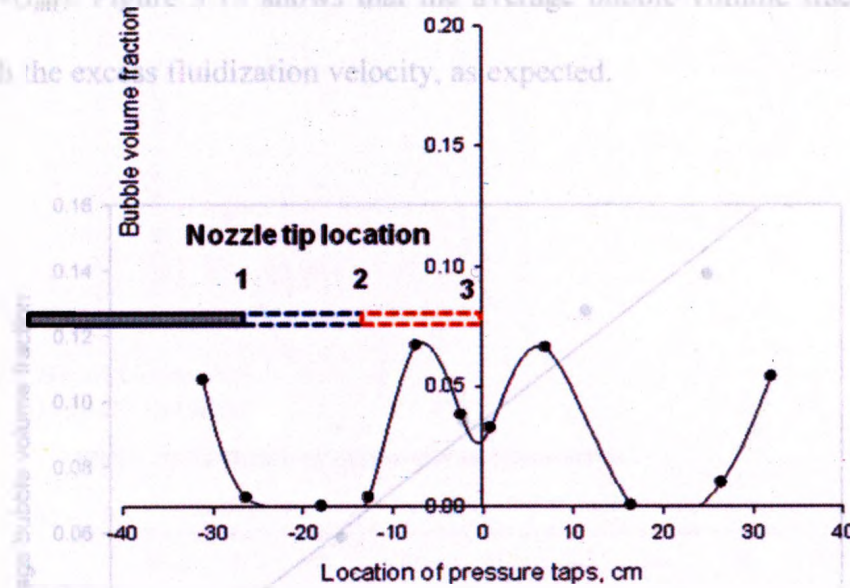


Figure 3.11: Bubble volume fraction profile along the width of bed at 0.1 m/s

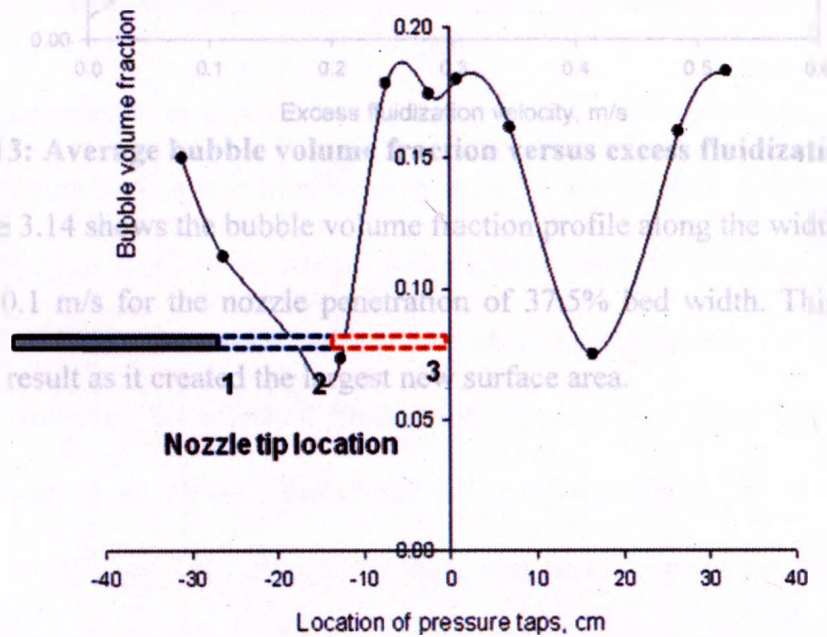


Figure 3.12: Bubble volume fraction profile along the width of bed at 0.5 m/s

The average bubble volume fraction at each fluidization velocity was also determined by taking the average of all the values obtained from each location. Figure 3.13 shows a plot of average bubble volume fraction versus the excess fluidization

velocity ($U-U_{mf}$). Figure 3.13 shows that the average bubble volume fraction increases linearly with the excess fluidization velocity, as expected.

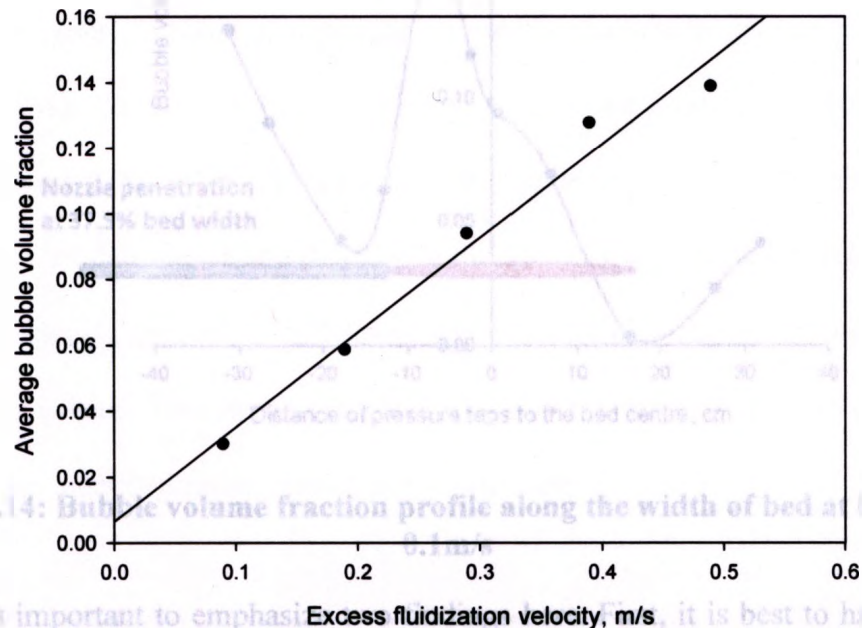


Figure 3.14: Bubble volume fraction profile along the width of bed at 0.5 m/s and 0.1 m/s for the nozzle penetration of 37.5% bed width.

Figure 3.13: Average bubble volume fraction versus excess fluidization velocity

Figure 3.14 shows the bubble volume fraction profile along the width of the bed at 0.5 m/s and 0.1 m/s for the nozzle penetration of 37.5% bed width. This combination gave the best result as it created the largest new surface area.

However, the effect of fluidization velocity on particle entrainment is not very clear. Hulet et al. (2003) studied the effect of superficial gas velocity on solid entrainment into gas jet. They found that there was no clear trend between fluidization velocity and entrainment rate. In some cases the entrainment rate increased with increasing fluidization velocity, while in the other cases it decreased. However, Hulet et al. (2003) did not determine the effect of the local bubble fraction. The effect of fluidization velocity on solid entrainment and attrition efficiency will be examined in the next section with the 2.8 mm nozzle.

3.3.2 Effect of nozzle scale with uneven gas distribution

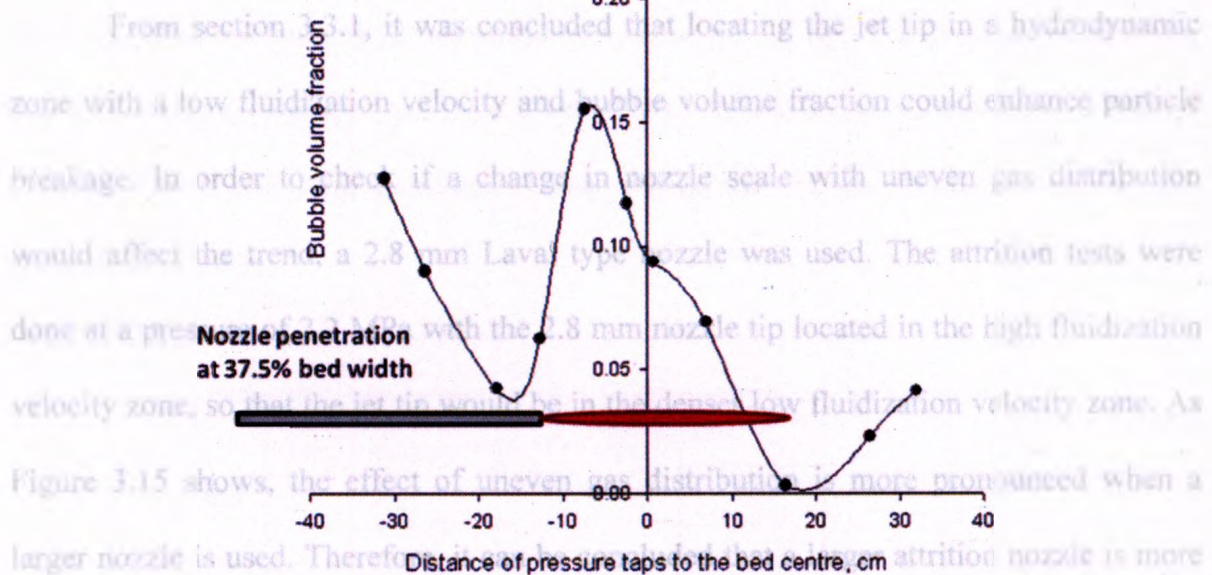


Figure 3.14: Bubble volume fraction profile along the width of bed at 0.5 m/s and 0.1 m/s

It is important to emphasize two findings here. First, it is best to have the jet tip located in a region with a low bubble fraction, as it will contact with a denser bed as discussed earlier in this study, which will enhance particle breakage. Second, it is probably best to locate the nozzle tip in a zone rich in gas bubbles to maximize particle entrainment. However, the effect of fluidization velocity on particle entrainment is not very clear. Hulet et al. (2003) studied the effect of superficial gas velocity on solid entrainment into gas jet. They found that there was no clear trend between fluidization velocity and entrainment rate. In some cases the entrainment rate increased with increasing fluidization velocity, while in the other cases it decreased. However, Hulet et al. (2003) did not determine the effect of the local bubble fraction. The effect of fluidization velocity on solid entrainment and attrition efficiency will be examined in the next section with the 2.8 mm nozzle.

3.3.2 Effect of nozzle scale with uneven gas distribution

From section 3.3.1, it was concluded that locating the jet tip in a hydrodynamic zone with a low fluidization velocity and bubble volume fraction could enhance particle breakage. In order to check if a change in nozzle scale with uneven gas distribution would affect the trend, a 2.8 mm Laval type nozzle was used. The attrition tests were done at a pressure of 2.2 MPa with the 2.8 mm nozzle tip located in the high fluidization velocity zone, so that the jet tip would be in the denser low fluidization velocity zone. As Figure 3.15 shows, the effect of uneven gas distribution is more pronounced when a larger nozzle is used. Therefore, it can be concluded that a larger attrition nozzle is more effective when operated under uneven gas distribution.

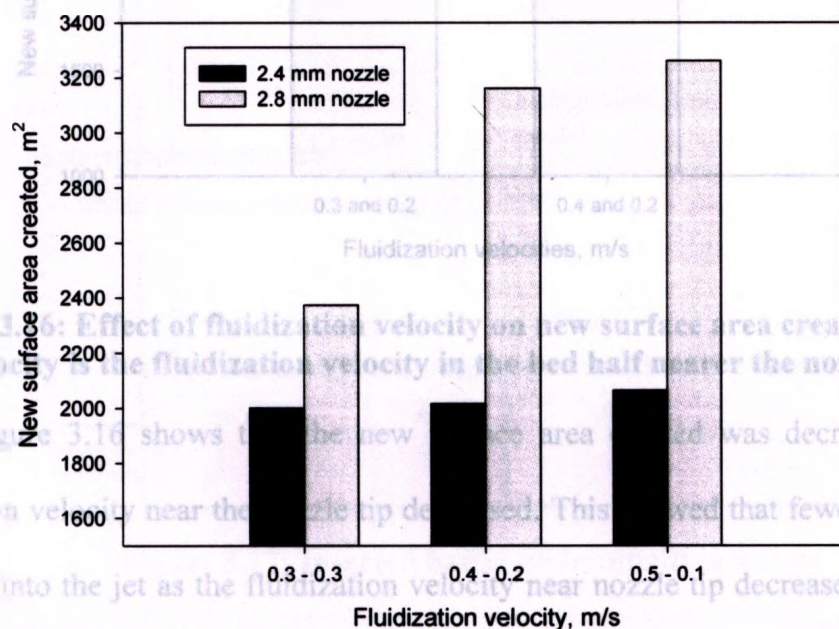


Figure 3.15: Effect of nozzle scale with uneven gas distribution (the first velocity is the fluidization velocity in the bed half nearer the nozzle port)

In order to check the effect of fluidization velocity on particle entrainment and attrition efficiency, an additional attrition test was carried out with the 2.8 mm nozzle operated at 2.2 MPa and compared with results obtained from 0.4 m/s and 0.2 m/s tests.

In this attrition test, the fluidization velocity near the jet tip was maintained at 0.2 m/s in order to create the same hydrodynamic zone near the jet tip. The fluidization velocity near the nozzle tip was changed from 0.4 m/s to 0.3 m/s, to show whether the fluidization velocity affects the solid entrainment near the nozzle tip, and ultimately affects the attrition efficiency.

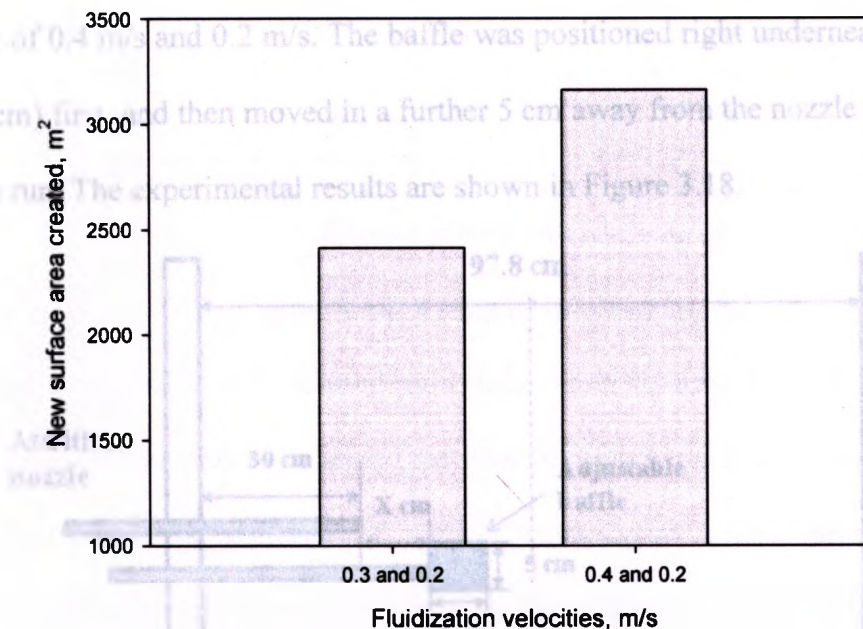


Figure 3.16: Effect of fluidization velocity on new surface area creation (the first velocity is the fluidization velocity in the bed half nearer the nozzle port)

Figure 3.16 shows that the new surface area created was decreased when the fluidization velocity near the nozzle tip decreased. This showed that fewer particles were entrained into the jet as the fluidization velocity near nozzle tip decreased, so that fewer particles were available for particle collision near jet tip. Therefore, it is best to keep a high fluidization velocity near the nozzle tip to maximize particle entrainment, and a low fluidization velocity near the jet tip to contact with a denser bed. Both conditions will help enhance particle attrition.

3.3.3 Effect of inserted baffle underneath the attrition jet

In order to further investigate the effect bed hydrodynamics on jet attrition, an adjustable baffle with a dimension of 5 cm by 5 cm was inserted 5 cm under the attrition nozzle (Figure 3.17). The baffle was moved along the jet cavity and its effect on new surface area created were determined. Experiments were conducted with the 2.8 mm Laval type nozzle with an upstream pressure of 2.2 MPa, at an uneven superficial gas velocity of 0.4 m/s and 0.2 m/s. The baffle was positioned right underneath the nozzle tip ($X = 0$ cm) first, and then moved in a further 5 cm away from the nozzle tip between each attrition run. The experimental results are shown in Figure 3.18.

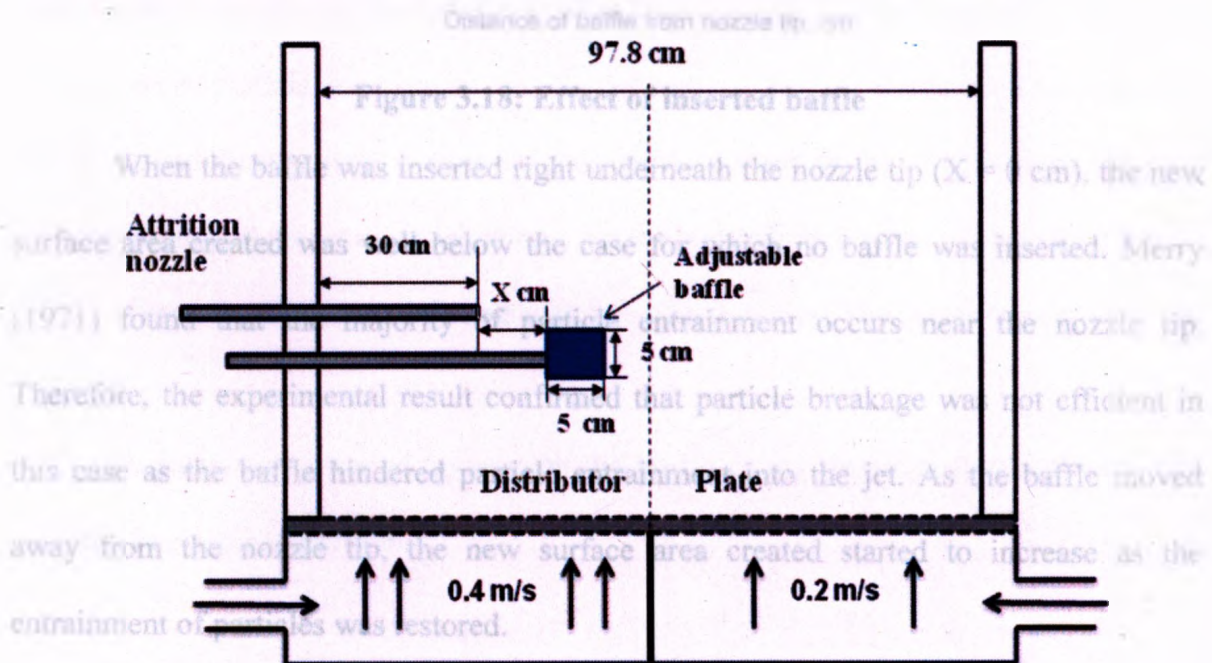


Figure 3.17: Inserted baffle under attrition nozzle

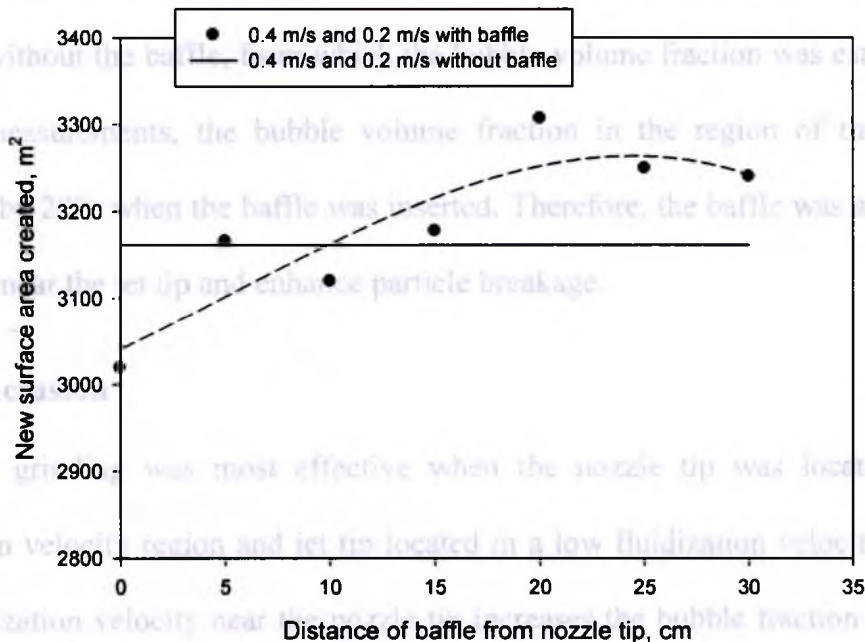


Figure 3.18: Effect of inserted baffle

When the baffle was inserted right underneath the nozzle tip ($X = 0$ cm), the new surface area created was well below the case for which no baffle was inserted. Merry (1971) found that the majority of particle entrainment occurs near the nozzle tip. Therefore, the experimental result confirmed that particle breakage was not efficient in this case as the baffle hindered particle entrainment into the jet. As the baffle moved away from the nozzle tip, the new surface area created started to increase as the entrainment of particles was restored.

The jet penetration depth could be estimated from the correlation developed by Benjelloun et al. (1995) as shown in Equation 3.3 earlier. For a 2.8 mm nozzle operated at 2.2 MPa, the jet penetration depth is approximately 33 cm. Therefore, when the baffle edge was 20 cm away from the nozzle tip, it densified a region between 20 and 25 cm from the nozzle tip, near the tip of the jet. According to Figure 3.18, the new surface area created increased when the baffle reduced the bubble fraction near the jet tip. In order to

check this argument, the local pressure gradient was measured through the pressure taps with and without the baffle, from which the bubble volume fraction was estimated. From the two measurements, the bubble volume fraction in the region of the jet tip was decreased by 28% when the baffle was inserted. Therefore, the baffle was able to densify the region near the jet tip and enhance particle breakage.

3.4 Conclusion

Jet grinding was most effective when the nozzle tip was located in a high fluidization velocity region and jet tip located in a low fluidization velocity region. The high fluidization velocity near the nozzle tip increases the bubble fraction in this region and enhances particle entrainment into the jet cavity. The low fluidization velocity near the jet tip reduces the local bubble volume fraction, ensuring that the particles entrained and accelerated in the jet cavity slam on a denser bed, enhancing particle breakage.

These results were confirmed with two nozzle scales. The larger nozzle was more effective.

A baffle was inserted underneath the jet tip cavity densified the local bed. This resulted in enhanced attrition.

3.5 Nomenclature

d_o Orifice diameter (m)

D_e Diameter at the nozzle exit (m)

g Gravity (m/s^2)

h Separation distance between the two pressure taps (m)

L_{jet} Jet penetration depth of attrition nozzle (m)

- P Pressure (Pa) ; Ullik, B. Performance of a fluidized bed jet mill as a function of operating parameters. *Int. J. Miner. Process* 1996, 43-43, 507-519.
- R_a Jet attrition rate (kg/s)
Boerefijn, R.; Gidde, N. J.; Ghadiri, M. Review of attrition of fluid cracking catalyst particles. *Powder Technology* 2000, 11, 145-174.
- u_o Jet velocity (m/s)
- U Fluidization velocity (m/s) ; Supersonic attrition nozzles in gas-solid fluidized beds. *Chemical Engineering and Processing: Process Intensification* 2010, 49, 225-234.
- U_e Gas velocity at the nozzle exit (m/s)
Dunlop D., Griffin, L., Moser, J., Particle size control in fluid coking. 1958, 54, 39-43.
- U_{mf} Minimum fluidization velocity (m/s)
Forsythe, W., Hertzog, W. Attrition characteristics of fluid cracking catalysts. *Ind. Eng. Chem.* 1960, 52, 100-104.
- U_{f1} Superficial gas velocity in zone 1 (m/s) (Eqn. 3.1)
- U_{f2} Superficial gas velocity in zone 2 (m/s) (Eqn. 3.1)
Entrainment and stability of a horizontal gas-liquid jet in a fluidized bed. *Int. J. Chem. React. Eng.* 2003.
- X_b Bubble volume fraction
Li, P., Particle attrition with supersonic nozzles in a high temperature fluidized bed. Ph.D. dissertation, The University of Western Ontario, London, Canada. 2011.

Greek letters

- ε Local bed voidage
McMillan, J.; Briens, C.; Berruti, F.; Chan, E. Particle attrition mechanism with a sonic jet. *Chemical Engineering Science* 2007b, 62, 3809-3820.
- ε_{mf} Voidage at minimum fluidization velocity
- ρ_{bed} Bed density (kg/m³)
Meibool, M.; Large, J. F.; Guigon, P. High velocity impact of particles on a target - An experimental study. *Exp. Therm. Fluid Dyn.* 1996, 44-45, 77-91.
- ρ_e Gas density at the nozzle exit (kg/m³)
- ρ_o Jet gas density (kg/m³)
Berry, J. A. The effect of a horizontal gas jet into a fluidised bed. *Trans. Inst. Chem. Eng.* 1971, 49, 189-195.
- ρ_p Particles density (kg/m³)
Olsson, P. A.; Almsedt, A. E. Influence of pressure and fluidization velocity on the particle size distribution in a fluidized bed. *Chemical Engineering Science* 1990, 45, 1733-1741.
- η Grinding efficiency (m²/kg)

3.6 References

- Benjelloun, F., Vanderschuren, J., and Liegeois, R., Penetration length of horizontal gas jets into atmospheric fluidized bed. *Proc. Fluidization-VIII*, J-F. Large and C. Laguerie Eds., Engineering Foundation, N.Y., 1995, 239-246.
- Bentham, A., Kwan, C., Boerefijn, R., Ghadiri, M., Fluidised-bed jet milling of pharmaceutical powders. *Powder Technol* 2004, 141, 233-238.

- Benz, M.; Herold, H.; Ulfik, B. Performance of a fluidized bed jet mill as a function of operating parameters. *Int. J. Miner. Process.* **1996**, 44-45, 507-519.
- Boerefijn, R.; Gudde, N. J.; Ghadiri, M. Review of attrition of fluid cracking catalyst particles. *Advanced Powder Technology* **2000**, 11, 145-174.
- Cruz, N.; Briens, C.; Berruti, F. Supersonic attrition nozzles in gas-solid fluidized beds. *Chemical Engineering and Processing: Process Intensification* **2010**, 49, 225-234.
- Dunlop D., Griffin, L., Moser, J., Particle size control in fluid coking. **1958**, 54, 39-43.
- Forsythe, W., Hertwig, W. Attrition characteristics of fluid cracking catalysts. *Ind. Eng. Chem* **1949**, 41, 1200-1206.
- Hulet, C., Briens, C., Berruti, F., Chan, E., Ariyapadi, S., Entrainment and stability of a horizontal gas-liquid jet in a fluidized bed, *Int. J. Chem. Rect. Eng.*, **2003**
- Li, F., Particle attrition with supersonic nozzles in a high temperature fluidized bed. Ph.D. dissertation, The University of Western Ontario, London, Canada. **2011**.
- McMillan, J.; Briens, C.; Berruti, F.; Chan, E. High velocity attrition nozzles in fluidized beds. *Powder Technol* **2007a**, 175, 133-141.
- McMillan, J.; Briens, C.; Berruti, F.; Chan, E. Particle attrition mechanism with a sonic gas jet injected into a fluidized bed. *Chemical Engineering Science*. **2007b**, 62, 3809-3820.
- Mebtoul, M.; Large, J. F.; Guigon, P. High velocity impact of particles on a target - An experimental study. *Int. J. Miner. Process.* **1996**, 44-45, 77-91.
- Merry, J. M. D.; Penetration of a horizontal gas jet into a fluidised bed. *Trans. Inst. Chem. Eng.* **1971**, 49, 189-195
- Olowson, P. A.; Almstedt, A. E. Influence of pressure and fluidization velocity on the bubble behaviour and gas flow distribution in a fluidized bed. *Chemical Engineering Science* **1990**, 45, 1733-1741.
- Pacek, A. W.; Nienow, A. W. An application of jet grinding to fluidised bed granulation. *Powder Technol* **1991**, 65, 305-310.
- Smith, J. M.; Van Ness, H. C.; Abbott, M. M. In *Introduction to chemical engineering thermodynamics*; McGraw-Hill chemical engineering series; McGraw-Hill: New York, 1996; pp 763.

Song, X.; Bi, H.; Jim Lim, C.; Grace, J. R.; Chan, E.; Knapper, B.; McKnight, C. Hydrodynamics of the reactor section in fluid cokers. *Powder Technol* **2004**, *147*, 126-136.

4.1 Introduction

Tasirin, S. M.; Geldart, D. Experimental investigation on fluidized bed jet grinding. *Powder Technol* **1999**, *105*, 337-341.

Werther, J.; Xi, W. Jet attrition of catalyst particles in gas fluidized beds. *Powder Technol* **1993**, *76*, 39-46.

Wiman, J.; Almstedt, A. E. Influence of pressure, fluidization velocity and particle size on the hydrodynamics of a freely bubbling fluidized bed. *Chemical Engineering Science* **1998**, *53*, 2167-2176.

Wu, S.; Baeyens, J.; Chu, C. -. Effect of the grid-velocity on attrition in gas fluidized beds. *Can. J. Chem. Eng.* **1999**, *77*, 738-744.

that is produced as a reaction by-product deposits on the fluidized coke particles. Therefore, there is a gradual increase of the coke particle size as the reaction proceeds. Moreover, the coke particles form agglomerates when several coke particles stick together due to poor feed distribution. If the increase in the coke particle size is unchecked, it leads to fluidization problems. Therefore, high velocity gas jets are applied to grind fluidized particles in order to maintain the particle size within an optimal range. However, jet attrition accounts for about 40% of the total steam consumption in Fluid Cokers (Li, 2011). If the steam consumption of the attrition nozzles could be reduced, it would lead to reduced energy consumption, a higher reactor throughput and reduced sour water treatment (Pougarich et al., 2010; McMillan et al., 2007a).

Different methods to improve particle attrition in fluidized bed have been studied by numerous researchers, such as using a target plate downstream of the nozzle, placing a shroud around the nozzle tip, using opposing nozzles and changing nozzle orientations. Dunlop et al. (1958) placed a target plate downstream of the attrition jet, which enhanced grinding by promoting particles and target collisions. However, this method has some

Chapter 4: Effect of Nozzle Inclination on Jet Attrition

4.1 Introduction

Particle size control is very important in many fluidized bed processes in order to maintain good fluidization and satisfactory operation. The Fluid Coking process is one that is just sufficient to reduce the particle to the required size. Tasirin et al. (1999) also particular example where the particle size of the fluidized particles must be kept within a well-defined range in order for the process to operate properly. Fluid Coking is used for upgrading heavy oils, such as bitumen extracted from oil sands, with non-catalytic thermal cracking to produce lighter, synthetic crude oil. During this process, solid coke that is produced as a reaction by-product deposits on the fluidized coke particles. Therefore, there is a gradual increase of the coke particle size as the reaction proceeds. Moreover, the coke particles form agglomerates when several coke particles stick entrained into the jet increased so that more particles were able to slam on the target together due to poor feed distribution. If the increase in the coke particle size is unchecked, it leads to fluidization problems. Therefore, high velocity gas jets are applied to grind fluidized particles in order to maintain the particle size within an optimal range. However, jet attrition accounts for about 40% of the total steam consumption in Fluid Cokers (Li, 2011). If the steam consumption of the attrition nozzles could be reduced, it would lead to reduced energy consumption, a higher reactor throughput and reduced sour water treatment (Pougatch et al., 2010; McMillan et al., 2007a).

Different methods to improve particle attrition in fluidized bed have been studied by numerous researchers, such as using a target plate downstream of the nozzle, placing a shroud around the nozzle tip, using opposing nozzles and changing nozzle orientations. Dunlop et al. (1958) placed a target plate downstream of the attrition jet, which enhanced grinding by promoting particles and target collisions. However, this method has some

drawbacks such as erosion of the target plate and generation of some unwanted ultra-fine particles. Tasirin et al. (1999) further studied the effect of a target plate on particle attrition. They claimed that there is an optimal separation distance between nozzle and the target plate, which would allow the particles to accelerate to an optimal impact speed that is just sufficient to reduce the particle to the required size. Tasirin et al. (1999) also found that the rate of grinding increased as the separation distance decreased, and that a single nozzle with a target required about half of the power consumption of two opposing nozzles to achieve the same grinding. McMillan (2007) studied the effect of a circular target on particle attrition with different separation distances between the nozzle and the target plate. They found that the grinding efficiency increased as the target moved away from the nozzle while remaining within reach of the jet, as the volume of particles entrained into the jet increased so that more particles were able to slam on the target (McMillan, 2007).

Hulet et al. (2007) studied the effect of a shroud on the entrainment of fluidized solids into a gas jet and found that the shroud helped to divert bubbles approaching the nozzle tip thereby minimizing the effect of cross flow on the jet momentum. With the shroud, the gas jet entrains more particles and less gas. McMillan et al. (2007) further studied the effect of a shroud on particle attrition and found that a nozzle with a shroud performed better than a free jet. They claimed that it was because the shroud helped to entrain more particles into the gas jet. As a result, more collisions happened between the entrained particles and the solids in the dense phase of the bed near the tip of the jet, which enhanced the attrition rate.

Yates et al. (1991) studied particle attrition of opposing vertical jets in their overlap region and found that the discharge location of gases affect the attrition rate. When the gases from opposing jets were discharged close to the wall, they found it had a significant influence on attrition. Tasirin et al. (1999) compared the grinding rate of both horizontal and vertical opposing jets with single jet. They found that two opposing horizontal nozzles gave only a slight increase in grinding compared to a single horizontal jet. But, the grinding rate of two vertical non-interacting nozzles was roughly twice that of one vertical nozzle. Tasirin et al. (1999) concluded that it is not advantageous to use

4.2 Experimental Setup

two interacting opposing jets, as the region between them has a lower particle concentration, which lead to fewer particle-particle collisions.

The studies on the effect of nozzle angle on particle attrition are very limited. Werther and Xi (1993) studied the effect of the orientation of a gas jet and found that a horizontal jet achieved the same attrition rate as an upward jet. However, the attrition rate was significantly higher with a downward jet. Midoux et al. (1999) used three different jet mills with two nozzle angles (63° and 67°) and found that the nozzle angle affected the grinding ratio of the product. Tuunila and Nystrom (1998) studied the effect of nozzle angle on particle attrition. They varied the angle of nozzle in three levels, which were 23° , 33° and 43° and found the largest angle (43°) gave the highest grinding rate. Tuunila and Nystrom (1998) found that their results were in agreement with Ahlbus (1992), who had found that an even larger angle (60°) was most effective. The limited amount of research work on nozzle angle was done using straight tube nozzles in most cases, except Midoux et al. (1999) who used abrupt and Laval shaped nozzles. The Laval type nozzle described by Benz et al. (1996) is able to provide a supersonic velocity jet as the gas

expands in the divergent section, which enhances the jet momentum and grinding rate. Therefore, the effect of the nozzle angle on particle attrition with supersonic jet needs to be systematically studied, with a wide range of nozzle angles.

The objective of this work is to investigate the effect of nozzle inclination angle on the jet attrition process. A high velocity Laval-type nozzle was used and the nozzle was adjusted from 0° to 90° . The effect of a baffle on the attrition rate obtained with inclined jets was also studied.

4.2 Experimental Setup

Attrition experiments were conducted in a pie-shaped fluidized bed with a height of 1.97 m and 0.69 m in width as shown in Figure 4.1. The bed is equipped with two external cyclones in series, a primary cyclone that returns entrained materials to the bed through a dipleg, and a secondary cyclone that collects the particles escaping from the primary cyclone with a container. The unit is fluidized with compressed air, whose flowrate is controlled by a bank of sonic nozzles with a pressure regulator. High pressure nitrogen gas is injected into the bed using a high velocity attrition nozzle to attrit the fluidized coke particles.

Experiments were conducted as follows. First, initial elutriation was performed at a superficial gas velocity of 0.6 m/s after loading the solids into the column, to eliminate fine particles from the bed. A bed sample was taken through the sampling port, after elutriation. The size distribution of the sample was analyzed using a laser diffraction apparatus (HELOS of Sympatec). The fines collected in the secondary cyclone container were discarded just before the attrition was started. Then, the bed was fluidized at a

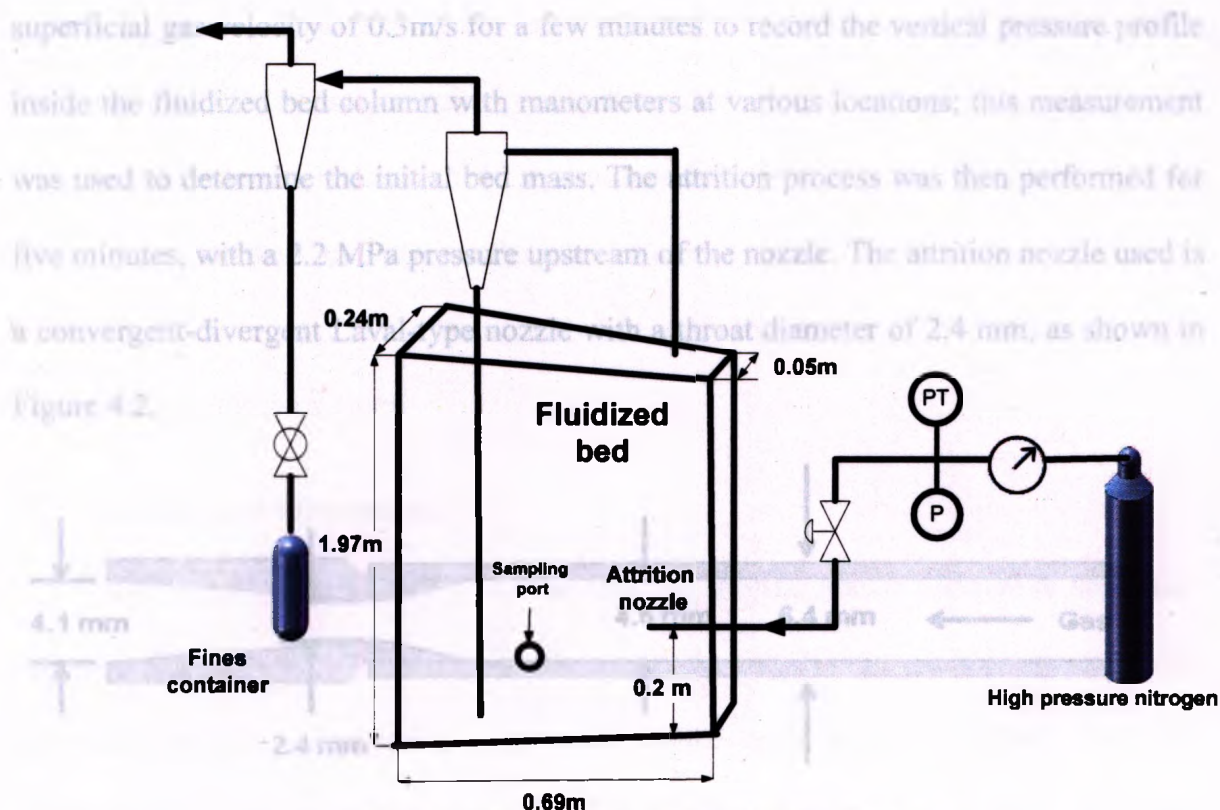


Figure 4.2: Laval type nozzle, $D_{th} = 2.4 \text{ mm}$

Figure 4.1: Experimental Set-up

After the attrition process, the superficial gas velocity was adjusted to 0.6 m/s to perform elutriation. The attrition nozzle was placed inside the bed at a height of 0.20 m above the grid. A bed sample was collected at the end of the elutriation process from the sampling port. The attrition gas was supplied from a high pressure nitrogen tank. The mass flowrates were determined from the pressure upstream of the nozzles, measured with a pressure transducer, using a prior calibration (because there was sonic flow through the nozzles, the gas flowrate was independent of downstream pressure).

The attrition nozzle was arranged so that the attrition gas was injected horizontally into the bed at first. Then, the angle of the attrition nozzle was adjusted by a superficial gas velocity of 0.6 m/s after loading the solids into the column, to eliminate fine particles from the bed. A bed sample was taken through the sampling port, after elutriation.

The effect of nozzle inclination on the particle size distribution was also determined. The size distribution of the sample was analyzed using a laser diffraction apparatus (HELOS of Sympatec). The fines collected in the secondary cyclone container were discarded just before the attrition was started. Then, the bed was fluidized at a superficial gas velocity of 0.6 m/s for a few minutes to record the vertical pressure profile inside the fluidized bed column with manometers at various locations; this measurement was used to determine the initial bed mass. The attrition process was then performed for five minutes, with a 2.2 MPa pressure upstream of the nozzle. The attrition nozzle used is a convergent-divergent Laval type nozzle with a throat diameter of 2.4 mm , as shown in Figure 4.2.

superficial gas velocity of 0.3m/s for a few minutes to record the vertical pressure profile inside the fluidized bed column with manometers at various locations; this measurement was used to determine the initial bed mass. The attrition process was then performed for five minutes, with a 2.2 MPa pressure upstream of the nozzle. The attrition nozzle used is a convergent-divergent Laval-type nozzle with a throat diameter of 2.4 mm, as shown in Figure 4.2.

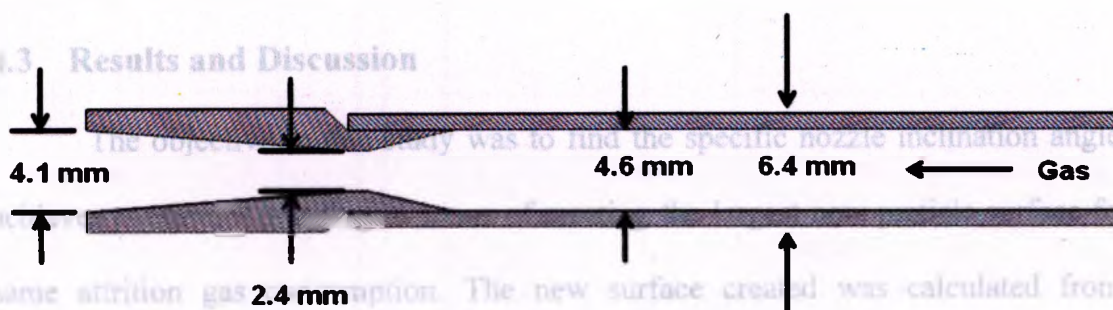


Figure 4.2: Laval type nozzle, $D_{th} = 2.4$ mm

After the attrition process, the superficial gas velocity was adjusted to 0.6 m/s to perform elutriation. A bed sample was collected at the end of the elutriation process from the sampling port. The fine particles collected in the secondary cyclone container were collected and analysed. Although some small amount of the fines were lost in the exhaust air, their impact on the final results were negligible.

The attrition nozzle was arranged so that the attrition gas was injected horizontally into the bed at first. Then, the angle of the attrition nozzle was adjusted by 15° toward the grid for each subsequent run.

The effect of nozzle inclination on the particle size distribution was also determined. The particle size distribution was measured for the bed particles and the cyclone catch. The results were then combined to obtain the average size distribution of the particles mix after attrition, including all the ground particles and the particles that

had not yet been ground. The results were reported with three size cuts: 0-30 μm (fines particles), 30-105 μm and particles greater than 105 μm (coarse particles). The 30 μm size cut was selected because there were no particles smaller than 30 μm in the bed before attrition and all particles smaller than 30 μm were, therefore, the result of attrition. Similarly, the 105 μm size cut was selected because there were no particles larger than 105 μm in the elutriated fines.

4.3 Results and Discussion

The objective in this study was to find the specific nozzle inclination angle that achieves maximum grinding in terms of creating the largest new particle surface for the same attrition gas consumption. The new surface created was calculated from the difference between the surface area of the original bed sample and the sum of surface areas created from the final (after attrition) bed samples and the generated fines.

Figure 4.3: Nozzle lay out

4.3.1 Effect of nozzle inclination on jet attrition

The effect of nozzle inclination on jet attrition was studied by changing the nozzle inclination angle from 0° to 90°. The attrition experiment was started with the nozzle inclination angle at 0°, which means the nozzle injects the attrition gas into the bed horizontally. Subsequently, the nozzle inclination angle was adjusted towards the grid by 15° for each run until 90°. At 90°, the nozzle injects the attrition gas directly towards the grid (against fluidization velocity). Due to the design constraint on the fluidized bed and nozzle, it can only adjust the nozzle to an inclination angle of 45° with the original location. For nozzle inclination angles over 45°, the nozzle was secured from the top of the fluidized bed as shown in Figure 4.3. To verify that the change of nozzle location did

not affect the results, the runs for a nozzle inclination of 45° were performed with both set ups.

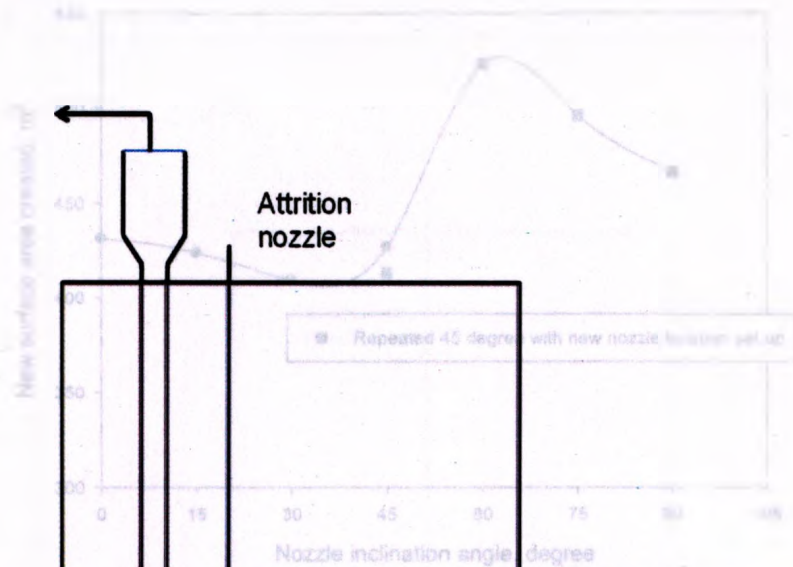


Figure 4.4: New surface area created vs. nozzle inclination angle

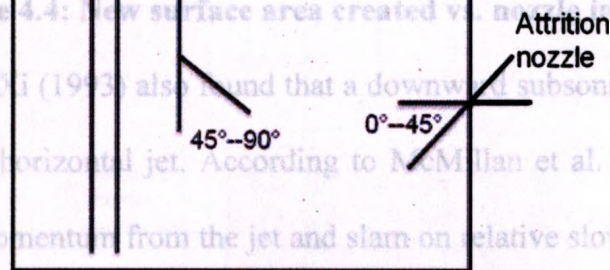


Figure 4.3: Nozzle layout

Figure 4.4 shows how the new surface area created varied with the nozzle inclination angle. First, the new surface areas created at a nozzle inclination angle of 45° were about the same for both nozzle setups. The new surface remained almost constant for nozzle inclinations between 0° to 45° . However, the new surface increased sharply as the nozzle inclination was increased beyond 45° , reaching a maximum value for 60° , and decreasing for larger inclinations. These results matched with findings from Ahlbus (1992), who also found that the grinding rate was a maximum for a nozzle angle of 60° , using subsonic jets.

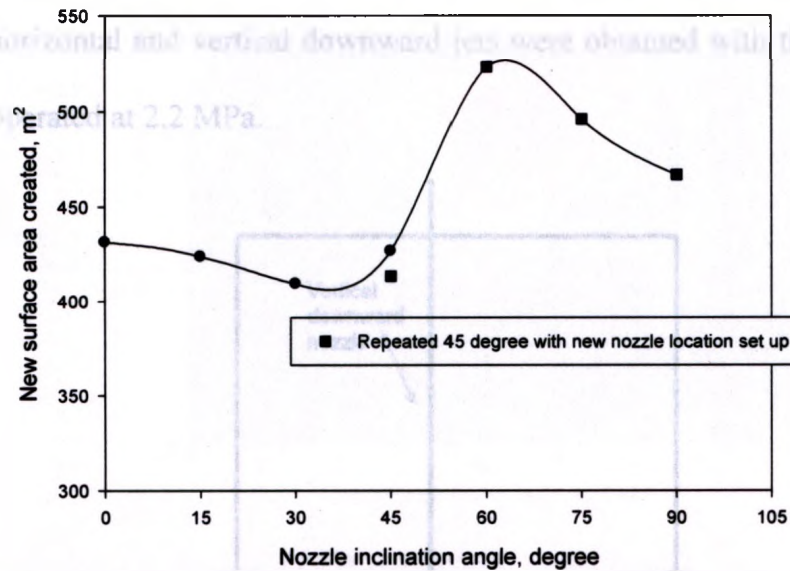


Figure 4.4: New surface area created vs. nozzle inclination angle

Werther and Xi (1993) also found that a downward subsonic jet achieved a higher attrition rate than a horizontal jet. According to McMillan et al. (2007b), the entrained bed particles gain momentum from the jet and slam on relative slow moving bed particles near the jet tip, where particle breakage occurs. The horizontal jet tip loses some of its momentum when it was pushed upward by the fluidizing gas, which weakens the particle breakage near the jet tip. On the other hand, when a downward jet is used, the upward fluidizing particles collide with the entire downward jet tip constantly thereby increasing the strength and number of particle collisions, which may enhance the particle attrition.

A novel electrical capacitance tomography technique developed by Hamidi (2011) was used to determine the voidage profile around the jet tip. As Figure 4.5 shows, a wooden window was installed on both sides of the fluidized bed near the expected jet tip region. Electrodes were adhered to the wooden window to obtain capacitance signals during jet attrition. The capacitance signals were analyzed after to generate the voidage contours around the jet tip. Due to the constraint of the electrode window size, the

contour for the inclined nozzle at 60° was not obtained. The jet tip contours for two extreme cases, horizontal and vertical downward jets were obtained with the supersonic attrition nozzle operated at 2.2 MPa.

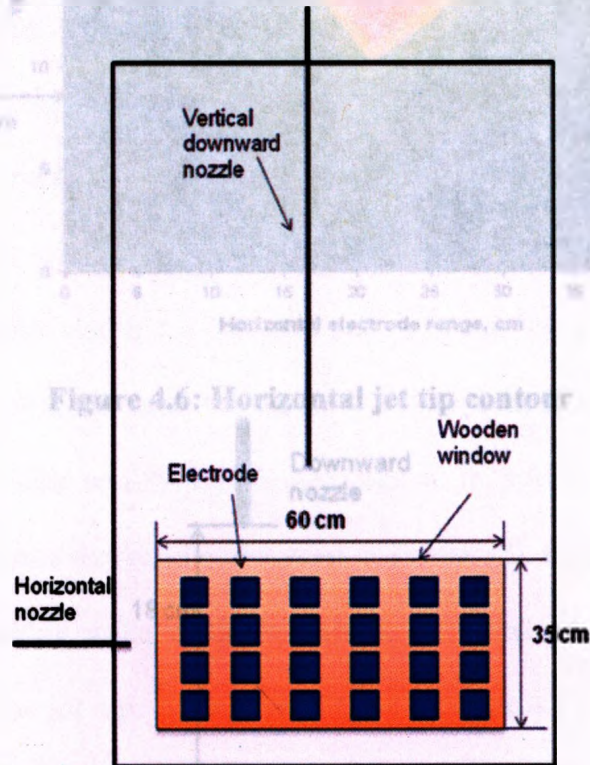


Figure 4.5: Electrodes on wooden window

The jet tip contour for horizontal and vertical downward jets are shown in Figures 4.6 and 4.7. From the horizontal jet tip contour, it is observed that the jet tip was pushed upward due to the influence of the upward fluidization gas. Moreover, the voidage of the jet tip core for the horizontal jet is lower than the downward jet.

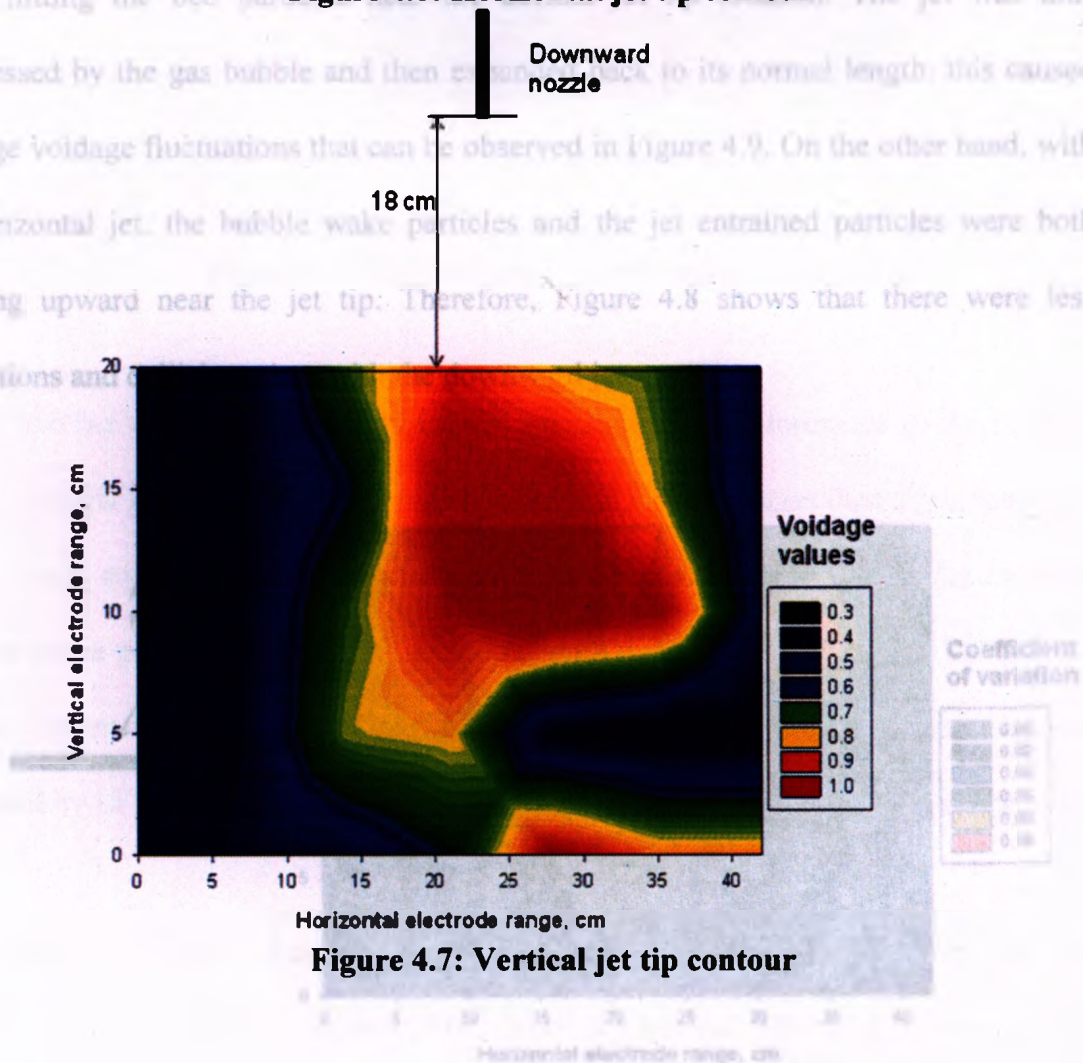
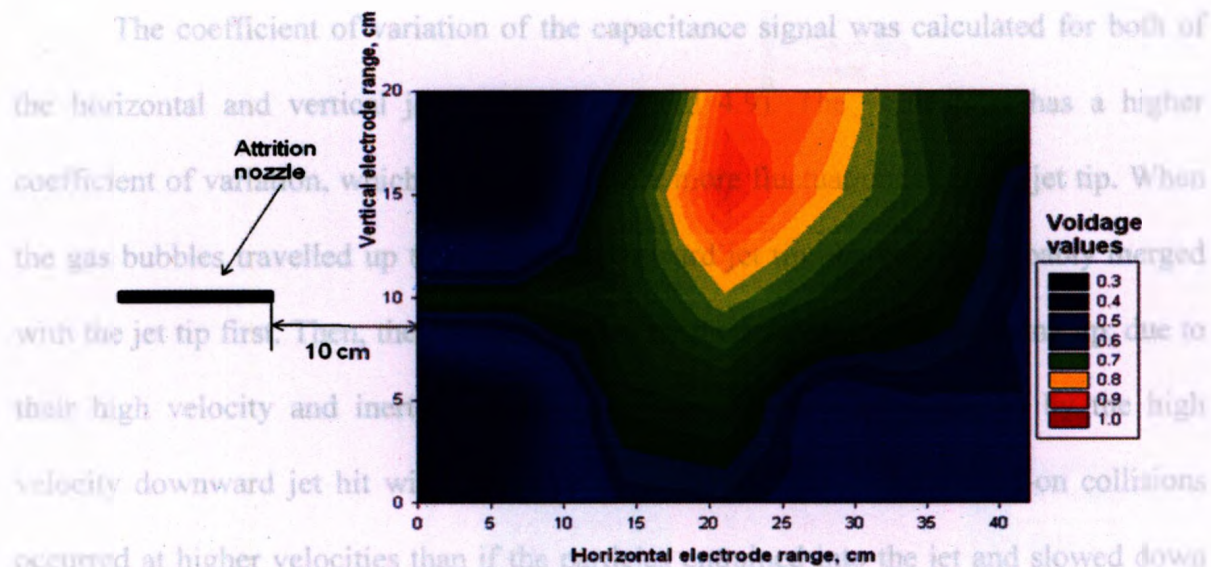


Figure 4.8: Coefficient of variation for horizontal jet

The coefficient of variation of the capacitance signal was calculated for both of the horizontal and vertical jets (Figures 4.8 and 4.9). The vertical jet has a higher coefficient of variation, which means there were more fluctuations near the jet tip. When the gas bubbles travelled up towards the downward jet tip, the bubble probably merged with the jet tip first. Then, the particles carried by the bubble wake keep going up, due to their high velocity and inertia. In the meantime, the particles entrained by the high velocity downward jet hit with these bubble wake particles. These head-on collisions occurred at higher velocities than if the particles entrained into the jet and slowed down before hitting the bed particles near the normal jet tip location. The jet was thus compressed by the gas bubble and then expanded back to its normal length: this caused the large voidage fluctuations that can be observed in Figure 4.9. On the other hand, with the horizontal jet, the bubble wake particles and the jet entrained particles were both traveling upward near the jet tip. Therefore, Figure 4.8 shows that there were less fluctuations and collisions than with the downward jet.

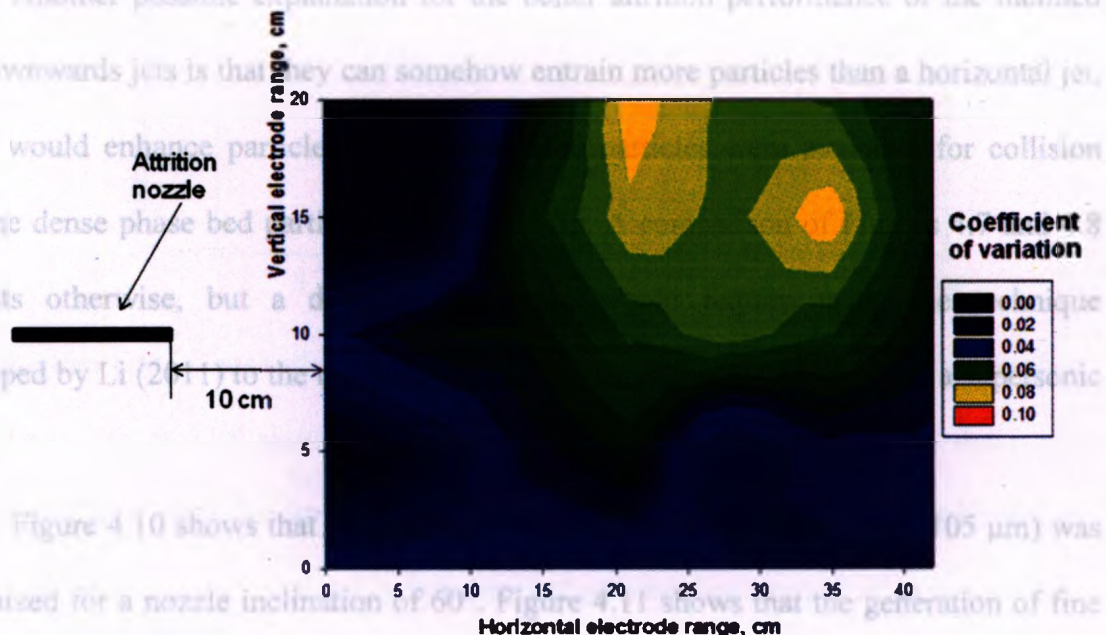


Figure 4.8: Coefficient of variation for horizontal jet

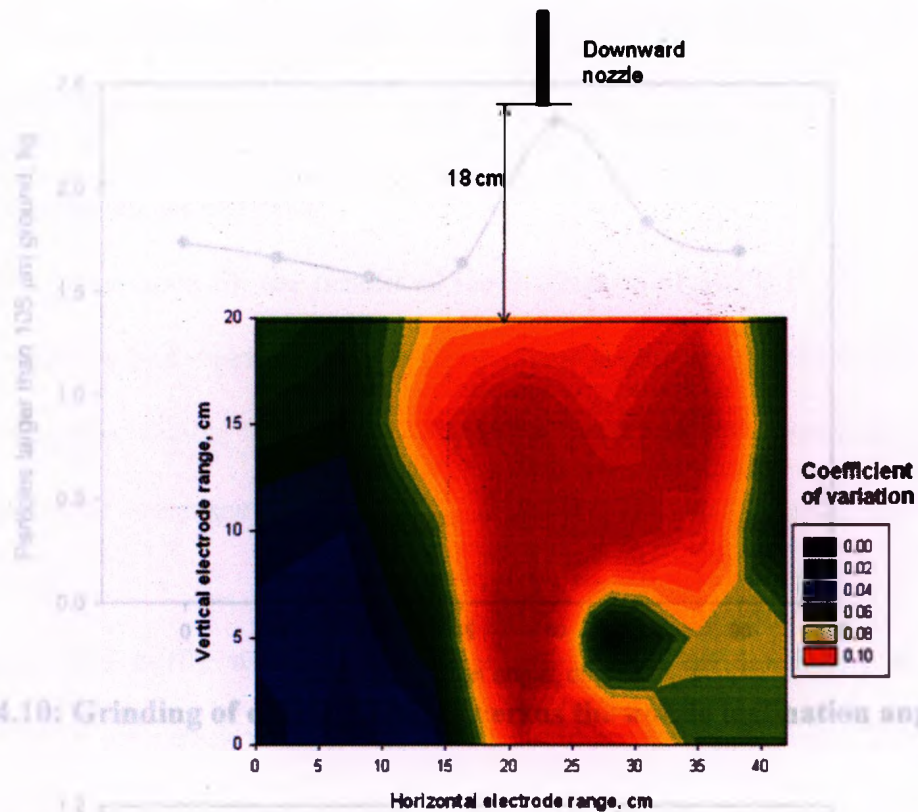


Figure 4.9: Coefficient of variation for vertical jet

Another possible explanation for the better attrition performance of the inclined and downwards jets is that they can somehow entrain more particles than a horizontal jet, which would enhance particle breakage as more particles were available for collision with the dense phase bed particles near the jet tip. A comparison of Figures 4.7 and 4.8 suggests otherwise, but a definite conclusion would require using the technique developed by Li (2011) to measure the entrainment of solid particles into a supersonic jet. From the results shown above, it is important to emphasize that the nozzle

Figure 4.10 shows that the grinding of coarse particles (greater than $105\ \mu\text{m}$) was maximized for a nozzle inclination of 60° . Figure 4.11 shows that the generation of fine particles ($0\text{--}30\ \mu\text{m}$) was not greatly affected by the nozzle inclination angle.

many fine particles would result in increased dust emissions from the Fluid Coker and poor fluidization in the reactor.

4.3.2 Effect of baffle on jet attrition

A possible explanation for the benefit of the inclination of 60° is the downward, inclined jet densifies the bed region below the jet tip. This means that particles entrained by the jet hit a denser region, causing more particle breakage. Experiments were, therefore, conducted to determine whether using a baffle to further density this zone would be beneficial.

In Chapter 3, a baffle was inserted underneath a horizontal attrition jet and improved the attrition efficiency when it was located near the jet tip, by densifying the region by deflecting gas bubbles from the attrition jet. In this section, a similar baffle was inserted underneath the attrition jet for the nozzle inclination angle at 60° (Figure 4.12).

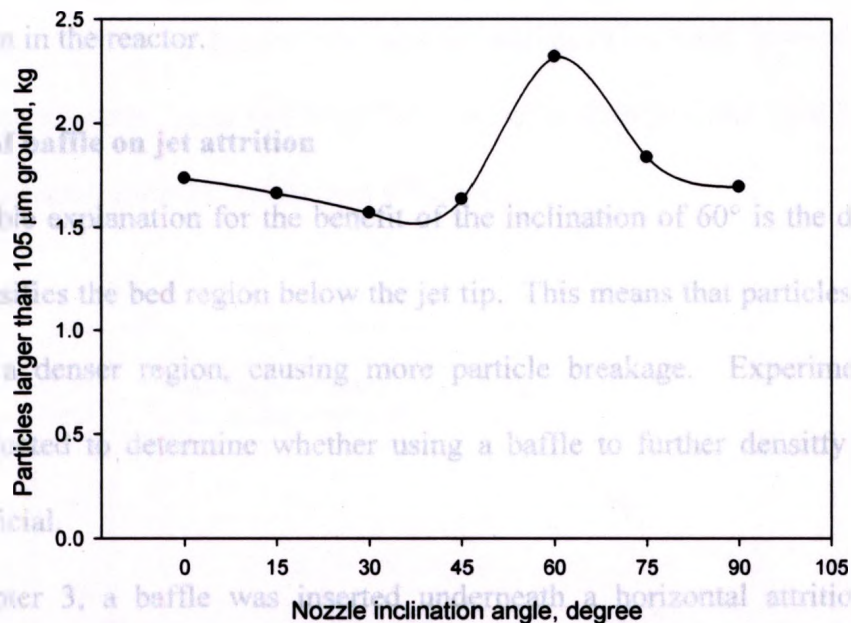


Figure 4.10: Grinding of coarse particles versus the nozzle inclination angle

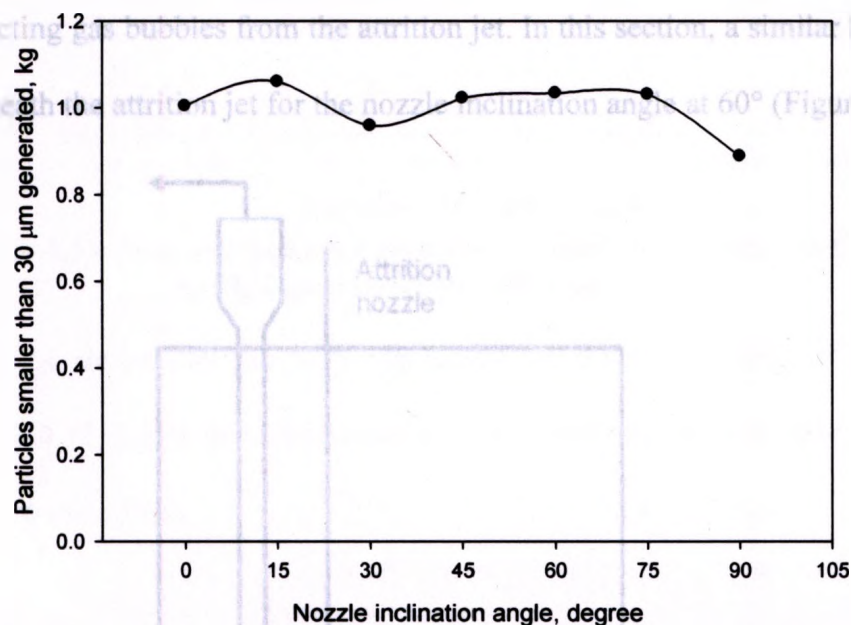


Figure 4.11: Generation of fine particles versus the nozzle inclination angle

From the results shown above, it is important to emphasize that the nozzle inclination of 60° gave the best result in terms of maximizing the new particle surface, grinding the most coarse particles, while generating a similar amount of unwanted fines when compared to the other inclinations. This is a very desirable condition since too

many fine particles would result in increased dust emissions from the Fluid Coker and poor fluidization in the reactor.

4.3.2 Effect of baffle on jet attrition

A possible explanation for the benefit of the inclination of 60° is the downward, inclined jet densifies the bed region below the jet tip. This means that particles entrained by the jet hit a denser region, causing more particle breakage. Experiments were, therefore, conducted to determine whether using a baffle to further densify this zone would be beneficial.

In Chapter 3, a baffle was inserted underneath a horizontal attrition jet and improved the attrition efficiency when it was located near the jet tip, by densifying the region by deflecting gas bubbles from the attrition jet. In this section, a similar baffle was inserted underneath the attrition jet for the nozzle inclination angle at 60° (Figure 4.12).

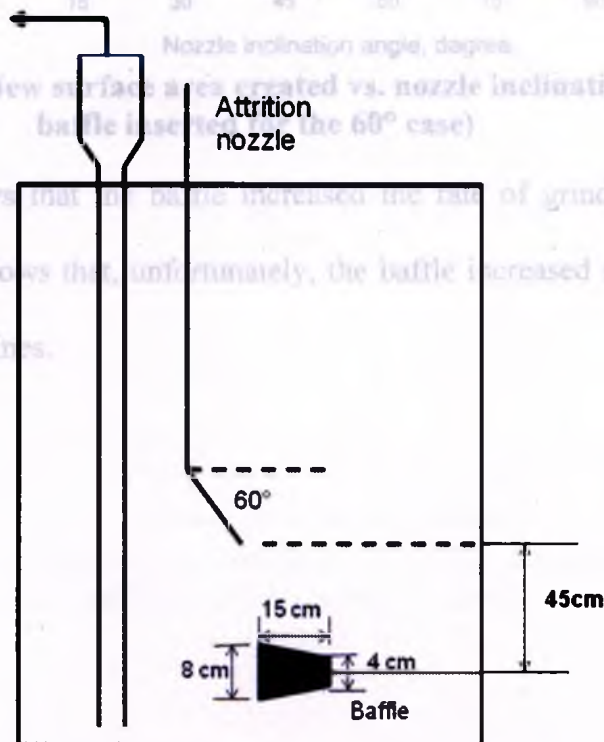


Figure 4.12: Nozzle position relative to baffle

Figure 4.13 shows that the baffle inserted underneath the attrition jet, at a nozzle inclination angle of 60° , increased the new particle surface. This result is consistent with the findings from Chapter 3 and confirms that the baffle densifies the local bed region near the jet tip, which improves the attrition efficiency.

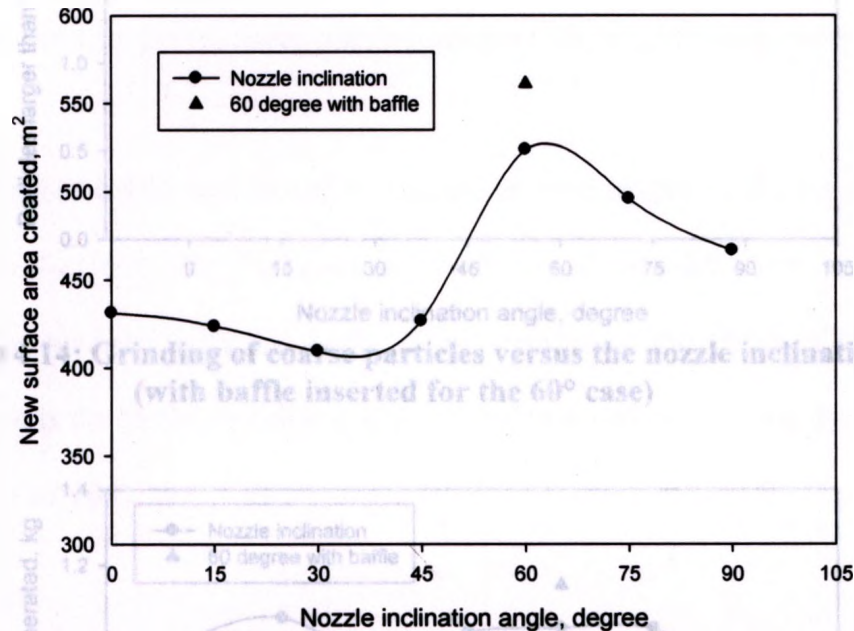


Figure 4.13: New surface area created vs. nozzle inclination angle (with baffle inserted for the 60° case)

Figure 4.14 shows that the baffle increased the rate of grinding of the coarse particles. Figure 4.15 shows that, unfortunately, the baffle increased slightly the rate of generation of unwanted fines.

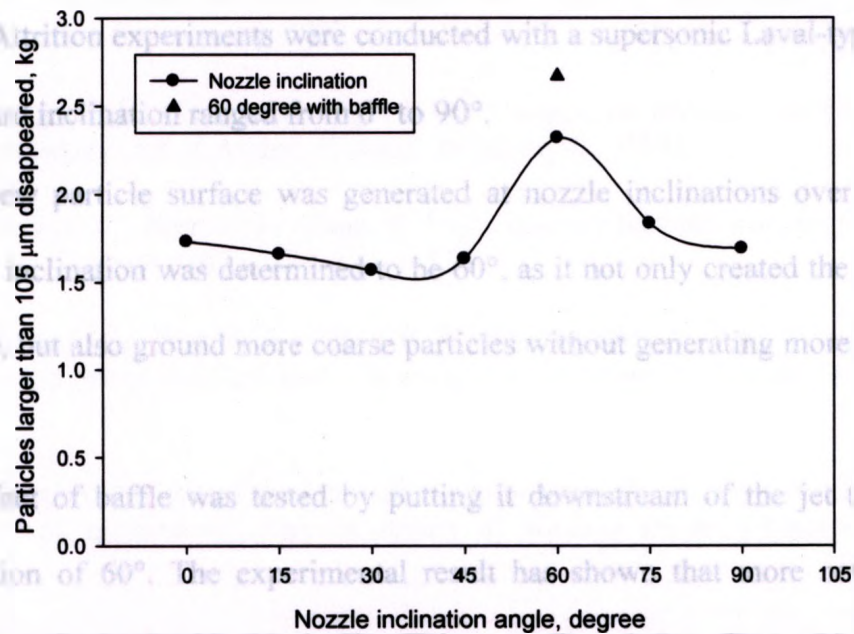


Figure 4.14: Grinding of coarse particles versus the nozzle inclination angle (with baffle inserted for the 60° case)

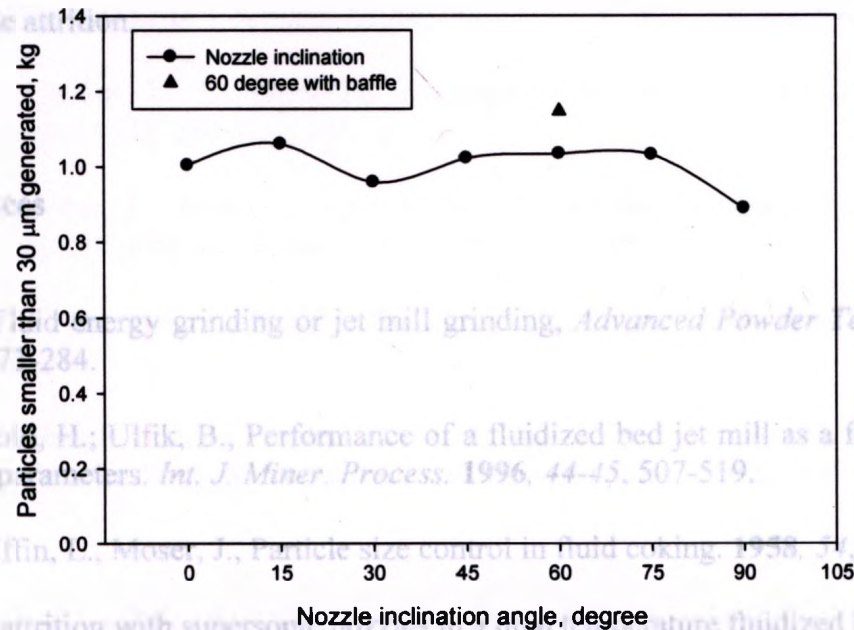


Figure 4.15: Generation of fine particles versus the nozzle inclination angle (with baffle inserted for the 60° case)

4.4 Conclusion

The effect of nozzle inclination on particle attrition was investigated in a gas-solid fluidized bed. Attrition experiments were conducted with a supersonic Laval-type nozzle, whose downward inclination ranged from 0° to 90°.

More new particle surface was generated at nozzle inclinations over 45°. The optimal nozzle inclination was determined to be 60°, as it not only created the most new particle surface, but also ground more coarse particles without generating more unwanted fines.

The effect of baffle was tested by putting it downstream of the jet tip for the nozzle inclination of 60°. The experimental result has shown that more new particle surface area was obtained with this baffle. This reconfirmed the effect of baffle from Chapter 3, which is the baffle was able to densify the local bed region near the jet tip and enhance particle attrition.

4.5 References

- Ahlbus, F.E., Fluid energy grinding or jet mill grinding, *Advanced Powder Technology*, **1996**, 3, 273-284.
- Benz, M.; Herold, H.; Ulfik, B., Performance of a fluidized bed jet mill as a function of operating parameters. *Int. J. Miner. Process.* **1996**, 44-45, 507-519.
- Dunlop D., Griffin, L., Moser, J., Particle size control in fluid coking. **1958**, 54, 39-43.
- Li, F., Particle attrition with supersonic nozzles in a high temperature fluidized bed. Ph.D. dissertation, The University of Western Ontario, London, Canada. **2011**.
- Hamidi M., Measurement of gas jet penetration in a gas-solid fluidized bed using ECT method. *Draft*, **2011**

Hulet, C.; McMillan, J.; Briens, C.; Berruti, F.; Chan, E. W. Visualization of the effect of a shroud on entrainment of fluidized solids into a gas jet. *International Journal of Chemical Reactor Engineering* **2007**, 5.

5.1 Conclusions

Mebtoul, M.; Large, J. F.; Guigon, P. High velocity impact of particles on a target - An experimental study. *Int. J. Miner. Process.* **1996**, 44-45, 77-91.

McMillan, J.; Briens, C.; Berruti, F.; Chan, E. High velocity attrition nozzles in fluidized beds. *Powder Technol* **2007a**, 175, 133-141.

McMillan, J.; Briens, C.; Berruti, F.; Chan, E. Particle attrition mechanism with a sonic gas jet injected into a fluidized bed. *Chemical Engineering Science* **2007b**, 62, 3809-3820.

McMillan, J.. Characterization of the interactions between high velocity jets and fluidized particles. Ph.D. dissertation, The University of Western Ontario, London, Canada. **2007**

Midoux, N.; Hošek, P.; Pailleres, L.; Authelin, J. R. Micronization of pharmaceutical substances in a spiral jet mill. *Powder Technol* **1999**, 104, 113-120.

Pougatch, K.; Salcudean, M.; McMillan, J. Simulation of particle attrition by supersonic gas jets in fluidized beds. *Chemical Engineering Science* **2010**, 65, 4829-4843.

Tasirin, S. M.; Geldart, D. Experimental investigation on fluidized bed jet grinding. *Powder Technol* **1999**, 105, 337-341.

Tuunila, R.; Nyström, L. Technical note: Effects of grinding parameters on product fineness in jet mill grinding. *Minerals Eng* **1998**, 11, 1089-1094.

Werther, J.; Xi, W. Jet attrition of catalyst particles in gas fluidized beds. *Powder Technol* **1993**, 76, 39-46.

Yates, J. G.; Cobbinah, S. S.; Cheesman, D. J.; Jordan, S. P. In *Particle attrition in fluidized beds containing opposing jets*; AIChE Symposium Series; 1991; Vol. 87, pp 13-19.

Chapter 5: Conclusions and Recommendations

5.1 Conclusions

1. The impact on jet attrition of operating conditions such as attrition pressure, nozzle scale and attrition time for a supersonic Laval-type nozzle was investigated. It was concluded that higher attrition pressures and bigger attrition nozzles are more effective. They can generate the same new particle surface while consuming less attrition gas. It was also found that using a higher attrition pressure and bigger attrition nozzles generated roughly the same amount of unwanted fine particles while consuming less attrition gas than using lower attrition pressures and smaller attrition nozzles. The only limitation is that potential erosion of fluidized bed internals should be avoided, as higher attrition pressures and larger attrition nozzles resulted in jets that penetrated further.
2. From the study on the effect of fluidized bed hydrodynamics on jet attrition, it was found that jet grinding was most effective when the nozzle tip was located in a high fluidization velocity region and jet tip located in a low fluidization velocity region. High fluidization velocity near the nozzle tip enhanced particle entrainment into the jet cavity. Low fluidization velocity near the jet tip reduced the local bubble volume fraction, so the entrained and accelerated particles in the jet cavity would slam on a denser bed, which enhanced particle breakage. These results were confirmed with two nozzle scales. A baffle inserted underneath the jet tip cavity was able to densify the local bed, which enhanced the attrition efficiency.

3. A study of the effect of nozzle inclination showed that more new particle surface was generated with a downward, inclined nozzle, with an angle of 60° with the horizontal direction. The optimal nozzle inclination was determined to be 60° , as it not only created the most new particle surface, but also ground more coarse particles without generating more unwanted fines. Particle attrition was further improved when a baffle was inserted underneath the jet cavity of the nozzle with a 60° inclination.

5.2 Recommendations

1. The study on the operating conditions of supersonic nozzles suggested that it is beneficial to use a nozzle at high attrition pressure, because it can save attrition gas when compared to low attrition pressure for the same surface area creation. Future work should investigate higher attrition pressures (2.2 MPa was the highest attrition pressure used in this study).
2. In the study on the effect of nozzle inclination, inclined jets beyond 45° were found effective, especially the 60° nozzle inclination angle. Future work should investigate the influence of inclined angle on solid entrainment with a technique such as Li (2011) developed. Also, the jet tip contour for nozzle angles other than horizontal and vertical should be investigated. Computational Fluid Dynamics (CFD) could also be used to model the hydrodynamics of inclined jets compare to horizontal jet.